M-Pos52 EFFECT OF PHOSPHORYLATION ON THE INTERACTION BETWEEN ACTIN AND RABBIT MUSCLE PHOSPHOFRUCTOKINASE. Michael A. Luther and James C. Lee, Department of Biochemistry, St. Louis University school of Medicine, St. Louis, MO 63104.

Rabbit muscle phosphofructokinase (PFK) has been shown to undergo phosphorylation-dephosphorylation. This post-translational modification of PFK is related to muscle activity. Upon stimulation of muscle contraction, PFK is phosphorylated to a greater extent than that of the resting muscle. To elucidate the role of phosphorylation-dephosphorylation in the regulation of PFK, the highly phosphorylated form was purified by the procedure previously published by this laboratory. The dephosphorylated form was prepared by treating the enzyme with alkaline phosphatase. Using these two forms of PFK, steady state kinetics, subunit self association and interaction between PFK and actin were studied. Results from steady state kinetics at pH 7.0, 23°C show that F-actin acts as a positive effector of phosphorylated PFK, while the kinetics of the dephosphorylated enzyme are not affected. Binding studies show that F-actin has a higher affinity for the phosphorylated form. Results from these *in vitro* studies are consistent with *in vivo* observations that the amount of PFK bound to the muscle matrix is increased with stimulation of muscle contraction. Hence, phosphorylation of PFK during muscle contraction increases the enzyme activity via its association with muscle protein, thus, providing energy to the cellular component where it is needed. (Supported by NIH grants NS-14269 and AM-21489.)

M-Pos53 PROTEIN UPTAKE OF CRYSTALLINE COMPOUNDS BY SOLUBILIZATION: THE REFERENCE STATE PROBLEM. Rex Lovrien, Biochemistry Dept., University of Minnesota, St. Paul, MN 55108.

When compounds (C) are quite insoluble in water (aromatic hydrocarbons, drugs, alkaloids) a commonly used device is to determine their solubility in (i) Solvent only, (ii) Protein in the same solvent. And from the data get $\bar{v}$ (bound), C_{free}, etc.; thence get a binding constant for a binding reaction: C_{free} + Protein $\rightleftharpoons$ C·Pr$_{\bar{v}}$. It is strongly implied - in fact said, from the way K ("binding constant") for the foregoing reaction is generally defined, that the reference state for the compound is the compound in solution, C_{free}. However that may not be realistic. It can be proven in at least two separate ways that *every* molecule so solubilized becoming bound to the protein, actually comes from the crystal or from whatever solid form the otherwise insoluble compound may have. Therefore two free energy contents determine the overall energetics and relevant Δ quantities: (i) That of compound-protein binding affinity, (ii) That of the compound bound to itself in crystal (or amorphous solid) reference state. Half the contribution to the overall energetics in any such solubilization originates in the thermodynamic properties of the crystal reference state. Although at final equilibrium the chemical potential of the compound is the same everywhere (C_{xtal}, C_{free}, C·Pr$_{\bar{v}}$) after the reaction is finished, the process of getting there is an integral process in which the controlling reference state is C_{xtal} during every step. Several consequences ensue. One consequence is that it becomes clear why in such experiments the observed protein driven solubilizations correlate so strongly with the thermodynamic properties of the organic crystal, e.g. ΔH_{fusion}, rather than simply with protein-ligand affinity.

M-Pos54 LIGHT SCATTERING STUDIES OF γ-CRYSTALLINS FROM CALF LENS. Michael R. Fisch, Roland J. Siezen and George B. Benedek, Massachusetts Institute of Technology, Dept. of Physics, Cambridge, MA 02139.

Cold cataract formation in young mammalian lens nuclei has been modelled as a phase separation. The phase separation temperatures associated with γ-crystallins suggest that these lens proteins may play a central role in the phenomena of cold cataract formation. We have studied the spectrum and intensity of the light scattered from solutions of pure γ-crystallins (0.05M phosphate pH 7) in the vicinity of the phase boundary. The phase separation temperature, T*, was determined for each concentration, c, as the temperature at which the intensity of the transmitted light decreased by 10% below its maximum temperature-independent value, measured at temperatures well above T*. Quasi-elastic light scattering measurements at 20°C above T* indicate the presence of two distinct populations of scatterers: (a) small scatterers with $\bar{R}_h$ = 30Å, and (b) large polydisperse scatterers with $\bar{R}_h$ = 600Å. The mean hydrodynamic radius of the small scatterers increases three-fold as T approaches T*, while that of the large scatterers increases approximately 30-fold. The $\bar{R}_h$ versus T-T* curve is essentially the same along all the measured isochores. This data allows various models of the phase separation to be examined.

M-Pos55 FAR ULTRA VIOLET RESONANCE RAMAN SPECTROSCOPY OF PROTEINS AND PROTEIN COMPONENTS Leland Mayne, Greg Harhay, and Bruce Hudson, Department of Chemistry and Institute of Molecular Biology, University of Oregon, Eugene, Oregon 97403 USA

Recent developments in laser technology have made possible the collection of resonance Raman spectra with excitation wavelengths into the vacuum ultra violet*. We have been applying this technique to the study of proteins and protein components. Excitation at these wavelengths provides resonance enhancement of some new chromophores such as the peptide bond and resonance with higher excited states of others such as the aromatic amino acid side chains. Studies have been carried out on several model compounds and many amino acids. Studies of actual proteins are underway beginning with ribonuclease. The necessity of avoiding laser damage to the sample while also maintaining native protein have lead to the development of novel sample handling techniques.

*Bruce Hudson and Leland Mayne, Methods in Enzymology, in press

M-Pos56 ^{1}H NMR INVESTIGATION OF THE BINDING OF L-GLUTAMINE TO GLUTAMINE BINDING PROTEIN OF E. COLI, by Q. Shen, V. Simplaceanu, P. F. Cottam, and C. Ho, Department of Biological Sciences, Carnegie-Mellon University, Pittsburgh, PA 15213, U.S.A.

^{1}H nuclear magnetic resonance (NMR) spectroscopy has been used to investigate the structure-function relationship of glutamine binding protein (GBP) of E. coli. Significant spectral changes are observed in the aromatic, aliphatic, and the ring-current shifted proton resonance regions upon binding of glutamine (Gln) to GBP. In addition, in the exchangeable proton resonance region (5.0 to 10.0 ppm downfield from the proton resonance of H_2O), we have observed the occurrence of six new resonances upon ligand binding. All of these spectral changes are completed at a 1:1 molar ratio of GBP to Gln, in agreement with the presence of one binding site per protein molecule. These spectral changes in the exchangeable proton resonance region of the NMR spectra are absent when GBP is titrated with asparagine or glutamate, indicating that these resonances reflect the highly specific interactions between the protein and its ligand. To assign these exchangeable proton resonances in the protein-ligand complex, two approaches have been used. First, the spectral changes in GBP upon titration with two known competitive inhibitors, γ-glutamylhydrazide and γ-glutamylhydroxamate, have been monitored. Second, ^{1}H-^{1}H nuclear Overhauser effect (NOE) measurements for each of the exchangeable proton resonances have been carried out. The results suggest that at least one of these exchangeable proton resonances originates from an intermolecular hydrogen bond between the amide proton of Gln and the GBP. The relevance of these results to the molecular mechanism for the specific recognition of the ligand by the binding protein will be discussed. [This work is supported by research grants from the NIH (GM-26874) and the NSF (DMB-8208829)].

M-Pos57 TRANSIENT ELECTRIC BIREFRINGENCE OF MYOSIN ROD AS A FUNCTION OF TEMPERATURE AND IONIC STRENGTH. Kusuma Thallam and Sonja Krause. Department of Chemistry, Rensselaer Polytechnic Institute, Troy, NY 12181.

The effect of ionic strength and temperature on rabbit skeletal myosin rod was studied using transient electric birefringence measurements. In all these studies a single relaxation time (τ) was found indicating a single macromolecular species in solution. Electric birefringence studies were done in the temperature range 5°C to 45°C in 10 mm and 2 mm pyrophosphate (PPi) buffers at pH 9.0 and in phosphate buffer at pH 7.0. The temperature corrected relaxation time remained constant up to 15°C at the value expected for a rigid myosin rod in both PPi solutions, and then dropped to another constant value above 30°C. The high temperature relaxation time in 2 mm PPi was 12% lower than the low temperature relaxation time, whereas in 10 mm PPi the high temperature relaxation time was 35% lower than the low temperature relaxation time. These results suggest that the rod is rigid at lower temperatures and that flexibility increases with increasing temperature, especially in 10 mm PPi solutions. In phosphate buffer at pH 7.0, the relaxation time was less then expected for a rigid rod at 5°C and immediately started decreasing to a high temperature constant value somewhat lower than in 10 mm PPi at pH 9. Relaxation times were constant with ionic strength (0.015 M to 0.02 M) at pH 9.0 at 20°C. The specific Kerr constant decreased with increasing ionic strength, from 29×10^{-6} esu to 12.0×10^{-6} esu, as expected for charged macromolecules in ionic solutions.

* Supported by the National Science Foundation

M-Pos58 ALLOSTERIC INTERACTIONS BETWEEN LIGAND-BINDING SITES OF SERUM ALBUMIN. D.O. Tinker & J.C. Hsia, Dept. of Biochemistry, University of Toronto, Toronto, Canada, M5S 1A8.

We have previously shown that the di-anionic spin-labelled ligand TOPG binds to the same sites on human serum albumin (HSA), and with the same order of affinities, as the binding sites for bilirubin, (Hsia et al (1982), J. Biol. Chem. 257, 1724-1729). We propose an allosteric domain model that accounts for the observed binding isotherms. The three binding sites for TOPG and bilirubin are postulated to co-incide with the three structural domains (Brown, J.R. (1976), Federation Proc. 35, 2141-2144), a primary site residing in domain 2 and two secondary sites in domains 1 and 3 (numbered from the NH_2-terminal). Allosteric interaction is postulated to exist between domains in different ligand states (occupied or unoccupied) with interaction co-efficients α and β. The molecular partition function is given in terms of free ligand concentration, [L], by

$$Q = [L]^3 + (\alpha + \beta)K_1[L]^2 + \alpha\beta K_1^2[L] + K_1^2K_2$$

where K_1 and K_2 are the intrinsic dissociation constants for ligand binding in domains 1 (or 3) and 2, the secondary and primary binding sites, respectively. For a wide range of values of α, β and the K_i's, Q yields a non-cooperative binding isotherm for the ligand, with simple competitive displacement of TOPG by bilirubin. On the other hand, the primary binding sites for saturated fatty acids are postulated to reside on domains 3 and 1. A striking enhancement of TOPG binding in the presence of fatty acid is predicted by the model, and found experimentally. The values for the interaction co-efficients found from the effects of bilirubin and palmitate on TOPG binding are comparable (range, 0.1 - 0.5). Thus the model succeeds in giving a unified quantitative description of ligand binding by HSA. (Supported by the Medical Research Council).

M-Pos59 ELECTROSTATIC ANALYSIS OF PROTEIN-PROTEIN INTERACTIONS: THIRD DOMAIN OF TURKEY OVOMUCOID AND STREPTOMYCES GRISEUS PROTEASE B, James H. Smith and Frank R. N. Gurd, Department of Chemistry, Indiana University, Bloomington, Indiana 47405.

The static accessibility modified Tanford-Kirkwood discrete charge model (Matthew et al., Biochemistry 18, 1919, 1979) has been used to analyze the interaction of a proteinase inhibitor, the third domain of the turkey ovomucoid (OMTKY3), with bacterial Protease B from S. griseus (SGPB). The overall association was found to be predominantly due to non-electrostatic forces, although weak electrostatic forces were implicated. The configuration of OMTKY3 from the complex was found to be electrostatically less stable, in terms of free energy, than the native configuration. When considered in the complex below pH 9, the additional electrostatic stabilizing forces gained by OMTKY3 were too small to compensate for the switch to the complex configuration from the native. When the interaction of the SGPB charge array with itself is also considered, the formation of the complex is found to be electrostatically stabilized, with the effect increasing with pH. The importance to the electrostatic stabilization of charge burial at the protein-protein interface was found to increase with pH. The electrostatic contribution to the docking process between SGPB and OMTKY3 was examined using three different methods. In a monopolar approximation the two were found to favorably associate between pH 6 and 8. A dipolar estimation predicted a net repulsion between the two, although the dipoles were aligned favorably. The aforementioned modified discrete charge model predicted a slightly stabilizing association process, increasing this effect with pH. In this model manifestations of electrostatic interactions were found to begin around a distance of 4 angstroms separation and to primarily affect the charge array at the protein-protein interface. (Supported by Public Health Service Research Grants HL-05556 and HL-14680.)

M-Pos60 INTERMEDIATE LIGATION STATES OF HEMOGLOBIN: THREE ENERGY LEVELS DEFINE TWO LIGAND AFFINITIES. Francine R. Smith and Gary K. Ackers, Dept. of Biology, The Johns Hopkins University, Baltimore, MD 21218.

During the course of ligand binding tetrameric hemoglobin molecules assume ten states which have different configurations of ligands bound to the heme sites. We have developed methods for determining the energetic properties of all the partially-ligated species of CN-met hemoglobins. The relative values of the Gibbs free energy levels for six of the ten possible forms have been determined as of this abstract deadline. These are the first free energies determined for partially-ligated hemoglobins in distinct microscopic configurations. We anticipate, using these new methods, that a complete partition function will soon be obtained. The present results define three Gibbs energy levels for the tetrameric molecule. The differences between these levels and the distribution of species within each level lead to the prediction of only two affinities for the stepwise binding of ligands. The results for CN-met hemoglobin are consistent with values we have obtained for energetic properties of partially-oxygenated hemoglobin. These findings provide a simple means of rationalizing much of the hemoglobin literature. Supported by grants from the NSF and NIH.

M-Pos61 SITE SELECTION SPECTROSCOPY OF IRON-FREE HEME PROTEINS. J. M. Vanderkooi, V.T. Moy, G. Maniara and K. G. Paul, Dept. of Biochemistry & Biophysics, Univ. of Penn., Philadelphia PA, and Department of Physiological Chemistry, University of Umea, Umea, Sweden.

The optical spectra of most chromophores in proteins are unresolved and hence uninterpretable; however, we have demonstrated that resolved spectra can be obtained for porphyrins in heme proteins under conditions of site selection. The fluorescence emission spectra of mesoporphyrin derivatives of horse radish peroxidase (types A and C), myoglobin and leg-hemoglobin and of iron-free cytochrome c were examined as a function of temperature, pH and excitation frequency. Highly resolved emission spectra were obtained at 4.2 K when the sample was excited with narrow bandwidth laser light into the low energy side of the Qx(1,0) vibrational band. Excitation at the high energy side or at higher temperatures resulted in broad spectra which are interpreted in terms of phonon interactions between the porphyrin and the polypeptide chain. The details of phonon interactions, the extent of inhomogeneous broadening and the resolution of the zero phonon lines varied with the proteins used, indicating porphyrin-protein interactions. An effect of pH on the spectra was interpreted in terms of effects of neighboring charged amino acids on the chromophore (Sponsored by NSF grant PCM 84-0844).

M-Pos62 QUANTITATION OF BACTERIORHODOPSIN, HALORHODOPSIN, AND SLOW RHODOPSIN IN H. halobium RETINYL PROTEIN MUTANT STRAINS. D.B. Bivin, S.L. Helgerson, H.W. Boyer and W.Stoeckenius. Cardiovascular Research Institute and Department of Biochemistry and Biophysics, UCSF, San Francisco,CA 94143.

Bacteriorhodopsin (bR) driven energetic systems can serve as models for studying proton dependent energy coupling mechanisms. However, the contributions of other electrogenic ion pumps (i.e. halorhodopsin (hR) and the respiratory chain) must be systematically excluded. We have characterized strains of H. halobium in which the mutational events leading to the loss of both bR and hR have been mapped [1]. The strains tested were II-7 (bR^+ hR^+ sR^+), IV-4 ($bR^-hR^-sR^+$) IV-13 ($bR^-hR^+sR^+$) ReIV-41 ($bR^+hR^+sR^+$) and O-3 ($bR^-hR^+sR^+$). The amounts of bR, hR and sR were determined in these strains. Amounts of bR were determined by light/dark difference spectroscopy; the amount of sR was determined by flash spectroscopy. The amount of hR was determined by photo steady state spectroscopy. This last method makes use of the fact that hR can exist in two spectrally distinct forms under certain conditions [2]. One form absorbs maximally at 408nm; the other absorbs maximally at 578nm. Illumination of the suspensions with orange light drives the hR into the 408nm form while illumination with blue light drives the hR into the 578nm form. The difference of the spectra of these two forms is characteristic of hR and can be used to detect hR when bR is also present. It is quantative when the ratio of bR/hR is less than 50.

References: 1. Betlach M,Pfeifer F,Friedman J, Boyer HW (1983) PNAS USA 80:1416-1420
2. Taylor ME, Bogomolni RA, Weber HJ (1983) PNAS USA 80:6172-6176
(Supported by NIH Program Project Grant GM-27057 and NIH GM-31785)

M-Pos63 CHARACTERIZATION OF THE CHROMOPHORE OF THE THIRD RHODOPSIN-LIKE PIGMENT OF HALOBACTERIUM HALOBIUM AND ITS PHOTOPRODUCT. Motoyuki Tsuda, Department of Physics, Sapporo Medical College, Sapporo 060, Japan, Burr Nelson, C.-H. Chang, Rajni Govindjee and Thomas G. Ebrey, University of Illinois, Department of Physiology and Biophysics, 524 Burrill Hall, 407 South Goodwin Avenue, Urbana, IL 61801 U.S.A.

Halobacterium halobium strain Flx 3 1c has been shown by Bogomolni and Spudich [Proc. Natl. Acad. Sci. USA 79, 6250 (1982)] to be lacking in bacteriorhodopsin and halorhodopsin but possesses a third rhodopsin-like pigment, tR_{590}, also called sR (slow rhodopsin). The photocycle of tR_{590} has a long-lived (~ 0.8 sec) short wavelength intermediate, tR_{370} [Tsuda et al., Biochem. Biophys. Res. Commun., 108, 970 (1982)]. Because of its long life-time tR_{370} accumulates in significant amounts under steady state red illumination. Retinal photoisomerization plays a key role in the excitation of visual cells in the retina and in proton pumping by the purple membrane of H. halobium. Thus, it is important to determine the isomeric form of the chromophore in tR_{590} and its photoproduct tR_{370}. Using high performance liquid chromatography we show that the chromophore extracted from tR_{590} is primarily all-trans retinal, and its conversion by light to tR_{370} causes the chromophore to isomerize primarily to the 13-cis conformation.

M-Pos64 LIGHT-INDUCED CHLORIDE TRANSPORT BY HALORHODOPSIN IN BLM WITH ATTACHED HALOBACTERIUM CELL-ENVELOPES. I.Vodyanoy, J.K.Lanyi, V.Vodyanoy. Dept. of Physiology and Biophysics, Univ. of Calif. Irvine, Irvine CA 92717

Halorhodopsin (HR) is a retinal protein related to bacteriorhodopsin (BR) but with many spectroscopic and photochemical properties quite different from those of BR. Recent results indicate that HR in the cell membrane is an inward-directed chloride pump (Schobert and Lanyi, J.Biol.Chem. 257:10306, 1982). We have studied a reconstitution system where well oriented HR-containing vesicles are attached to a bimolecular phospholipid membrane (BLM) made of phosphatidylcholine, modified with proton carrier SF 6847 (3,5-di-tert-butyl-4-hydroxybenzylide). The BLM was formed of a lipid monolayer, using a closed chamber method (Vodyanoy and Murphy, BBA 687:189, 1982). The membrane area was about 1 sq. mm. We have analyzed this system using a simple topological model and its corresponding electrical circuit diagram. Using just the dependence of membrane conductance on vesicle concentration, we could determine the conductance of that part of the membrane area which is free of vesicles. The chloride pump in our circuit acts as a light-sensitive voltage generator with a serial resistance. Analysis of this circuit shows that the results of three independent measurements i.e. short-circuit "light-current", "light" and "dark" current-voltage (I-V) dependence fully define the system parameters. These are: resistance of the BLM-vesicle contact, resistance of vesicle membranes, equivalent voltage potential of the pump and its electromotive force. The parameters derived describe very well the observed I-V dependence of the system ("dark" and "light"). We evaluated also the apparent affinity of HR to chloride ions (which is about 40 mM), thus confirming independent studies with cell envelope vesicles in suspension (Lanyi and Schobert, Biochemistry 22:2763, 1983).

M-Pos65 CONFORMATION AND ENVIRONMENT OF THE β-IONONE RING AND ADJACENT CHAIN IN BACTERIORHODOPSIN. Harbison, G.S. and Herzfeld, J., Harvard Medical School; Smith, S. and Mathies, R., University of California, Berkeley; Pardoen, H. and Lugtenburg, J., University of Leiden, Netherlands; Griffin, R.G., Francis Bitter Nat'l Magnet Laboratory, Massachusetts Institute of Technology, Cambridge, MA 02139. Introduced by E.A. Dawidowicz.

^{13}C Solid state magic angle sample spinning NMR spectra of various specifically retinyl-labeled bRs has enabled us to deduce that the conformation of bR about the ring-chain linkage is planar s-*trans*. This conclusion rests on three independent measurements, vis: (a) The ^{13}C-5 chemical shift (144.6 ppm) which is much closer to (albeit downfield of) the ^{13}C-5 shifts of crystalline 6-s-*trans* retinoids (134-136 ppm) than to 6-s-*cis* derivatives (127-129 ppm). (b) The ^{13}C-8 chemical shifts of bR (131.6, 132.7 ppm) which show the sterically-induced upfield shift noted in 6-s-*trans* compounds (σ_I = 131-133 ppm), absent in 6-s-*cis* derivatives (σ_I = 138-140 ppm). (c) The ^{13}C-18 longitudinal relaxation time(T_1), which in methyl groups is usually dominated by dipole-dipole relaxation due to hops about the C_3 axis, and which is long (>15 s) in bR and in 6-s-*trans* retinoids, and short (<4 s) in 6-s-*cis* compounds. The large additional downfield shift at C-5 supports the external point-charge hypothesis of Honig and Nakanishi; a negative charge closely associated with C-5 is expected to deshield it and thus shift its resonance downfield. The combined point charge and s-*trans* linkage are expected to have a synergistic effect on λ_{MAX}. Additionally, circumstantial evidence will be presented for a positively charged amino-acid sidechain associated with C-7 and C-19, which may be the point-charge counterion.

M-Pos66 ^{13}C NMR STUDIES OF BACTERIORHODOPSIN: EXPERIMENT AND THEORETICAL METHODS FOR INTERPRETING DATA. Hillary S. Rodman, B. A. Wallace, Alan Croteau*, Barry H. Honig. Department of Biochemistry & Molecular Biophysics, Columbia University, NY, NY 10032. *Department of Chemistry, Columbia University, NY, NY, 10027.

A retinal with a ^{13}C label on carbon 15 was incorporated into bleached bacteriorhodopsin. Dark adapted bacteriorhodopsin was then incorporated into dimyristoyl phosphatidylcholine vesicles and the ^{13}C NMR spectrum was obtained. One broad peak for the retinal was observed indicating the environment of carbon 15 in the 13-cis and all-trans isomers found in dark adapted bacteriorhodopsin are similar. Other ^{13}C peaks in the bacteriorhodopsin chromophore have been identified by Harbison et al. (1984) using solid state techniques. The carbon 15 peak was found to be about 14 ppm upfield from model compounds, the largest shift observed in bacteriorhodopsin chromophore relative to model compounds. This large shift may be due to a steric interaction between the Schiff base end of the chromophore and the protein, or a modified electronic environment due to charged residues on the protein.

Interpretation of ^{13}C chemical shifts by theroetical means has proven to be difficult. We have however, found that there is a high correlation between changes in charge densities (calculated with CNDO/S) between similar molecules and changes in their chemical shifts. We are using this technique and the ^{13}C NMR data on the chromophore of bacteriorhodopsin to model it's binding site in the protein.

M-Pos67 STABILITY OF TRANSMEMBRANE SEGMENTS OF BACTERIORHODOPSIN STUDIED BY PROGRESSIVE PROTEOLYSIS. M.E. Dumont, J. Trewhella*, D.M. Engelman and F.M. Richards, Department of Molecular Biophysics and Biochemistry, Yale University, P.O. Box 6666, New Haven, Ct. 06511 and *Life Sciences Division, Los Alamos National Laboratory, Los Alamos, N.M. 87545

Extensive proteolysis of purple membranes from Halobacterium halobium has been carried out with the aim of characterizing the membrane-embedded regions of bacteriorhodopsin. Products of proteinase K digestions of purple membranes for up to 24 hours at an enzyme:substrate ratio of 1:2 (w/w) were separated by reverse phase HPLC. Amino acid compositions of HPLC fractions were fit to segments of the bacteriorhodopsin sequence using a computerized search procedure. Effects of digestion on the membranes were also monitored by SDS-urea polyacrylamide gel electrophoresis, x-ray diffraction, determination of the amount of ^3H leucine remaining associated with the membranes, and measurement of the visible absorption spectrum.

Mild proteolysis leaves bacteriorhodopsin largely intact, with cleavage only in segments which have previously been identified as being exposed to the aqueous surface of the membrane. After longer digestion times, some hydrophobic sequences are removed from the membrane. This is most simply explained by destabilization of transmembrane segments subsequent to cleavage of aqueous loop regions of the protein. The individual segments may experience motion in and out of the plane of the membrane, allowing access to proteases. These results demonstrate a need for caution in interpreting proteolytic digestions in the study of membrane protein topology. (Supported by grants GM-21714 and AI-20466 from the National Institutes of Health.)

M-Pos68 THERMODYNAMIC MEASUREMENTS OF PURPLE MEMBRANE. S. Tristram-Nagle, C.P. Yang, J.F. Nagle. Departments of Biological Sciences and Physics, Carnegie-Mellon University, Pittsburgh, Pa. 15213

In order to investigate suggested phase changes in purple membrane, we are performing high precision dilatometric and calorimetric measurements. To increase sensitivity we use higher concentrations of membrane (12.6 mg/ml) than previous high precision calorimetric measurements (Jackson, M.B. and Sturtevant, J.M. (1978), Biochem. 17:911). In the temperature range 5 to 30° C the apparent coefficient of expansion, α, has an average value of 6.2×10^{-4}/deg in good agreement with the value obtained by J. Marque (personal communication). In addition, we observe that α increases by 14% from 5° to 28° C and then decreases for higher temperatures. Our preliminary calorimetric measurements are consistent with a slight change in slope of the specific heat at 28° C. If these measurements are to be interpreted in terms of phase changes, then the transition is very broad and involves far fewer degrees of freedom than typical lipid bilayer phase transitions. Since it is known that the purple membrane lipids melt at very low temperatures (J.S. Chen et al. (1974), Biochim. Biophys. Acta 352:202), any transition presumably involves the protein or protein-lipid interactions.

Preliminary isothermal differential dilatometric measurements have been made with and without light and indicate that a small volume change accompanies light adaptation.

M-Pos69 **PATCH CLAMPING OF BACTERIORHODOPSIN AND ITS RECONSTITUTION IN A POLYMERIZABLE LECITHIN.** **Paul Yager, Code 6190, Bio/Molecular Engineering Branch, Naval Research Laboratory, Washington, DC 20375-5000**

Patch clamping, to date used primarily as a research tool for the study of membrane proteins, might be used in a method of fabricating biologically-based sensors if the bilayer at the electrode tip were made more rugged. Stabilization of lipid bilayers by polymerization is a potential solution. Bacteriorhodopsin (as a test protein) was reincorporated in liposomes of a polymerizable diacetylenic lecithin, di-(10,12 tricosadiynoyl) phosphatidylcholine by cosonication above the transition temperature of the lecithin. The liposomes sustained the function of the protein before and after polymerization as determined by the change in pH of the external medium induced by illumination by visible light. Bacteriorhodopsin was also reincorporated into an asolectin monolayer at the air-water interface, from which it was transferred as a bilayer onto a patch electrode tip. Such patches probably contained fewer than 20,000 protein monomers under the reconstitution conditions used. When illuminated with pulses of 514.5 nm light the lipid/protein patch produced a current spike corresponding approximately to the buildup of the 412 nm intermediate. Work is in progress to test the influence of polymerizable lipids on the function of the protein in this configuration.

M-Pos70 MEMBRANE-ORGANIZATION AND FUNCTION RELATIONSHIP OF THE PURPLE MEMBRANE.
S.C. Hartsel, J.E. Draheim, B.J. Kolodziej and J.Y. Cassim, Department of Microbiology, The Ohio State University, Columbus, Ohio 43210

The relationship between membrane organization and function was investigated by a comparative study of a contracted lattice form (cPM) and the native lattice form (nPM) of the purple membrane (PM) by absorption, fluorescence and circular dichroic (CD) spectral analysis. Results indicated no major differences in protein structure between these lattice forms. The only difference observed was that the excitonic contribution to the protein visible CD and the protein fluorescence was enhanced in the cPM relative to that of the nPM. Moreover, changes associated with the bR568 to M412 phototransformation in the PM were also similar in both forms. However, there was a marked difference in the photoresponse of the two forms: cPM M412 decay half-life was slower by greater than two orders of magnitude, cPM light-dependent hydroxylamine bleaching was much more rapid and cPM dark-adaptation was markedly slower relative to that of nPM. These results suggest that a subtle yet strong relationship exists between membrane organization and photoresponse. The significance of this relationship will be discussed in view of our recently proposed deformation wave model for the photoinduced vectorial proton transport in the PM (1).

(1) Draheim, J.E., N.J. Gibson, S.C. Hartsel and J.Y. Cassim, 1984, Biophys J., 45:211a.

M-Pos71 CROSSLINKING OF BACTERIORHODOPSIN PROVIDES FURTHER SUPPORT FOR THE DEFORMATION WAVE MODEL OF PROTON TRANSPORT
N.J. Gibson and J.Y. Cassim, Department of Microbiology, The Ohio State University, Columbus, Ohio 43210

In an effort to understand the mechanism by which bacteriorhodopsin pumps protons, purple membrane has been crosslinked with dimethyl adipimidate (DMA), bleached, and then examined spectroscopically. Circular dichroism spectra of the purple membranes, both in solution and oriented as films, were compared. While the spectra suggest that crosslinking alone causes no change in the secondary or tertiary structure of the protein, bleaching of native and crosslinked membranes results in a tilting of the α - helical segments away from the membrane normal. The average tilt for bleached membranes is estimated to be 28° while the tilt for crosslinked - then - bleached samples is approximately 35° . A similar phenomenon has been seen on a smaller scale in the photointermediate M-412 and has led to the suggestion that protons are translocated via a deformation wave caused by the tilting helices (1). In view of previous findings that crosslinking with DMA causes a decrease in photocycling yet an increase in proton pumping (2,3), it is postulated that the degree of tilting may be correlated with the number of protons pumped. This further supports the hypothesis that a large scale global structural change of the protein is essential to proton pumping. Furthermore, it suggests that the variable stoichiometry observed is due to differing degrees of tilting and, by extension, to resultant deformation waves of differing magnitudes. Work is currently underway to investigate the conformational state of the intermediate M-412 in crosslinked purple membrane.

(1) Draheim, J.E., N.J. Gibson, S.C. Hartsel and J.Y. Cassim. 1984, Biophys. J., 45: 211a.
(2) Konishi, T. and L. Packer, 1976, Biochem. Biophys. Res. Comm., 72:1437-1442.
(3) Konishi, T., S. Tristram and L. Packer, 1979, Photochem. Photobiol. 29: 353-358.

M-Pos72 BACTERIOOPSIN PIGMENT WITH MODIFIED RETINAL CHAIN HAS PHOTOCHEMISTRY AND PUMPS PROTONS
J. Zingoni, Y. S. Or, R. Crouch, C. H. Chang, R. Govindjee, and T. G. Ebrey, Medical University of South Carolina, Charleston, SC, and University of Illinois, Urbana, IL

Bacteriorhodopsin undergoes a light activated photocycle establishing a proton gradient across the membrane. The chromophore is all-trans retinal 1 without which the protein does not undergo the light energy conversion. Retinal analogues containing one less (2) and one additional (3) carbon in the side chain have been synthesized and the all-trans isomers characterized. In both

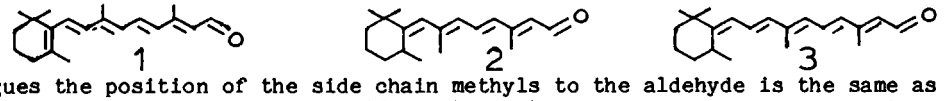

analogues the position of the side chain methyls to the aldehyde is the same as for retinal. With 2, bacterioopsin forms a pigment (λ max 470 nm) which undergoes a photocycle with a M intermediate at 355 nm ($T_{\frac{1}{2}}$ =11 msec). Some proton pumping is observed. The extended analogue (3) also forms a pigment with bacterioopsin with λ max of 518 nm. This pigment also undergoes a photocycle with a M intermediate at 395 nm ($T_{\frac{1}{2}}$ =11 msec). A strong light induced pH change is observed with this pigment. Both pigments are moderately stable to hydroxyl amine and all-trans retinal. Studies with acyclic retinals have shown that the retinal ring has no role in the photochemistry or proton pumping activity of bacteriorhodopsin. These results imply that the polyene side chain length is key to the proton pumping activity and that the full length of the retinal side chain is required to obtain a fully functionally active bacterioopsin pigment. (Supported by grants NIH EY04939, NSF PCM-01924, and DEA ER12087.)

M-Pos73 THE ORDER OF PROTON UPTAKE AND RELEASE BY BACTERIORHODOPSIN AT LOW pH.
Drake Mitchell and G. W. Rayfield, Physics Department, University of Oregon, Eugene, OR 97403.

The order of proton uptake and release in an aqueous suspension of purple membrane in response to a light flash has been investigated at lowered pH. pH indicator dyes and a flashspectrophotometer were used for the study. At pH 7 it was found that the release of protons from the purple membrane precedes uptake as reported by other investigators. At pH 5 and pH 4.1 it was also found that release precedes uptake. Both purple membrane sheets and bacteriorhodopsin containing vesicles were used in this study. Our preliminary results are not in agreement with those of previous investigators.

The number of protons pumped per bacteriorhodopsin molecule photocycling was also measured at various values of pH. The change in absorbance at 400nm and the differential extinction of the M412 state were used to determine the number of BR molecules photocycling.

M-Pos74 THE CHROMOPHORE RETINAL CONTROLS THE PROTON/HYDROXYL ION FLUX ACROSS BACTERIORHODOPSIN.
Norbert A. Dencher and Petra A. Burghaus (Intr. by H. Otto). Biophysics Group, Dept. Physics, Freie Universität Berlin, Arnimallee 14, D-1000 Berlin 33, FRG.

Experiments had been performed to answer the question whether the chromophore retinal in bacteriorhodopsin (BR) influences the proton/hydroxyl ion flux through this light-energized proton pump. Transmembrane pH-gradients were quickly established across BR/BO-dimyristoyl-phosphatidylcholine-phosphatidylserine vesicles and the induced fluorescence changes of the enclosed pH-sensitive optical probe pyranine were measured. The H^+/OH^- flux through bacterioopsin was faster than the one through native bacteriorhodopsin and through bacteriorhodopsin reconstituted from bacterioopsin (BO) and retinal. Whereas the imposed transmembrane pH-gradient across the BO-lipid vesicles decayed with a single lifetime of τ= 213 s, upon regeneration of ≈ 80% of the BO with retinal to BR the overall decay rate was considerable slower and composed of two exponentials with τ_1= 200 s, A_1 = 29% and τ_2= 1230 s, A_2= 71% (8.0°C, molar lipid to BO ratio of 35, 1 mM phosphate buffer and 50 mM K_2SO_4 in the vesicle interior). Our results support investigations previously described by Konishi and Packer (FEBS Lett. 89, 333-336, 1978) and might indicate that the chromophore retinal either is part of the proton/hydroxyl ion path across the protein moiety of bacteriorhodopsin or indirectly controls this path. The dependence of the H^+/OH^- permeability on both the isomeric configuration of retinal and the aggregation state of the membrane protein shall be discussed to gain further insight into the molecular properties involved.

M-Pos75 CONTROL OF PROTONATION STATES OF GROUPS IN PROTEINS BY ADJUSTMENT OF H-BOND GEOMETRY.
Steve Scheiner, Department of Chemistry & Biochemistry, Southern Illinois University, Carbondale, IL 62901.

The competition between various groups for a proton is studied by ab initio molecular orbital methods. It is found that reorientations of the two groups involved in a H-bond can reverse the equilibrium position of the proton shared between them. Specifically, the carbonyl and hydroxyl groups were modeled by H_2CO and HOH. In the H-bond between these two groups, association of the proton with the carbonyl $(H_2COH\text{--}OH_2)^+$ was favored over the hydroxyl $(H_2CO\text{--}HOH_2)^+$ when the latter group is situated along a lone pair of the carbonyl oxygen. However, displacement of the water to the C=O axis between the two carbonyl lone pairs reverses the situation and $(H_2CO\text{--}HOH_2)^+$ is more stable. A similar reversal of stability is observed in the H-bond involving a Schiff base (modeled by CH_2NH) and amine (NH_3). In one arrangement where the lone pairs of the two groups point toward one another, the proton prefers the Schiff base to the amine, i.e. $(H_2CHNH\text{--}NH_3)^+$ is more stable than $(H_2CHN\text{--}HNH_3)^+$. On the other hand, rotation of the lone pair of the amine away from the Schiff base nitrogen results in proton transfer across to the amine. These shifts in stability correspond to reversal of relative pK of the groups involved. A fundamental principle emerging from the calculations is that ion-dipole electrostatic interactions favor transfer of a proton to the group which is positioned as closely as possible to the negative end of the dipole moment vector of the other. The ideas developed here suggest a number of means by which conformational changes may be utilized to shift protons from residue to residue within a protein molecule such as an enzyme or bacteriorhodopsin. (supported by NIH grants GM29391 and AM01059)

M-Pos76 FACTORS INFLUENCING THE CARBON-NITROGEN STRETCHING FORCE CONSTANT IN SCHIFF'S BASES AND PROTONATED SCHIFF'S BASES. Juan Lopez-Garriga, Gerald T. Babcock and James F. Harrison, Department of Chemistry, Michigan State University, E. Lansing, MI 48824-1322 USA

The C-N stretching frequency $\nu_{C=N}$ has been studied in a series of aromatic Schiff's bases, their protonated derivatives and in their reaction products with other Lewis acids. In general, $\nu_{C=N}$ increases upon protonation or reaction with a Lewis acid; the magnitude of the increase is dependent on the extent of conjugation in the aromatic system, on the nature of the substituent on the nitrogen Schiff's base, and on the strength of the Lewis acid. A similar trend has been observed by others for the C≡N stretching modes in nitriles. This suggests that the behavior of the nitrogen lone pair is involved in determining the properties of the $C=N^+$ and $C\equiv N^+$ vibrational modes. *Ab initio* calculations have been carried out at the GVB level for methylimine and methylenimonium ion and show that upon protonation of methylimine the sp^2 character of the lone pair is decreased significantly (~30%); consequently, there is a reorganization of the electron density around the nitrogen which leads to an increase in the overall sp^2 character of the C-N sigma bond. This observation is in agreement with NMR data which indicate an increase in the electronegativity of the nitrogen upon protonation of the Schiff's bases. Furthermore, potential surfaces calculated for the C=N and $C=N^+$ vibrational modes indicate that the $C=N^+$ stretching force constant increases relative to the C=N force constant by ~0.5 mdyn/Å; these calculations also show a slight decrease in the C=N bond length upon protonation. Therefore, the change in the nitrogen lone pair and the accompanying change in electronegativity play important roles in determining the behavior of the $C=N^+$ and $C\equiv N^+$ stretching frequencies.

M-Pos77 N-H BOND LENGTHS AND HYDROGEN BONDING IN CRYSTALLINE AMINO-ACIDS, PEPTIDES, SCHIFF BASES AND BACTERIORHODOPSIN.
Harbison, G.S. and Herzfeld, J., Harvard Medical School, Boston, MA; Roberts, J.E. and Griffin, R. G., Francis Bitter Nat'l Magnet Lab, Massachusetts Institute of Technology, Cambridge, MA 02139.

The "Dipshift" technique of Munowitz et al. (J. Chem. Phys. 76, 2848) allows separation of the dipolar and chemical shift interactions in magic angle sample spinning NMR spectra. By carefully measuring the multiple pulse scaling factor, we have been able to determine to high accuracy (≤ 0.01 Å) the ^{15}N-^{1}H dipolar interaction and thus the NMR bond length for several amino-acids and peptides for which high resolution neutron crystallographic structures are available. The two measurements are strongly correlated, with the NMR bond lengths uniformly 0.03-0.04 Å greater than those from neutron diffraction. This divergence is adequately explained by vibrational corrections to the NMR bond length. Since N-H bond lengths are inversely correlated with the strength of the hydrogen bond between N-H and a Lewis donor, we therefore have a probe of hydrogen bond strength in biomolecules. We have applied this technique to a series of solid retinal Schiff-base salts. As we previously reported these salts possess ^{15}N chemical shifts which span a 27 ppm range and which were inferred to be primarily determined by hydrogen bonding. N-H bond lengths are indeed strongly correlated with the ^{15}N chemical shifts, long N-H distances being associated with downfield ^{15}N shifts and strongly hydrogen-bonding counterions. We shall present data obtained by this method on the ^{15}N-^{1}H dipolar interaction of the bR Schiff base, which on the basis of its ^{15}N chemical shift appears to be very weakly hydrogen-bonded to its counterion.

M-Pos78 EFFECT OF TRITON X-100 ON LIGHT - INDUCED ION RELEASE FROM PURPLE MEMBRANES.[†]
Tim Marinetti and David Mauzerall, The Rockefeller University, 1230 York Avenue, New York, NY 10021

Transient ion release and uptake by purple membrane (pm) fragments after light flashes (585 nm, 1 μs, <1 mj) were measured using a 100 kHz AC conductivity bridge. Conductivity changes (ΔK) due to H^+ can be distinguished from those due to other ions by varying buffer composition at constant pH.[1] At pH 7 in 1M NaCl, ΔK is positive and varies by <10% under conditions where it should have inverted sign, showing that most of the transient is due to ions other than H^+. Addition of Triton X-100 (TX; 0.025% v/v) causes an immediate 2-3-fold increase in both ΔK and its ~20 ms decay time. This could be due to the dispersal of occluded pm fragments. When [TX] >0.1%, ΔK decreases in magnitude and its decay becomes complex: a rapid (30-60 ms) negative swing followed by a slow (0.3 to >1 s) recovery; increasing [TX] to 5% causes no large effect on either amplitude or kinetics. Although buffer variation new changes ΔK by ~30% (corresponding to H^+ release), the bulk of the signal is still due to ions other than H^+. Also, the size of the negative swing in ΔK compared to the baseline shift due to heating by the absorbed light implies transient ion binding by the pm-TX complex rather than a thermal effect. Experiments to identify which non-proton ions are responsible are in progress.

† This work is supported by NIH grant GM 32955-01.

[1] Marinetti and Mauzerall, PNAS (USA), 80 178-180 (1983).

M-Pos79 THE ROLE OF CATIONS ON THE PHOTOCHEMISTRY AND REGENERATION OF BACTERIORHODOPSIN. C.-H. Chang, J.-G. Chen, R. Govindjee and T. Ebrey. University of Illinois, Department of Physiology and Biophysics, 524 Burrill Hall, 407 S. Goodwin Avenue, Urbana, IL 61801 U.S.A.
We have studied the role of cations on the photocycle and proton pumping function of bacteriorhodopsin (BR) by substituting Ca^{++} and Mg^{++} with La^{+++}, K^{+} or Na^{+}. Flash-photolysis measurements at pH 6.7 show that the decay kinetics of the photointermediates M and O are slowed down, and the amplitude of the O intermediate is reduced by La^{+++} substitution in purple membrane sheets, or PM incorporated into egg phosphatidylcholine vesicles or PM incorporated in polyacrylamide gels (7.5%). At higher pH(8.0) the decay time of M intermediate increased by approximately 10^3. There is little difference in the M decay between the native PM and K^{+} or Na^{+} substituted PM. However the amplitude of the O intermediate in the Na^{+} or K-PM is reduced. The rate of proton uptake by La^{+++}-BR is significantly slower compared to native BR. The La^{+++} effect on both proton pumping increases at higher pH. The rate of proton uptake is unaffected by Na^{+} or K^{+} substitution. The results will be discussed in relation to the effect of pH on the binding affinity of the cations. When purple membrane is bleached and washed with distilled water, elemental analysis shows that it no longer binds Ca^{++} and Mg^{++}. Well-washed bleached membranes were used to regenerate pigments using several retinal isomers. We find that 13-cis retinal forms a pigment readily but that all-trans retinal forms very little pigment. 9-cis retinal did not form pigment; however 11-cis retinal formed a pigment with max = 550 nm. The rate of pigment regeneration and the photocycle of the 11-cis pigment is very slow compared with bacteriorhodopsin.

M-Pos80 **A PHOTOCHEMICAL STUDY OF THE BACTERIORHODOPSIN IN THE BROWN HOLO-MEMBRANE.** **S.C. Hartsel, B.J. Kolodziej and J.Y. Cassim, Department of Microbiology, The Ohio State University, Columbus, Ohio 43210**

A comparative study of the conformational stability of the bacteriorhodopsins of the purple membrane and its precursor, brown holo-membrane has been undertaken to assess the relationship between membrane supramolecular structure and protein photoresponse. Although x-ray diffraction has indicated a similarity in the lattice parameters of the two membrane forms, brown holo-membrane exibits strikingly different photoresponses under various environmental conditions. At low temperature (-70°C), bR568 of brown holo-membrane is in equilibrium with a 460 nm absorbing species, bR460, which is pH, as well as temperature, dependent. No detectable bR460 species is present in the purple membrane under identical conditions. Irradiation of the bR460 species with 460 nm light does not produce either the M412 or the bR568 species, but instead results in a reversible 365 nm absorbing species. On the other hand, similar irradiation at 570 nm converts the remaining bR568 species to the typical M412 species. Addition of NaCl to brown holo-membrane suspensions enhances the stability of the bR460 species at ambient temperature. Circular dichroic analysis indicates the absence of excitonic coupling of the chromophoric retinals in bR460 species, suggesting a randomization of the chromophoric positions. Furthermore, the bR460 chromophoric retinals may be more accessible to the external medium as considerable dark bleaching of the brown holo-membrane with hydroxylamine is possible. These results suggest that a definite relationship exists between the membrane supramolecular structure and the photoresponse of the membrane bacteriorhodopsins.

M-Pos81 SLOW PHOTOCYCLES IN BACTERIORHODOPSIN IMMOBILIZED IN NaCl PELLETS.
Vitaly Vodyanoy, Bela Karvaly and Janos K. Lanyi, Department of Physiology and Biophysics, University of California, Irvine, CA 92717 and Bioelectromagnetics Laboratory, Michigan State University, East Lansing, MI 48824

When a purple membrane suspension containing NaCl is freeze-dried under controlled conditions, the bacteriorhodopsin (BR) is not denatured and the dry BR-NaCl mixture can be compressed into translucent pellets. Light-adapted BR will dark-adapt in the pellets, but dark-adapted BR will not light-adapt. In these pellets both slow (several mins to hrs) and rapid (less than 100 msec) photoreactions are observed. The slow photolysis events originate from considerably blue-shifted parent species: one previously proposed by Lazarev and Terpugov (Biochim.Biophys.Acta 590, 324-338, 1980) at 506 nm for the light-adapted photocycle, and another at 480 nm for the dark-adapted photocycle. In contrast, the fraction of BR in the pellets whose spectrum is not shifted shows only rapid photoreactions characteristic of light and dark-adapted BR. The kinetics of the slow events suggest the existence of two distinct M intermediates, which decay via two routes: one directly (on a 1 min time-scale) and another through the O intermediate (on a 5 min time-scale). We attribute these phenomena to a slowed down all-trans photocycle. Dark-adapted pellets show, in addition to these changes, a separate and independent absorption change at 600 nm (which decays on a 1 hr time-scale), originating from a parent species which absorbs at 480 nm. When illumination is terminated the concentration of the 600 nm species continues to rise, suggesting that during the illumination this species is efficiently photoconverted back to its parent. We attribute these phenomena to a slowed down 13-cis photocycle.

M-Pos82 BACTERIORHODOPSIN PHOTOCYCLE: DISTRIBUTED KINETICS ANALYSIS OF FLASH PHOTOLYSIS ABSORBANCE DATA. A. H. Xie[1], J. F. Nagle[1], and R. H. Lozier[2]. [1]Department of Physics, Carnegie-Mellon University, Pittsburgh, PA 15213 and [2]CVRI, University of California, San Francisco, CA 94143.

Previous interpretations of flash photolysis data of bacteriorhodopsin in purple membrane have assumed ordinary first order kinetics for the basic kinetic steps. No kinetic model using this assumption has yet been found that can account for our previous data without making the unphysical assumption that the spectrum of O is strongly temperature dependent. We have performed a mathematical analysis of a model in which the L to M decay obeys distributed (Austin et al, Phys. Rev. Letts. 8, 403 (1974)), rather than ordinary, first order kinetics. This model corresponds to a physical model for which the L to M decay is subject to random Gaussian fluctuations which decay more slowly than the L state. Our previously developed procedure for analyzing extensive data taken at multiple wavelengths (Nagle et al, Biophys. J. 38, 161 (1982)), with the appropriate modifications to accommodate the new mathematics, is then employed to test the unidirectional unbranched model with distributed L to M kinetics. We find that the distributed kinetics (DK) model is slightly superior to previous models employing ordinary first kinetics. In particular, the temperature dependence of the O spectrum is slightly smaller, but there are still significantly large negative extinctions in the blue when the slowest rate constant corresponds to the M to O transition. New data taken under better controlled conditions is being analyzed and indicates some significant changes. In particular, using the same analysis there are no negative extinctions in the O spectrum.

M-Pos83 PHOTOCYCLE OF TYROSINE-64-NITRATED BACTERIORHODOPSIN. Richard H. Lozier and Peter Scherrer, CVRI and Dept. of Biochem. and Biophys., UCSF, San Francisco, CA 94143.

Bacteriorhodopsin can be nitrated with high specificity on the aromatic moiety of Tyrosine-64 (Scherrer and Stoeckenius, Biochemistry, in press). We have invéstigated the photocycle of this pigment. Absorbance changes induced by 10ns 500nm vertically polarized laser flashes were measured from .001 to 300 ms following the flash at 5, 20, and 35°C in a sample suspended in 10mM NaCl. Data were taken at fifteen measuring wavelengths from 380 to 680nm. At each wavelength the absorbance changes were measured with three different polarizations of the measuring beam re the laser beam polarization - parallel, perpendicular, and at the magic angle (54.7 degrees). The magic angle data for all 15 wavelengths were analyzed simultaneously with the multiexponential fitting program VARP. Convergent results were obtained using one to six terms at each temperature, but the improvement in the fit was small beyond the 4 term fit. The same was true when the (A(parallel)+2A(perpendicular))/3 data were analyzed, and the corresponding parameters up to the 4 term fit were comparable to those from the magic angle data. All but the fastest rate parameter (which was near the instrument response time) exhibited excellent Arrhenius behavior. Spectra for four intermediate states (corresponding to K, L, M, and O of the normal bacteriorhodopsin cycle) were calculated assuming an unidirectional-unbranched model. The spectra of the intermediates were independent of temperature within the experimental noise. A somewhat surprising finding is that the calculated absorption maximum of the O spectrum is not significantly red-shifted from the parent pigment. Rather, it is decreased in intensity and broadened. Invoking (temperature independent) branching from M to bR would red-shift the maximum for O.

M-Pos84 A NANOSECOND-DIODE-ARRAY-SPECTROMETER FOR FLASH PHOTOLYSIS. Josef Sedlmair and David C. Mauzerall, The Rockefeller University, 1230 York Avenue, New York, NY 10021

We have designed and built a Nanosecond-Diode-Array-Spectrometer for kinetic absorbance studies in the visible and near ir that acquires a 1000-point spectrum 600 nm wide in 17 ms. Employing fluorescent dyes pumped by a nitrogen laser as a novel light source, it allows an optimal time resolution of 10 ns and a spectral resolution of 2.4 nm. Noise is photon-limited and typically 0.003 A in a single scan at a sample absorbance of 0.6 A. Varying the dye mixture allows tailoring the emission spectrum to match the absorption of the observed species, resulting in nearly constant S/N ratio across the spectrum. The S/N ratio is independent of the delay between pumping and probing flashes; no artefacts from the lasers are seen at any time.

Some sample studies show the range and versatility of this spectrometer:
We studied electron transfer in a porphyrin with a quinone moiety rigidly held 10 A above the macrocycle plane (Lindsey et al., J. Am. Chem. Soc. (1983) 105, 6528-9). A very broad absorption band from 405-540 nm, attributed to the porphyrin cation, grows in within 400 ns and decays with a half-life of 1.4 us. Blocking the electron transfer by reducing the quinone leaves only a triplet spectrum which decays similarly to ZnTPP within hundreds of us.

Our results on bacteriorhodopsin confirm the previously reported transient spectra (Lozier et al., Biophys. J. (1975) 15, 955-62) with a large red shift in the first 100 ns, followed by an even larger blue shift after 500 us which lasts about 5 ms. Changing the pH from 6 to 8 does not change the spectra substantially.

This research was supported by The Rockefeller University and the Ferry Fund.

M-Pos85 SUB-MILLISECOND INFRARED KINETICS OF BACTERIORHODOPSIN USING AN FTIR SPECTROMETER. Gavin Dollinger, Laura Eisenstein, Physics Department, University of Illinois, Urbana, IL 61801; Allan A. Croteau, James O. Alben, Department of Physiological Chemistry, Ohio State University, Columbus, OH 43210.

We are beginning to acquire kinetic IR data on bacteriorhodopsin (bR) with a spinning sample designed to be placed as an accessory in an FTIR spectrometer. The device consists of two Irtran 2 plates mounted on the shaft of a sine-cosine wave controlled stepper motor with a maximum frequency of 22 Hz. A film of bR is dried along the circumference of one Irtran plate, hydrated and sealed with the other. While spinning, the film is illuminated at one point with 2W of continuous 514.5 nm light from an Argon Ion laser and monitored in another spot with the IR beam of the spectrometer. The IR beam is focussed with a 6x beam condenser. The angular separation of the two beams can be converted into a time difference. Different times can be monitored by changing this angular separation and/or the rotational period. The maximum resolution is limited to 50 μs by the diameters of the Irtran 2 plates (20 cm) and the IR and visible light beams (≈ .5 mm) and the rotational period of the plates. The rotational period is limited to approximately five times the half-life of the bR photocycle ($t_{1/2}$ ≈ 10 ms). The device takes full advantage of the FTIR spectrometer's ability to acquire all wavelengths in the IR region (4000-800 cm^{-1}) simultaneously. This technique can also be used to study bR solutions and other photoreactive systems such as carboxymyoglobin. Preliminary data on bR will be presented. This work was supported in part by grants HEW PHS GM32455 and HEW PHS RR01739.

M-Pos86 VISIBLE AND INFRARED STUDIES OF THE KINETICS OF THE M-TO-BR TRANSITION AT LOW TEMPERATURE (210K). Agnes Janoshazi, Laura Eisenstein, Joseph Vittitow (Intr. by Enrico Gratton), Department of Physics, University of Illinois, 1110 West Green Street, Urbana, IL 61801.

The decay of the M intermediate of well-hydrated films of bacteriorhodopsin (bR) was studied at low temperature (210K) in the infrared and visible regions. Using Fourier-transform infrared difference spectroscopy (with 1s time resolution) we observed different rates for different modes (e.g. the Schiff base and the C = C stretch) of M and bR. Each decay was multi-exponential. In the visible the rise of the light-adapted bR peak at 567 nm was also multi-exponential. We also measured the IR kinetics of bR with its carboxyl tail removed by papain digestion. The M kinetics were significantly slowed by removal of the carboxyl terminus. This work was supported in part by HEW PHS GM32455.

M-Pos87 THE INVOLVEMENT OF TRYPTOPHAN AND TYROSINE IN THE PHOTOREACTIONS OF BACTERIORHODOPSIN. Gavin Dollinger, Laura Eisenstein, Mi Kyung Hong, Shuo-Liang Lin and Joseph Vittitow, Physics Department, University of Illinois, 1110 W. Green St., Urbana, IL 61801.

Here we report some results of our FTIR work on bacteriorhodopsin (bR) from Halobacterium halobium grown on standard medium and on media containing L-[$\delta_1,\varepsilon_3,\zeta_2,\zeta_3,\eta_2$-$^2H_5$] tryptophan or L-[$\varepsilon_1,\varepsilon_2$-$^2H_2$] tyrosine. Preliminary results were reported earlier (Bagley et al., Biophys. J. 45, 211a (1984)). A comparison of the difference spectra of native bR and those of $^2H_5$TRP bR reveals that no line in the spectra of the dark adapted (bR^{DA}) to light adapted (bR^{LA}) or the bR^{LA} to K transitions can be assigned to tryptophan. Solution spectra of TYR and $^2H_2$TYR in both H_2O and ^2H_2O at high and low pH (pD) have been acquired with an attenuated total reflectance cell. These solution spectra and the bR^{DA}/bR^{LA} difference spectra of native bR and $^2H_2$TYR bR show that during the bR^{DA} to bR^{LA} transition a tyrosine becomes deprotonated. The results for the bR^{LA} to K transition are more complicated and somewhat more speculative. A tyrosine that is ionized in the bR^{LA} state is protonated in K and another tyrosine which is protonated in the bR^{LA} state either deprotonates or undergoes a change in environment during this transition. To determine which tyrosines are involved in these transitions, we studied the IR difference spectra of bR in which either TYR26 or TYR64 was specifically nitrated at one of the ε positions. These results suggest that TYR26 is not involved but the data for TYR64 are not as conclusive. The deuterated tyrosine and tryptophan bR were generously supplied by E. Oldfield and the nitrated samples were generously provided by R. Bogomolni and P. Scherrer. This work was supported in part by HEW PHS GM32455.

M-Pos88 DARK NOISE OF ISOLATED RETINAL RODS IN LOW EXTERNAL CALCIUM: EFFECTS OF CESIUM AND TEA. Gary G. Matthews, Dept. of Neurobiology & Behavior, SUNY, Stony Brook, NY 11794

In low-calcium saline, the mean and variance of the dark current increase transiently after bright-flash responses (*Biophys. J., 45,* 337a). I now report that perfusion of the inner segment with saline containing cesium (Cs) or TEA blocks this variance increase. TEA also has large effect on the mean level, while Cs does not. The effect of Cs and TEA on variance may be due to blockade of voltage-sensitive channels that respond to voltage changes during the increased dark current. The effect of TEA on mean dark current suggests that TEA also affects the inner segment (outward) path for the dark current, whereas Cs apparently does not. The results suggest that the variance increase associated with increased dark current is due to voltage fluctuations set up by a current source other than the light-sensitive current. If voltage fluctuations drive the noise in outer segment (OS) membrane current, the low-frequency response of the OS current to voltage fluctuations might be limited by OS capacitance under conditions where OS conductance is low. For example, in normal calcium, dark current noise arising from voltage fluctuations might be low-pass filtered by the input time-constant and high-pass filtered by OS capacitance. This result was observed in experiments in which a suction electrode was placed on the inner segment to pass current, while OS current was recorded via a second suction electrode: the spectrum of the resulting noise rolled off at both high and low frequencies. These results indicate that voltage fluctuations can be a source of current fluctuations in the OS and specify factors that are important in shaping such noise events. Results of patch-recordings from the OS in low-calcium saline will also be discussed.

Supported by the Alfred P. Sloan Foundation and by NIH Grant EY03821.

M-Pos89 PHOTOTRANSDUCTION OCCURS IN THE ABSENCE OF TRANSMEMBRANE CALCIUM GRADIENTS IN ISOLATED FROG ROD PHOTORECEPTORS. G.D. Nicol, U.B. Kaupp, and M.D. Bownds, Laboratory of Molecular Biology, University of Wisconsin, Madison, Wisconsin 53706.

We have examined the hypothesis that light-induced changes in internal Ca^{++} concentration cause suppression of a current that flows in the dark. Using isolated rod outer segments still attached to their inner segments (OS-IS) and suspended in 10^{-8}M Ca^{++} Ringer's, we have found that conditions expected to equilibrate Ca^{++} gradients [addition of the Ca^{++} ionophore A23187 (10 μM)] do not affect the dark current or the photoresponse. Complete suppression of the dark current and the photoresponse is observed when A23187 is added to OS-IS in 1 mM Ringer's; the suppression is reversed if external Ca^{++} is lowered to 10^{-8}M by EGTA addition. Effectiveness of the ionophore was shown by suspending purified OS-IS in 10^{-6}M Ca^{++}, K^{+}-Ringer's (to prevent loss of internal Ca^{++} by Na/Ca exchange); addition of 5 μM A23187 caused the loss of >95% of Ca^{++} (1 Ca^{++}/rhodopsin, measured by arsenazo III spectroscopy).

The experiments demonstrate that photoresponses can be obtained in the absence of Ca^{++} gradients across the disk and plasma membranes, making it unlikely that changes in internal Ca^{++} are required for transduction in rod cells. Further, after suppression of the dark current and photoresponse by A23187 in 1 mM Ca^{++}, both can be restored by addition of 50 μM IBMX. This suggests that conditions known to elevate internal cyclic GMP can restore light sensitivity.

M-Pos90 INVOLVEMENT OF cGMP IN PHOTOTRANSDUCTION BY ISOLATED FROG RODS IN THE ABSENCE OF TRANSMEMBRANE CALCIUM GRADIENTS. R.H. Cote, S.A. Burke, G.D. Nicol and M.D. Bownds, Laboratory of Molecular Biology, University of Wisconsin, Madison, Wisconsin 53706.

Both Ca^{2+} and cGMP are thought to be involved in controlling the cation permeability of rod photoreceptors. Using a suspension of isolated frog rod outer segments still attached to the ellipsoid portion of the inner segment, we have altered the extracellular Ca^{2+} concentration and compared changes in total cGMP concentration with changes in membrane current. Consistent with the membrane voltage data of Woodruff and Fain (J. Gen. Physiol. 80:537, 1982), we find that as the Ca^{2+} concentration is lowered from 1 mM to 1 μM, no change in cGMP levels is observed, even though increases in the dark current are seen. When the Ca^{2+} concentration is lowered from 1 mM to 10 nM, there is a 1 min lag prior to the cGMP increase; in contrast, this lowering of external Ca^{2+} increases the dark current within seconds. In the dark, Ca^{2+} appears to influence the dark current independently of cGMP.

Intradiscal and cytoplasmic Ca^{2+} can be equilibrated with external Ca^{2+} by addition of the ionophore A23187. In a 10 nM Ca^{2+} medium containing 10 μM A23187, the dark current is still suppressed by light, and 2-fold decreases in cGMP concentration are measured. The subsecond kinetics of the cGMP decrease under this condition of "Ca^{2+} clamp" are as rapid as the response seen in the absence of ionophore. Under both conditions, the kinetics of the cGMP decrease and the kinetics of the photoresponse are comparable. Thus, light-induced suppression of the dark current may be initiated by changes in cGMP under conditions where the Ca^{2+} concentration does not vary.

M-Pos91 CYTOPLASMIC pH IN ROD OUTER SEGMENTS AND HIGH-ENERGY PHOSPHATE METABOLISM DURING PHOTOTRANSDUCTION. *S. Yoshikami and W.A. Hagins*, Lab. of Chemical Physics, NIADDK, NIH, Bethesda, MD 20205.

Rod outer segments (o.s.) contain light-coupled GTPase, cyclases, phosphodiesterases and other enzymes that transfer ~P groups among high-energy intermediates or produce inorganic phosphate (P_i). In isolated intact o.s., light bleaching 1% of rhodopsin causes enzymatic loss of millimolar amounts of CrP and GTP with appearance of equivalent P_i within 20 s. Since net transfer of ~P from CrP to P_i adds base to the cytoplasm, does o.s. cytoplasm show pH changes during the light response?

~1 mM 6-carboxyfluorescein (6-CF) was introduced into live rods of isolated frog retinas by incubation with 6-CF diacetate. 100 μm thick retinal slices were mounted in a flow chamber on the stage of a fluorescence microscope. The long axes of the o.s. were normal to the light path. 6-CF was seen only in the receptor layer. Using the pH-sensitive fluorescence efficiency of the dye (pK_a 6.25, 480 nm excitation, 520 nm emission), 40 μm long zones of outer segments were monitored by fluorescence microscopy. o.s. cytoplasm has a pH of about 6.90 and a buffering power of ~1mM base per pH unit as determined by NH_4Cl perfusion. During stimulation of the outer segments by exciting light that caused $10^4 - 10^6$ photoisomerizations sec^{-1} per o.s., no pH changes exceeding .002 unit were seen between 0.1 and 20 s. after onset of illumination. The net production or consumption of protons during such strong light stimuli was thus < 2μM in o.s. cytoplasm. Since transfer of ~P from a phosphagen such as CrP to P_i consumes 0.5 mol of protons per mol reacting at pH 7 and conversion of NTP to NMP by the cyclase-phosphodiesterase pathway yields 1 mol of protons/mol reacting, the lack of pH changes is surprising. Either (1) the nucleotide hydrolysis seen in isolated frog o.s. [Robinson &Hagins, *Nature*,280, 398, (1979)] does not occur in live rods, or (2) the ~P transfer and hydrolysis is in exact proton balance, or (3) ~P catabolism is exactly balanced by anærobic glycolysis within the o.s. cytoplasm during phototransduction.

M-Pos92 OPTIMIZED PROCEDURE FOR REASSOCIATION OF cGMP PHOSPHODIESTERASE ACTIVITY WITH ROD DISK MEMBRANES. James L. Miller[1], Edward A. Dratz[2], Burton J. Litman[1], (1) Department of Biochemistry, Univ. of Va. School of Medicine, Charlottesville, VA 22908; (2) Chemistry Board, University of Calif., Santa Cruz, CA 95064. Sponsored by Jay Fox[1].

The GTP-binding protein (GBP) and cGMP phosphodiesterase (PDE) found in vertebrate rod outer segments are peripherally bound to the disc membrane in isotonic buffers, but may be eluted from the membrane by either hypotonic or hypertonic conditions. Investigations which have exploited this reversible binding to the disc membrane, usually produce reassociated preparations with substantially lower sensitivity to light, a reduced V_{max} of the PDE, and slower activation kinetics when compared to isolated ROS. We have compared the PDE activity which can be recovered by each of several different reassociation protocols and may now reproducibly recover virtually all the light sensitivity and V_{max} of the PDE in reassociated preparations. The most common practice which involves mixing the protein extract and membranes immediately prior to the assay recovers only 20-30% of the original PDE activity and the early activation kinetics are considerably slower (at low rhodopsin bleaches). Incubating this mixture for 3 hours under isotonic conditions can double the recoverable PDE activity. The optimized reassociation protocol involves mixing both membranes and extrinsic proteins, under hypotonic conditions, such that the [rho] $\geq$ 1-2 mg/ml, and dialyzing this mixture against isotonic buffer. The high [rho] during reassociation greatly enhances the recovery of both light sensitivity and the early kinetics of PDE activation. In summary, the optimized reassociated preparation retains the stoichiometry of rhodopsin:GBP:PDE, light sensitivity, V_{max} of the PDE and early activation kinetics found in isolated ROS.

M-Pos93 EVIDENCE THAT cGMP HYDROLYSIS IS CAUSAL IN PHOTOTRANSDUCTION. R. Heyman, A. Ames III, T. Walseth, M. Barad, R. Graeff & N. Goldberg (Intr. by H. Lee) Dept. of Pharmacology, Univ. of Minnesota, Minneapolis 55455 and Massachusetts General Hospital, Boston 02114

We recently reported that light induces incremental increases in cGMP metabolic flux, independent of changes in cGMP levels; and we proposed that cGMP hydrolysis is a biochemical event of functional importance and integral to phototransduction (JBC 258:9213,1983). This was uncovered by monitoring cGMP flux in the isolated rabbit retina as a function of phosphodiesterase (PDE)-promoted incorporation of ^{18}O from [^{18}O]water into endogenous guanine nucleotide α-phosphoryls. We have extended these studies to examine the relationship between cGMP metabolic flux and photoreceptor dark current measured by the aspartate-isolated mass receptor potential and to determine the stoichiometry of the response. Increasing frequency of flashing light accelerates cGMP flux in correspondence with increases in the voltage-time integral of the electrical response without changes in retinal cGMP concentration. The electrical response saturates at a lower frequency of flashing light than the biochemical response. With increasing intensities of continuous photic stimulation the inhibition of dark current closely parallels increases in cGMP flux independent of changes in cGMP levels. At the lowest light intensity tested, 4300 molecules of cGMP are hydrolyzed per photon absorbed. IBMX, an inhibitor of PDE, increases dark current coincident with diminished cGMP metabolic flux. These results demonstrate that the dark current and cGMP flux are closely correlated whether phototransduction is activated or inhibited and that the biochemical event is temporally resolved as rapidly and takes place over the same range of stimulus intensities as the electrical response. These observations support the hypothesis that light-evoked acceleration of cGMP hydrolysis independent of change in cGMP steady state levels plays a causal role in phototransduction. NIH EY04877,GM28818,NS10828.

M-Pos94 RHODOPSIN - G-PROTEIN INTERACTIONS MONITORED BY RESONANCE ENERGY TRANSFER. Hamutal Borochov-Neori, Dept. Physics, University of California San Diego, La Jolla, CA 92093.

The interactions between photoexcited rhodopsin (*Rho) and the photoreceptor G-protein (G) appear to be crucial in visual transduction. We investigated these interactions by measuring resonance energy transfer (RET) between fluorescently labeled *Rho and G, in an extension of our earlier study on Rho-Rho interactions within the membrane(1). Rho and G were labeled with several fluorescence sulfhydryl reagents. The activity of both labeled proteins was preserved. The spectral properties of the conjugates (e.g. quantum yield) were sensitive to the formation of the *Rho·G complex. To measure RET, membranes containing *Rho labeled with the energy donor pyrene (P) were supplemented with G labeled with the energy acceptor diethylaminophenylmethylcoumarin (C). Fig.1 shows the fluorescence excitation spectrum of purified P-*Rho reconstituted in phospholipid vesicles supplemented with C-G. The emission was measured at 465nm, the maximum for C. RET between P-*Rho and C-G was evident by the increase in emission intensity measured with excitation at 313,327 and 342nm, absorption maxima of P. RET disappeared upon addition of GppNHp, known to dissociate *Rho·G. Similar results were obtained with P-*Rho in stripped disc membranes and with bimane labeled G. Thus, RET between these fluorescent protein derivatives provides a sensitive tool to investigate Rho-G interactions. The measurements will be extended to derive structural and kinetic parameters of the system. Supp. NIH EY04596 (H. B-N.) and EY02084 (Dr. M. Montal). (1) Borochov-Neori et al (1983) Biochemistry 22, 206.

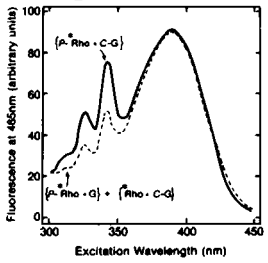

Fig.1: Excitation spectra of P-*Rho-lipid vesicles + C-G, (—) measured (--) predicted. Protein-0.15mg/ml, each. 5mM Tris, 0.5mM $MgCl_2$, 2mM DTT, BSA 1mg/ml, pH7.5.

M-Pos95 cGMP STIMULATED CALCIUM RELEASE FROM PURIFIED BOVINE RETINAL DISCS. K.L. Puckett, A.J. Rawji, and S.M. Goldin. Dept. of Pharmacology, Harvard Medical School, Boston, MA 02115.

Parallel lines of evidence have suggested that light initiates changes in both cGMP and Ca metabolism in rod outer segments (ROS). Both Ca and cGMP have been hypothesized to play a role in phototransduction (rod cell hyperpolarization). We report observations suggesting that cGMP may regulate Ca fluxes in a purified ROS disc preparation. Discs were isolated from ROS by hypoosmotic shock, flotation on 5% Ficoll, and separation into two distinct subpopulations on a linear 5-20% Ficoll density gradient. The major subpopulation, the "R-band," had an ATP-dependent Ca uptake activity as previously described (Puckett et al., Biochem. (1985) in press).

Discs were preloaded with ^{45}Ca (in the presence versus the absence of ATP); external Ca was then removed via elution through cation exchange resin. The preloaded discs were retained on glass fiber filters, and then constantly perfused with buffer and/or test solutions. The perfusate was collected at 10 sec intervals to determine ^{45}Ca release from the discs. cGMP, at physiological levels (50-100 μM), caused release of ~20% of the total Ca associated with the discs (maximal rate within 10 sec). Exponential decay of the ^{45}Ca release event immediately followed the initial peak of release ($t_{1/e} \approx 30$ sec). In the absence of cGMP, initial ^{45}Ca release was only 12-15% of that observed in the presence of cGMP. The cGMP-stimulated Ca release occurred only when the discs were actively loaded (in the presence of ATP); there was no effect of cGMP on discs passively loaded with ^{45}Ca (in the absence of ATP). Neither cAMP nor GTP showed any effect on ^{45}Ca release.

Of interest is the molecular mechanism responsible for cGMP regulation of Ca release, the possible role of this mechanism in controlling phototransduction, and the identity of the transport system responsible for this Ca release.

M-Pos96 ROLE OF CHROMOPHORE CHARGE IN RHODOPSIN MEDIATED ACTIVATION OF GTPASE. R.D. Calhoon and R.R. Rando, Dept. of Pharmacology, Harvard Medical School, Boston, MA 02115.

The chromophore of bovine rhodopsin was modified in order to study the effect of chromophore isomer and charge on the rhodopsin mediated activation of GTPase, the only known biochemical reaction directly affected by rhodopsin.

All-trans-retinal derivatives were introduced to see if the all-trans chromophore triggered GTPase activation. All-trans isomers do not result in activation of GTPase when added as all-trans retinal, all-trans retinal oxime, or retinoyl fluoride, which covalently binds to the active site lysine of opsin via a peptide bond to form all-trans retinoyl opsin. Thus, deformation of rhodopsin by the trans isomer is not sufficient to trigger GTPase activation.

The peptide bond of 9-cis-retinoyl opsin lacks the charge of the protonated Schiff base, and hence allows separation of the effect of isomerization from that of charge movement in the functioning of rhodopsin. 9-cis retinoyl opsin photoisomerizes to its all-trans congener, but does not activate GTPase, consistent with the notion that a protonated Schiff base is critical for the function of rhodopsin and that photoisomerization is not is and of itself.

The above experiments are consistent with the idea that charge movement is important in the functioning of rhodopsin but do not tell how the charge might move. One set of proposed mechanisms involves photochemically induced migration of the positive charge from the Schiff base to the β-ionone ring. If this is the case, then a pigment formed from 7,8-dihydroretinal should not activate the GTPase. 7,8-dihydro-11-cis and 9-cis-retinals form bleachable pigments with opsin which activate GTPase upon photolysis. This appears to eliminate any mechanism involving a photochemically mediated charge transfer to the β-ionone ring.

M-Pos97 CAN MECHANICAL COUPLING ACCOUNT FOR AMPLIFICATION AND ADAPTATION IN VISUAL TRANSDUCTION ?
Lucian V. Del Priore* and Aaron Lewis, Dept. of Applied Physics, Cornell University, Ithaca, NY 14853 (* Current address: Wilmer Eye Institute, Johns Hopkins Hospital, Balt., MD 21209)

Chemical transmitter hypotheses were introduced at a time when rod outer segment (ROS) discs were felt to be physically isolated from the plasma membrane, but recent electron micrographs demonstrate numerous elastic filaments interconnecting adjacent discs to one another and the plasma membrane. In view of this observation, we propose a mechanical coupling model of visual transduction that incorporates the following known facts on ROS physiology: (1) light extrudes Ca from ROS; (2) rapid light-induced G-protein binding to metarhodopsin II causes ROS shrinkage; (3) 4×10^5 cyclic GMP (cG) sec^{-1} are hydrolyzed after single photon absorption in vitro; (4) cG hydrolysis decreases Ca binding to unknown intracellular binding sites; and (5) increasing the surface area of an excitable membrane can increase the membrane Na current.

We suggest that the observed light-induced ROS shrinkage caused by G-protein binding to meta II decreases the surface area of the plasma membrane via the interconnecting filaments, and results in membrane hyperpolarization. Sensitivity control can be accounted for if background light decreases intracellular mechanical coupling, and Ca and cG may be involved in this regulation. We suggest that Ca is bound to the 1.6×10^7 filaments/toad ROS in the dark, and that there is extensive mechanical coupling with Ca bound. Light-induced cG hydrolysis decreases Ca binding and causes the observed extrusion of 3×10^7 Ca/toad ROS (i.e., ≈ 2 Ca/filament). Ca release may change the filament conformation and thereby decrease mechanical coupling and ROS sensitivity. Interestingly, this model predicts outer segment movement on the time scale of visual transduction, and these movements have recently been demonstrated by other workers in the invertebrate squid retina.

M-Pos98 VISUALIZATION OF ACTIN IN RETINAL ROD PHOTORECEPTORS BY LIGHT MICROSCOPY.
Lucian V. Del Priore*, William W. Carley**, Aaron Lewis, and Watt W. Webb, Dept. of Applied Physics, Cornell University, Ithaca, NY 14853 (*Current address: Wilmer Eye Institute, Johns Hopkins Hospital, Balt. MD 21209, ** Yale University School of Medicine, New Haven, CT 06510)

Actin has been visualized by light microscopy in retinal rod photoreceptors by utilizing a fluorescently-labeled acidic derivative of phalloidine, a potent phallotoxin that specifically binds to and stabilizes F-actin. We have confirmed the presence of filaments of F-actin extending from the calyceal processes surrounding the base of outer segments to the supranuclear region of rod cells in Bufo marinus. Our techniques provide a unique view of the three-dimensional organization of these intracellular filaments that have not previously been visualized by light microscopy. Actin has also been localized at the junction of the inner and outer segment in a band oriented perpendicular to the long axis of the rod cell, and in a continuous ring in the supranuclear region of toad receptors. The pattern of staining as a function of bleaching will be discussed and the composition of the numerous filaments that are known to connect the periphery of adjacent disc membranes to one another and to the plasma membrane will be considered.

M-Pos99 ^{2}H-NMR LINESHAPE AND SPIN-LATTICE RELAXATION STUDIES OF 3α-^{2}H-CHOLESTEROL/CEREBROSIDE BILAYER MEMBRANES.

M.J. Ruocco, D.J. Siminovitch, E.T. Olejniczak and R.G. Griffin. Francis Bitter National Magnet Laboratory, Massachusetts Institute of Technology, Cambridge, MA 02139.

^{2}H-NMR spectra of 3α-^{2}H-Cholesterol (CHOL)/Cerebroside (NPGS) bilayer (1:1; mol ratio) dispersions at $T \leq 53°C$ contain rigid lattice and motionally narrowed components. ^{2}H-spectra of 3α-^{2}H-CHOL monohydrate crystalline powder and X-ray diffraction studies, which demonstrate separate CHOL and NPGS lamellar phases coexist,[1] are used to assign the rigid component ($\Delta\nu_Q$ = 116 KHz) to the lamellar CHOL monohydrate crystal phase. The motionally narrowed ^{2}H-spectral component ($\Delta\nu_Q$ = 46.8 KHz) corresponds to residual CHOL in the cerebroside bilayers. As the temperature is increased to 66°C, all of the CHOL is incorporated into the cerebroside bilayers resulting in a single, motionally averaged axially symmetric lineshape ($\Delta\nu_Q$ = 46.8 KHz). The rigid lattice spectrum reappears upon cooling below T < 53°C as CHOL crystallizes out of the cerebroside bilayers.

Spin-lattice relaxation studies of 3α-^{2}H-CHOL/NPGS bilayers at 69°C yield partially relaxed lineshapes which exhibit T_1 relaxation anisotropy across the powder pattern. Experimental spectra can be simulated using a molecular long axis jump model with the C(3)-^{2}H bond at 73.5° with respect to the motional axis(director). Analysis of the spin-lattice relaxation times of the perpendicular (90°) and parallel (0°) edges $\left(T_1(90°)/T_1(0°) \simeq 2\right)$ suggests that CHOL executes large angle jumps rather than small angle jumps.

1.)Ruocco, M.J., E. Oldfield and G.G. Shipley (1983) Biophys. J. 41:117a.

M-Pos100 NEUTRON DIFFRACTION ON MATRIX PORIN FROM THE OUTER MEMBRANE OF ESCHERICHIA COLI.

Maja Mischel[1], Manfred Hentschel[1], Jürg P. Rosenbusch[2] and Georg Büldt[1]. 1. Dept. of Physics/Biophysics, Freie Universität Berlin, Arnimallee 14, D-1000 Berlin 33, FRG. 2. Dept. of Microbiology, Biozentrum, Universität Basel, CH-4056 Basel, Switzerland.

It is known from black lipid membrane experiments that matrix porin from the outer membrane of Escherichia coli forms a large channel of about 10 Å diameter which can be opened and closed dependent on voltage (H. Schindler, J.P. Rosenbusch, Proc. Natl. Acad. Sci. USA 75, 3751, 1978). Transmission electron microscopy on negatively stained two dimensional porin lattices shows a trimer in the elementary cell. The experiments suggest that in each monomer the channel starts separately on one side of the membrane and the three channels in the trimer combine to form one pore on the opposite side (D.L. Dorset, A. Engel, A. Massalski, J.P. Rosenbusch. Biophys. J. 45, 128, 1984). The aim of our neutron diffraction experiments was to test this model by H_2O/D_2O exchange experiments. Matrix porin was reconstituted into vesicles of dimeristoyllecithin with a phospholipid-to-protein weight ratio of about 0.7. The vesicles were ultracentrifuged in order to form flat pellets. Neutron experiments on the diffractometer D16 at the Institut Laue Langevin, Grenoble, gave diffraction rings up to 8 Å resolution. Several sets of data were collected from one large pellet with different water content in the membrane and variing H_2O/D_2O ratio. The data were analysed in three different ways: (i) Fourier difference density maps were calculated from the moduli of structure factors extracted from these data together with phases from electron diffraction experiments on matrix porin. (ii) The distance of the channels in porin trimers were estimated from radial autocorrelation functions calculated from the intensities using no phase information. (iii) Model calculations.

M-Pos101 SOURCE OF INCREASED LIPID AND PROTEIN IN HEATED CELLS.

E.D. Werts, J.J. Gipp and M.B. Yatvin, Department of Human Oncology, University of Wisconsin, Madison, WI 53792

We have previously shown that changes in cellular membrane lipids influence thermal sensitivity. In this study, changes in membrane composition of P-388 mouse leukemia cells were correlated with the development of thermal tolerance. Cells were cultured and heated in αMEM plus 10% fetal bovine serum and heated in a circulating water bath for 25 minutes at 44°C. Aliquots were transfered to a 37° incubator for an additional 24 hours of growth. Following Percoll gradient centrifugation of heated and control cells to remove debris, the remaining cells were greater than 95% viable by acridine orange/ethidium bromide fluorescent staining. Aliquots were disrupted and the membrane fractions prepared for analysis of cholesterol, phospholipid, and total protein content. Twenty-four hours after heating, the respective membrane concentrations of these components rose by 39%, 36%, and 69% compared to unheated controls. Despite the marked increases, heated and unheated cells were of equal diameter. To assess synthesis of new membrane components, heated cells were incubated for 24 hrs with ^{3}H-labelled glucose. Uptake fell to 29% of control values for the chloroform-methanol extracts of these membranes. To determine the source of the increased cholesterol, it was measured in whole cells and in isolated membranes of heated and control cells. Both total and membrane cholesterol levels were elevated in the heated cells. Incorporation of cholesterol from the serum containing medium is the most likely explanation to account for our observation. We are currently testing the hypothesis that the increases in protein, phospholipid and cholesterol observed in heated cells is derived from extracellular sources. (Supported by NIH grant CA-24872-05)

M-Pos102 ANALYSIS OF PROTEIN SECONDARY STRUCTURE AND HYDROGEN/DEUTERIUM EXCHANGE BY INFRARED SPECTROSCOPY FOR PHOTORECEPTOR MEMBRANE AND PURPLE MEMBRANE. N. W. Downer, T. J. Bruchman, and J. H. Hazzard. Dept. of Biochemistry, Univ. Of Arizona, Tucson, AZ 85721

Infrared spectroscopy on membranes in D_2O in the interval from 1800 to 1300 cm^{-1}(amide bands) was used to investigate the secondary structure and hydrogen exchange behavior of bacteriorhodopsin and bovine rhodopsin. The amide I band for bacteriorhodopsin could be fit with a minimum of three theoretical bands with peak positions at 1664, 1638, and 1625 cm^{-1}. Corresponding bands for rhodopsin were seen at 1657, 1639, and 1625 cm^{-1}. For both these membrane proteins, the amide I spectrum suggests that α-helix is the predominant form of secondary structure, but that a substantial amount of β-sheet conformation may be present as well. Whereas the amide I band for bacteriorhodopsin was invariant with pH in the range from 5 to 7, the bands at 1639 and 1625 cm^{-1} in the spectrum of photoreceptor membrane were replaced by a band at 1630 cm^{-1} when pH was lowered to 5. This result indicates significant pH-induced conformational rearrangement in the non-helical regions of membrane-bound rhodopsin.

The fraction of peptide groups in very slowly exchanging secondary structure was estimated from the absorbance ratio ($A_{amideII}/A_{amideI}$) that reached a plateau value after 10 hours of exchange at room temperature, pH 7. The value found for bacteriorhodopsin, 0.71, is in good agreement with expectation for all structural models proposed for this protein. The corresponding fraction for rhodopsin was estimated to be ≤ 0.60. Taken together, the results of this study suggest that the membrane domain of bovine rhodopsin is not likely to be structurally equivalent to the bacteriorhodopsin molecule.

M-Pos103 EVIDENCE FOR SPECIALIZED MACRO-DOMAINS IN PURIFIED GASTRIC MICROSOMES. Tushar K. Ray and J. Nandi, Department of Surgery, SUNY-Upstate Medical Center, Syracuse, New York 13210.

Gradient purified dog gastric microsomes are highly enriched in 5^1 - nucleotidase, K^+-pNPPase, H^+, K^+-ATPase and associated Mg^{+2}-ATPase activities. Absence of ouabain-sensative Na^+, K^+-ATPase, succinic dehydrogenase and cytochrome-C oxidase activities suggest negligible contamination from basolateral and mitochondrial membranes. Almost identical enzyme profiles were found in microsomes purified from enriched (80-90%) parietal cells from rabbit fundus demonstrating parietal origin of the microsomes. The question of whether the microsomal Mg^{+2}-ATPase is a part of the H^+, K^+-ATPase was sought. Treatment of the microsomes with 0.033% SDS at 21°c in a medium containing 2 mM ATP, 0.5 mM DTT, 250 mM sucrose and 50 mM Tris-glycine buffer (pH 8.5) followed by continuous sucrose density gradient (20-40%) centrifugation (150,000xg, 18h) resulted in distinct fractions; a light band (d=1.08), an intermediate zone ($d_{av.}$=1.10) and a heavy band (d=1.11). The light band contained all the Mg^{+2}-ATPase and 5^1-nucleotidase while the H^+, K^+-ATPase and K^+-pNPPase were localized exclusively in the heavy band. The intermediate zone had all of the enzyme activities. SDS-PAGE of the light and heavy bands were distinctly different showing nearly homogenous H^+, K^+-ATPase in the latter. Phospholipid and cholesterol content (mg/100 mg protein) were 163.8±5.4 and 52.0±1.4 for the light and 104.8±7.9 and 34.1±4.2 for the heavy fractions respectively. Distinct differences in the levels and fatty acid compositions of various individual phospholipids were noted. The data suggest that both the light and heavy membranes are derived from discrete and functionally specialized regions of the gastric microsomal surface.

M-Pos104 LANOSTEROL AND CHOLESTEROL HAVE DIFFERENT EFFECTS ON PHOSPHOLIPID ACYL CHAIN ORDERING. Philip L. Yeagle, Department of Biochemistry, SUNY/Buffalo, Buffalo, NY 14214.

D-2 nuclear magnetic resonance (NMR) spectra of dioleoylphosphatidylcholine labelled at positions 9 and 10 in the acyl chains of the phospholipid with deuterium were obtained as a function of the mole percent sterol in the membrane, where the sterol was either cholesterol or lanosterol. The spectra show in all cases three quadrupole splittings. One is due to the deuterium on position 10 of the sn-1 chain and another to the deuterium on position 10 of the sn-2 chain. The third deuterium quadrupole splitting arises from the deuterium at position 9 of both chains. Cholesterol, at increasing concentration, produces an increase in the quadrupole splitting from position 9, corresponding to an increase in order of that C-D bond segment arising from the inclusion of cholesterol in the membrane. Little effect is noted on the quadrupole splittings arising from position 10 of either chain. In contrast, lanosterol appears to have no effect on the quadrupole splittings from position 9. Lanosterol has no effects on the quadrupole splittings from position 10 of both chains, as in the case of cholesterol. These data therefore suggest little disorganization of the membrane structure due to the 14 methyl group of lanosterol. However, the 14 methyl group prevents lanosterol from increasing the motional order of the phospholipid hydrocarbon chains, a phenomenon characteristic of cholesterol.

M-Pos105 PREPARATION AND CHARACTERIZATION OF PHOSPHOLIPID ENRICHED SYNAPTIC PLASMA MEMBRANES. M. Myers and E. Freire, Dept. of Biochemistry, University of Tennessee, Knoxville, TN 37996-0840.

A detergent dialysis procedure has been developed to selectively enrich synaptic plasma membranes (SPM) with either DMPC or DPPC and purified gangliosides. This technique allows incorporation of exogenous lipid up to a mole fraction of 0.8 of the total phospholipid. Electron microscopy reveals that the selectively enriched synaptic membranes (SESM) are homogeneous vesicular structures with an average diameter of 0.7±0.1μm. Additional characterization of SESMs has been performed by sucrose density gradient centrifugation, high sensitivity DSC, fluorescence spectroscopy and enzymatic analysis. Unlike intact synaptic plasma membranes, SESMs exhibit a phase transition detectable by calorimetry and fluorescence spectroscopy. The thermotropic behavior of the SESM depends on the nature of the exogenous lipid, its mole fraction and its interactions with endogenous components of the synaptic membrane. DMPC enrichment results in a single, broad calorimetric peak centered at 24°C. This peak shows no evidence of any fine structure suggesting that DMPC is uniformly distributed within the synaptic membrane. Further enrichment with gangliosides result in an additional broadening of the calorimetric peak. Ganglioside Gd_{1a} SESMs show evidence of phase separation in the presence of enkephalins. By selecting appropriate exogenous lipid compositions, it is possible to prepare SESMs of different fluidity. At 37°C, the steady state DPH anisotropy of intact synaptic plasma membranes is ~0.23; enrichment of DMPC up to a 0.8 mole fraction lowers this value to 0.1. SESMs appear to be an ideal model system to study the effects of lipid composition and physical state on the properties of synaptic plasma membranes. (Supported by NIH Grant NS-20636.)

M-Pos106 MODELLING THE PAIR-CORELLATION FUNCTION IN GAP JUNCTION PELLETS ACCOUNTS FOR INTER--PARTICLE INTEREFERENCE EFFECTS IN THEIR X-RAY DIFFRACTION PATTERNS.--*Sunil Maulik, D.L.D. Caspar, W.C.Phillips, and +D.A. Goodenough, *Graduate Biophysics Program and Rosenstiel Basic Medical Sciences Research Center, Brandeis University, Waltham, MA.,02254. +Dept. of Anatomy, Harvard Medical School, Boston, MA.,02II5.

In order to obtain accurate electron density profiles from gap junction x-ray diffraction patterns, inter-particle intereference effects have been divided out by modelling the pair--correlation function that describes the small, disordered domains of membrane-pairs in pellets stacked by centrifugation. The refinement method used earlier by Makowski et al.(J. Cell Biol. 74:629-645(I977)) to obtain profiles and pair-correlation functions was found to be inapplicable in specimens where the stacking effects were prominent. Instead, a procedure that iteratively refines both the structure of the unit (described by the electron density profile) and the structure of the lattice (described by the pair-correlation function) has been devised based on simple starting models for both. With this model-building procedure and structure refinement method good fits were obtained to diffraction data from specimens analysed as a function of hydration where the intereference effects varied markedly. In addition, an estimate of the solvent (reference) density could also be obtained. The methodology of modelling the pair--correlation function can be applied to a variety of systems, including disordered one-dimensional biological arrays and liquid crystals.

M-Pos107 ANALYSIS OF SURFACE ELECTRICAL STRUCTURE OF PHOTORECEPTOR MEMBRANES.
Francis C. Tsui, Steven A. Sundberg and Wayne L. Hubbell, Jules Stein Eye Institute, and Department of Chemistry and Biochemistry, UCLA School of Medicine, CA 90024

A zero-order model for the structure of bovine rhodopsin in photoreceptor membranes base on hydrophobicity predictions indicates an interesting charge distribution in which the cytoplasmic surface of the protein bears a net charge of +4 and the intradiscal surface a net charge of -6 at neutral pH. To test this model as well as to study the spatial charge distribution on the protein at each surface and the asymmetry of charged phospholipids in the disc membrane we have carried out measurements of both cytoplasmic and intradiscal surface potentials as a function of ionic strength and pH in both native and reconstituted membranes using the approach recently discribed by Sundberg and Hubbell (1983). The reconstituted membranes used contain no charged phospholipids and have a roughly symmetric distribution of rhodopsin. A critical test to the model is the prediction of approximate zero net charge at the surface of the reconstituted membranes (isoelectric at neutral pH); this is found to be true. Analysis of the native membranes indicates a charge density of -5 to -6 per rhodopsin on the cytoplasmic surface and -6 per rhodopsin at the intradiscal surface. This result can be reconciled with the above if a major proportion of the charged lipids reside at the cytoplasmic surface. Internal consistency of measured potentials, charge densities derived from the extended Debye-Huckel theory and predictions of the model require that the charge not be extended far from the membrane surface. All these results and their biological significance will be discussed.

Sundberg, S.A. and Hubbell, W.L. (1983) Biophysical Journal vol. 41, 192A

M-Pos108 **PROPERTIES OF THE MEMBRANE-BOUND FUMARATE REDUCTASE OF ESCHERICHIA COLI.** C. Fronticelli, B. P. Rosen, A. Zachary, C. Orth, and E. Bucci. Dept. Biol. Chem., Univ. Maryland Sch. of Med., Baltimore, MD 21201.

Under conditions of anaerobic growth the membrane-bound fumarate reductase serves as the terminal component of the respiratory chain of E. coli. When cultures of E. coli HB101 bearing a recombinant plasmid (pFRD63) which encodes the fumarate reductase operon are grown under anaerobic conditions in glycerol-fumarate medium, the fumarate reductase activity is overexpressed. Everted membranes prepared by French press lysis were purified by isopycnic banding on sucrose density gradients. The fumarate reductase complex comprised between 70 and 90% of the inner membrane protein and is found to be associate with both phospholipid vesicles and tubules. Using these vesicles conformational and functional properties of the membrane bound enzyme were investigated. Analysis of circular dichroism (CD) spectra indicated that between pH 6.0 and 11.0 the secondary structure of the protein was 55% α helix and 33% β structure. At pH 12 there was an abrupt transformation to 100% β structure. This transition was partially reversible by titration to neutral pH. Titration of the sulfhydryl groups showed that the alkaline-induced conformation change is associated with burial of 4 of the 10 titratable sulfhydryl groups. The enzyme was active between pH 5.0 and 9.0 and was not sensitive to anions. Reaction with p-mercuribenzoate or mercuriphenylsulfonate induced a modification of the visible CD spectra without effect on the absorption spectra over the same span. Addition of an 8 molar excess of mercuriphenylsulphonate reduced the specific activity of the enzyme by 25%, but higher concentrations did not inhibit further. Fractions enriched in either the vesicles or tubules could be prepared by sucrose density centrifugation. The vesicular fraction showed lower helical content and lower specific activity than the tubular fraction. Small differences between the two in the visible CD and absorption spectra were detected.

M-Pos109 CHANGES IN LIPID DIFFUSION WITH CAPACITATION IN MOUSE SPERM. Wolf, D.E. and Hagopian, S.S. Worcester Foundation for Experimental Biology, Shrewsbury, Mass 01545 (Intr. by R. Vallee).

Mammalian sperm are transformed in the female reproductive tract so that they develop the ability to fertilize ova - a process known as capacitation. In the mouse this process can be induced in vitro by incubation in 30 mg/ml BSA for 2 hrs at 37°C. We have measured changes in lipid diffusion for the fluorescent lipid analogue C_{16}diI which result from capacitation using fluorescence recovery after photobleaching (FPR). In cauda epididymal sperm, diffusion was faster on the midpiece and tail of sperm than the head. Capacitation resulted in a slight increase in tail diffusion rate. In contrast, mock-capacitation in medium without BSA resulted in a decrease in diffusion rate in all regions.

CAPACITATION OF MOUSE SPERM WITH BSA:DIFFUSION OF C_{16}DiI

Diffusion coefficient X 10^9 cm^2/s

	Head			
	Anterior	Posterior	Midpiece	Tail
Control	1.11 ± .12	1.92 ± .13	5.64 ± .46	5.04 ± .48
Capacitated	2.65 ± .29	2.08 ± .34	6.06 ± 1.1	7.77 ± 1.5
Mock-capacitated	1.24 ± .21	1.31 ± .26	2.85 ± .58	1.65 ± .34
	% Recovery			
Control	61 ± 2	56 ± 2	58 ± 3	77 ± 2
Capacitated	45 ± 3	46 ± 4	45 ± 5	53 ± 6
Mock-capacitated	60 ± 4	53 ± 4	49 ± 5	69 ± 9

Physiologically, capacitation manifests itself in hyperactivated motility and a membrane fusion process known as the acrosome reaction.

M-Pos110 CONFORMATION AND ION SELECTIVITY OF THE IONOPHORE A204A. W.A. Pangborn*, W.L. Duax and D.A. Langs*, Molecular Biophysics Department, Medical Foundation of Buffalo, Inc., Buffalo, New York 14203

The ionophore A204A is a member of the family of monocarboxylic acid, polycyclic, polyether antibiotics. It induces monovalent cation permeability and exhibits selectivity for K^+ over Na^+. Structures have previously been reported for the free acid (Smith et al., Acta Cryst., B34, 3436 (1978)) and both the Na^+ and Ag^+ complexes (Jones et al., J. Amer. Chem. Soc., 95, 3399 (1973)) of A204A. The structure of the Na^+ complex reported exhibited anomalously long Na-ligand distances. Single crystals of the Na^+ and K^+ complexes of A204A have each been grown from water/acetone solutions. These crystals are monoclinic, space group C2, and isomorphous with each other and the previously reported structures. Data were collected on a Nicolet P3 diffractometer using Nb-filtered Mo radiation. Data were considered observed on the basis of a 2σ(I) test. The solution and refinement of these structures indicate that the previously reported Na-A204A comples was incorrectly identified and was actually the K^+ -complex. Tha Na-A204A complex in the present investigation exhibits normal Na-ligand distances. The conformations of the Na^+ and K^+ complexes are very similar. Empirical calculations of the bond strength on the basis of the coordination bond lengths indicate a stronger binding of K^+ over Na^+, which is consistent with the ion selectivity of this ionophore.

	a(Å)	b(Å)	c(Å)	β(°)	No. of data	Obs. data
Na-A204A	27.223(7)	14.529(3)	14.369(3)	91.18(2)	8653	7457
K-A204A	27.669(7)	14.491(8)	14.362(3)	91.61(2)	5341	4440

Supported by grants GM32812 and AM07368 form NIH, DHHS.

M-Pos111 CORRELATION BETWEEN SENDAI VIRUS-INDUCED LEAKAGE AND TARGET MEMBRANE PHASE BEHAVIOR. Yung-Shyeng Tsao, Ernesto Freire and Leaf Huang, Department of Biochemistry, University of Tennessee, Knoxville, TN 37996.

The Sendai virus-induced leakage of large liposomes containing egg phosphatidylethanolamine (PE) and different mole fractions of ganglioside GD1a have been investigated by fluorescence spectroscopy, using the self-quenching fluorescent dye calcein. The kinetics of leakage was obtained by following the enhancement of fluorescence intensity at 520 nm (excitation wavelength was 490 nm) as a function of time. Leakage of the entrapped dye was only observed when F-protein was present on the Sendai virus. Removal of the F-protein by trypsin digestion resulted in negligible leakage rates. The leakage rate was also dependent on the mole fraction of ganglioside GD1a and was maximal at 6.5 mole percent from 20° to 35° C. Arrehnius plots of the leakage rates showed breaks in the 20-25° C temperature range. Calorimetric, DPH steady state anisotropy and excimer formation experiments revealed that the breaks were associated with the gel-liquid crystalline phase transition of the liposomes. High sensitivity differential scanning calorimetry studies indicate that mixed PE-GD1a liposomes undergo a broad phase transition centered between 17° and 21° C depending on the ganglioside mole fraction. The enthalpy change for the transition was dependent upon the ganglioside mole percent and had a maximum at ~17 mole percent. It must be noted that under the conditions of the experiments, neither PE or GD1a are able to form bilayer structures by themselves and that liposome formation is the result of interactions between the PE and ganglioside molecules. (Supported by NIH Grant GM-31724).

M-Pos112 INTERACTION OF POLYAMINES WITH PHOSPHOLIPID MEMBRANES. S. Ohki, J. Duax and H. Ohshima. Dept. of Biophysical Sciences, State University of New York, Buffalo, NY 14214.

The interaction of polyamines (spermine, spermidine, etc.) with phospholipid membranes was studied: effects of polyamines on aggregation of small unilamellar phosphatidylserine vesicles as well as phosphatidylserine/phosphatidylcholine vesicles (1:1), electrophoretic mobility of multilamellar phosphatidylserine vesicles, surface tension of a phosphatidylserine monolayer and fusion of phosphatidylserine/phosphatidylcholine (1:1) vesicle to a phosphatidylserine monolayer.

It was found that polyamine molecules do adsorb strongly, probably electrostatically on a negatively charged membrane surface, but seem not to alter the conformation of such membrane molecules upon its binding. This result compares well with the facts that polyamines do cause aggregation of negatively charged lipid vesicles to a greater extent at a very small concentration (e.g., spermine ∿ μM range) but do not induce fusion of such lipid membranes even up to a relatively high concentration (e.g., spermine ∿ mM range). The binding capability of these polyamines to acidic phospholipid membranes and membrane fusion effect are discussed in comparison with metal polyvalent cations.

M-Pos113 THE EFFECTS OF PRESSURE ON THE FUSION OF LIPID VESICLES by E. L. Chang and P. Yager. Biomolecular Engineering, Code 6507, Naval Research Laboratory, Washington, D. C., 20375-5000.

The fusion of lipid membranes can occur through many different means such as cation-induced fusion, fusion mediated by fusogenic proteins, or spontaneous fusion of small unilamellar vesicles. The mechanism of fusion is not known but it is generally believed that the bilayer must undergo a non-bilayer deformation before fusion can be completed. We report here a study of the dependence of spontaneous fusion of vesicles on hydrostatic pressure. The vesicles are composed of dioleoylphosphatidyl ethanolamine/dioleoylphophatidyl choline/cholesterol (3:1:2) and are known to undergo a bilayer-to-hexagonal II phase transition around 50 C. This phase transition is accompanied by fusion of the sonicated vesicles. The fusion event was monitored by photon correlation spectroscopy; the resulting correlation functions were inverted to obtain histograms of the size distribution as a function of temperature and pressure. We find that pressure will inhibit the advent of fusion, but that increasing pressure alone will not suppress fusion of the vesicles. These results will be discussed in detail.

M-Pos114 A LIPID MIXING ASSAY TO MONITOR Ca^{2+}-INDUCED MEMBRANE FUSION AND PHASE SEPARATION. Roberta A. Parente and Barry R. Lentz. (Intr. by R. Faust) Biochemistry Department, University of North Carolina, Chapel Hill, NC 27514.

We have developed an assay to monitor the mixing of lipids during membrane fusion utilizing the observation that the fluorescence lifetime of 1-palmitoyl-2-(4'-carboxyethyl)-6-diphenylhexatriene-3-*sn*-phosphatidylcholine (DPHPC) is a sensitive function of lipid/probe ratio, especially for membranes containing greater than 1 mol % probe. Experimentally, a small number of vesicles containing a high concentration of probe (2 mol %) are mixed with a large number of vesicles devoid of probe. Upon addition of a fusogen, mixing of bilayer lipids associated with fusion is observed as an increase in the fluorescent lifetime of DPHPC resulting from loss of concentration-related quenching. By this assay, Ca^{2+}-induced fusion of bovine brain phosphatidylserine vesicles (0.22 mM lipid) occurred with a half-time of about 10 sec. while phase separation (between the PS head groups of bulk lipid and the PC head groups of our probe) was not significant until approximately 10 min. after Ca^{2+} addition and was completely reversible by EDTA addition. The results from our assay are in agreement with fusion measurements using the Tb^{3+}/dipicolinic acid contents mixing assay and the NBD-PE/Rh-PE lipid mixing assay. However, the advantage of DPHPC over NBD-PE/Rh-PE as a probe of membrane fusion is that the fluorescent moiety is located in the hydrophobic region of the bilayer where it is protected from the direct influence of added fusogenic agents. In this regard, we have shown that fluorescence quenching by Ca^{2+} interferes with the interpretation of data obtained with the NBD-PE/Rh-PE assay. Supported by USPHS Grant GM32707 and by an Established Investigator Award to BRL by the American Heart Association.

M-Pos115 FUSION OF LIPOSOMES INDUCED BY A HYDROPHOBIC PROTEIN FROM THE ACROSOME GRANULE OF ABALONE SPERMATOZOA. Keelung Hong and Victor D. Vacquier,* Cancer Research Institute, University of California, San Francisco, CA, and *the Marine Biology Research Division, Scripps Institution of Oceanography, University of California at San Diego, La Jolla, CA.

Lysin, a hydrophobic protein of m.w. 16K from the acrosome granule of the abalone, is responsible for the dissolution of egg vitelline layer. Lysin breaks the hydrophobic bonding of the vitelline layer fibers nonenzymatically. Here, we report that lysin nonselectively associates with phospholipid membranes and causes a spontaneous release of carboxyfluorescein from liposomes. The association of lysin with neutral vesicles suggests that there is a hydrophobic interaction between lysin and lipid bilayers. The binding of lysin to phospholipid vesicles in Ca^{2+}-free medium results in the aggregation of phosphatidylserine (PS)-containing vesicles, but this is not observed in neutral phosphatidylcholine vesicles. Resonance energy transfer was used to determine whether lysin induces fusion among the aggregated vesicles. When lysin was added, the energy transfer in PS-containing vesicles significantly decreased. That no fusion between neutral phosphatidylcholine vesicles and PS-containing vesicles was observed suggests that PS is required for lysin-induced liposome fusion. The interaction of lysin with liposomes is inhibited by Ca^{2+} and Mg^{2+}, which are known to modulate or facilitate membrane fusion. Our observations suggest that lysin may utilize its hydrophobic domain to interact with the hydrophobic region of phospholipid bilayers and facilitate the fusion of membranes, which are in close apposition to each other, because of the polycationic nature of the lysin. We propose that lysin may play two roles in fertilization: dissolution of the egg vitelline layer and facilitation of fusion between sperm and egg plasma membranes.

M-Pos116 FUSION OF SONICATED DIPALMITOYLPHOSPHATIDYLCHOLINE VESICLES: TEMPERATURE, SALT, NONIONIC SOLUTE AND CHOLESTEROL DEPENDENCE. Daniel S. McConnell and Stephen E. Schullery, Chemistry Department, Eastern Michigan University, Ypsilanti, MI 48197.

The fusion of sonicated DPPC vesicles was studied as a function of temperature, ionic strength, permeant and impermeant osmolarity, and vesicle cholesterol composition. As the temperature decreased from 35.5°C to 1°C, the fusion rate increased from undetectable, to about 10%/week at 30°C, then to about 90%/day at 1°C. At 13°C and above, fusion occurs to the 700 Å diameter vesicles previously reported at 21°C (Schullery, S.E., Schmidt, C.F., Felgner, P., Tillack, T.W. and Thompson, T.E. (1980) Biochemistry 19, 3919-3923). At 8°C and below, fusion occurs to the 950 Å form previously reported at 4°C (Wong, M., Anthony, F.W., Tillack, T.W. and Thompson, T.E. (1982) Biochemistry 21, 4126-4132). However, complete conversion to the 700 Å form prior to appearance of the 950 Å vesicles, as reported by Wong et al., was not observed.

The fusion rate was slower in increasing concentration (up to 1.00 M) NaCl or impermeant nonionic solutes glucose & trehalose. In contrast, the fusion rate was dramatically increased by up to 1.00 M permeant solutes glycerol, ethylene glycol, propylene glycol and ethanol. Fusion to approximately 700 Å vesicles was essentially complete in 30 minutes in 1.0 M ethanol at 22°C. Under these fast-fusion conditions, 10-65% incorporation of various water-soluble markers was achieved.

Incorporation of cholesterol into the sonicated vesicles inhibits the fusion process.

M-Pos117 INTERACTIONS OF Na^+, Li^+ AND Ca^{2+} WITH PHOSPHATIDIC ACID (PA), PHOSPHATIDYLGLYCEROL (PG) AND PHOSPHATIDYLSERINE (PS) BILAYERS. J. Mattai and G.G. Shipley. Biophysics Institute, Boston University School of Medicine, Boston, MA 02118.

Differential scanning calorimetry (DSC) has been used to investigate the interactions of excess Na^+, Li^+ and Ca^{2+} with dimyristoyl-, dipalmitoyl- and distearoyl- PA (DMPA, DPPA and DSPA) and PG (DMPG, DPPG and DSPG). For DPPA, the reversible bilayer gel → liquid crystalline transition, T_c for Na^+, Li^+ and Ca^{2+} are 68.2°C (ΔH = 8.9 Kcal/mol), 69.5°C (ΔH = 8.3 Kcal/mol), and 78.4°C (ΔH = 10.3 Kcal/mol). For DPPG, corresponding values are 43.0°C (ΔH = 10.6 Kcal/mol), 46.5°C (ΔH = 10.1 Kcal/mol) and 93.9°C (ΔH = 16.9 Kcal/mol). With the exception of Ca^{2+}, the changes in Tc are dependent on the screening ability of the metal ions.

DSC and x-ray diffraction have investigated Na^+, Li^+ and Ca^{2+} interactions with DPPC:DPPS (1:1, molar). For Na^+, a single transition is observed at ∿ 48.5°C (ΔH = 9.25 Kcal/mol); with both Li^+ and Ca^{2+}, two transitions are observed, relatively sharp peaks at ∿ 48.7°C (ΔH = 3.8 Kcal/mol) and 55°C (ΔH = 8.7 Kcal/mol), and broader transitions at ∿ 85°C (ΔH = 4.2 Kcal/mol) and ∿ 137°C. The higher transitions correspond to melting of the crystalline PS:Li^+ and PS:Ca^{2+} complexes while the lower transitions correspond to DPPC-rich phases. At 23°C, x-ray diffraction of Na^+ : DPPC/DPPS shows a 1/4.1 $(Å)^{-1}$ reflection which converts to a diffuse reflection at 1/4.56 $(Å)^{-1}$ at 61°C (L_β → L_α transition). For Li^+ :DPPC/DPPS (1:1) at 23°C, in addition to the 1/4.1 $(Å)^{-1}$ reflection, reflections are observed from 1/6.6 → 1/3.4 $(Å)^{-1}$, corresponding to the crystalline (L_c) Li^+:PS complex. At 61°C, the 1/4.6 $(Å)^{-1}$ reflection of a DPPC-rich L_α phase is present, but the reflections characteristic of the L_c phase persist. These results demonstrate that Li^+ and Ca^{2+} induce lateral phase separation of DPPS from a 1:1 DPPC/DPPS.

M-Pos118 SYNEXIN INTERACTIONS WITH FATTY ACIDS AND SPERMINE IN MEMBRANE FUSION. Paul Meers, Keelung Hong, and Demetrios Papahadjopoulos. Cancer Research Institute and Department of Pharmacology, University of California, San Francisco, CA 94143.

Synexin, a protein found in adrenal medulla and other cells, induces aggregation of chromaffin granules and fusion of certain liposomes in the presence of calcium. Certain fatty acids appear to allow chromaffin granules, aggregated by synexin and calcium, to fuse. Using a contents mixing assay (terbium and dipicolinic acid), we have found that fatty acids or synexin alone increased the rate of calcium-induced fusion of phosphatidate (PA)/phosphatidylethanolamine (PE) 1/3 liposomes. The fusion rates for synexin and arachidonic acid (AA) together were equal to or less than the sum of the separate rates, indicating that they act independently. When synexin was preincubated with levels of AA that were subthreshold for rate effects in the absence of synexin, no effect on the fusion by synexin plus calcium was observed. Thus, even though the AA-to-synexin ratio exceeded 50:1 in the preincubations, there appeared to be no specific effect of AA on synexin under the conditions of these experiments. Preincubation of synexin with 2 mM Ca^{++}, with or without AA, polymerized the synexin and reduced or eliminated the synexin enhancement of calcium-induced fusion. This suggests that monomers or oligomers are more effective than large polymers.

Spermine alone was found to polymerize synexin. Spermine-induced fusion of PA/PE 1/3 liposomes was inhibited by synexin, and synexin spun down with PA/phosphatidylcholine 1/1 multilamellar vesicles in the presence of spermine. These facts suggest spermine-mediated binding of synexin to the membrane surface and that polymerization conditions are related to membrane binding conditions.
(Supported by grant #PF 2398, American Cancer Society.)

M-Pos119 CHOLESTEROL MODULATES DIVALENT CATION-INDUCED PHASE TRANSITIONS AND FUSION OF PHOSPHATIDYLSERINE VESICLES. P. Wood, J. Bentz, and N. Düzgüneş, Cancer Research Institute and Departments of Pharmacy and Pharmaceutical Chemistry, University of California, San Francisco, CA 94143.

The kinetics of fusion of large unilamellar vesicles (approx. 100 nm diameter) composed of phosphatidylserine and cholesterol, induced by Ca^{2+}, Ba^{2+} and Sr^{2+}, was investigated by following the intermixing of Tb nitrilotriacetate and Na dipicolinate encapsulated in two vesicle populations. The size distribution of vesicle preparations with varying cholesterol content was estimated by dynamic light scattering and the encapsulated volume. The presence of 30 mol % cholesterol reduced the initial rate and extent of fusion by several fold at 10°C and by an order of magnitude at 30°C. These temperatures are, respectively, below and above the midpoint of the gel-liquid crystalline temperature (Tc) of the Ba^{2+} or Sr^{2+} complexes of phosphatidylserine/cholesterol. Leakage of aqueous contents, measured by carboxyfluorescein fluorescence, was delayed considerably for vesicles containing 20 and 30 mol % cholesterol, compared to vesicles composed of pure phosphatidylserine and its mixture with 10 mol % cholesterol. The shift of the endothermic transition of the bilayers to higher temperatures by Ba^{2+} and Sr^{2+}, determined by differential scanning calorimetry, was about 5°C lower for membranes containing 30 mol % cholesterol compared to pure phosphatidylserine, indicating a fluidizing effect of cholesterol.

(Supported by a Grant-in-Aid from the American Heart Association with funds contributed by the California Affiliate, and NIH Grant GM28117.)

M-Pos120 INTERACTIONS OF SYNAPTIC VESICLES WITH PLANAR BILAYERS. M. S. Perin and R. C. MacDonald, Dept. Neurobiology & Physiol. Northwestern University, Evanston, Il. 60201

We have investigated the interaction of synaptic vesicles with horizontal planar bilayers by fluorescence microscopy. Electric organ synaptic vesicles freeze-thawed in the presence of 200 mM calcein become fluorescent and increase in diameter by about four times. Such freeze-thawed synaptic vesicles (FTSV's) entrap high, partially self-quenched concentrations of calcein presumably due to rupture and fusion during freeze-thawing. In the presence of high concentrations of calcium chloride (25 mM), FTSV's adhere to black lipid membranes (BLM's, 4% phosphatidylserine 1% phosphatidylethanolamine in decane or 2.5% PS 2.5% PE in squalene). FTSV's aggregate on the surface of decane-based BLM's and lenses appear to form around the aggregated vesicles. Upon addition of untreated synaptic vesicles, a multitude of small lenses forms on the membrane. In contrast to decane-based BLM's, FTSV's bind individually to squalene-based BLM's and do not induce lens formation. With both types of membranes, other divalent ions including magnesium (25 mM) and cobalt (100 μM) can substitute for calcium in mediating adhesion. Release of concentrated calcein from FTSV's adhering to BLM's results in brightflashes of fluorescence. Such flashes, which can be due to either fusion or lysis, are diminished in the presence of cobalt ion (a calcein fluorescence quencher). The persistence of large flashes when cobalt ion is present on only one side of the BLM suggests that both fusion (trans release) and lysis (cis release) occur. Supported by NIH grant NS20831.

M-Pos121 pH-DEPENDENT FUSION OF PHOSPHOLIPID VESICLES USING A TITRATABLE POLYCATION. Paul S. Uster and David W. Deamer. Dept. of Zoology, University of California, Davis, CA 95616.

Poly-L-lysine-promoted membrane mixing of phospholipid vesicles occurred only if the buffer pH was at or below the pK_a of the lysyl residue. This suggested that the onset of liposome fusion could be regulated in a physiological pH range if poly-L-histidine was substituted as the fusogen. Fluorescence assays were used to monitor the rate and extent of lipid bilayer mixing, or mixing of entrapped contents. Microgram quantities of poly-L-histidine were added to 0.1 mM suspensions of phospholipid vesicles, but no fusion was detected at pH 7.4. When the pH of the buffer was lowered to 6.9 or below, fusion was rapid and substantial as measured by the mixing assays. The kinetics of Ca^{2+}-induced liposome fusion are contrasted with the kinetics of the pH-triggered poly-L-histidine fusion reaction. The lipid composition requirements, rapid kinetics, and triggering of vesicle coalescence in a physiological pH range suggest that polyhistidine-phospholipid vesicle interactions may be a useful model system of some biological fusion events. (Supported by NSF grant PCM 80-01953 and a Jastro-Shields Research Award.)

M-Pos122 FUSION OF PHOSPHOLIPID VESICLES WITH PLANAR MONOGLYCERIDE BILAYERS Walter D. Niles Dept. Physiology, Albert Einstein College of Medicine, Bronx, NY 10461

One possible role of osmotic pressure in vesicle-planar bilayer fusion is to remove water molecules interposed between the two phospholipid bilayers. This hydration barrier results from the ordering of water molecules in the polarization field extending away from any charged or zwitterionic surface. Since monoglycerides, such as glyceromonooleate (GMO), lack polar head groups, the force to remove associated water is expected to be less. To test this possibility, I examined the osmotic dependence of the fusion of 4:1 PC/PE vesicles, containing the ion-channel porin as a vesicular membrane marker, to planar GMO bilayers. In most experiments, a small rate of fusion (10 events/min) was observed in the absence of an osmotic gradient. This rate of fusion was unaffected by making the vesicle-containing compartment hyperosmotic with urea until the gradient exceeded 0.6 osmol/l (Osm), at which point the rate of fusion increased to the level seen with phospholipid planar bilayers sustaining a 0.1 Osm gradient. It was not possible to obtain vesicles attached to the planar GMO bilayer in a pre-fusion state, indicating that phospholipid vesicles form transitory, unstable contacts with GMO films. Vesicles having sufficient surface energy and approaching close to the planar film fuse without osmotic swelling. Osmotic-induced fusion, however, occurs only with gradients capable of producing enough water flow to swell the vesicle during the short lifetime of the vesicle-bilayer contact. The removal of water from between apposed bilayers may be a secondary effect of the osmotic gradient in this system. The results suggest a role for polar head groups in vesicle-membrane attachment. Supported by NIH grant #GM08549-02.

M-Pos123 FREE FATTY ACIDS AFFECT H^+- AND CA^{++}-INDUCED FUSION OF MODEL MEMBRANES. P.A. Baldwin,N. Düzgüneş and D. Papahadjopoulos, Cancer Res. Inst., Univ. of CA, San Francisco, CA 94143

Liposomes composed of phosphatidylethanolamine and oleic acid (PE:OA 7:3) fuse in response to lowered pH (Duzgunes et al., J. Cell Biol. 97:178a 1983). Recently, we have shown that addition of Ca^{++} also causes fusion and that both Ca^{++}- and H^+-induced fusion result in mixing of internal aqueous contents. Since cis-unsaturated fatty acids (FAs) act as fusogens of isolated chromaffin granules in the presence of Ca^{++}, but trans-unsaturated and saturated FAs are ineffective (Creutz, J. Cell Biol. 91:247, 1981), we have investigated the role of free FA structure in the fusion of PE liposomes. Liposomes were made from pure PE at pH 9.5 or from mixtures of PE and arachidonic acid (AA), elaidic acid (EA), stearic acid (SA) or OA. Fusion and leakage were monitored by the aqueous content mixing assay of Ellens et al. (Biophys. J. 45:70a, 1983). Pure PE liposomes were stable at pH 9.5. Addition of Ca^{++} resulted in a small degree of fusion (~3%/min). All the FAs increased the initial rate of content mixing in response to added Ca^{++} at pH 9.5; however only OA and AA caused large increases (3-5-fold) in the extent of fusion. Similar results were obtained for Ca^{++}-induced fusion of FA-PE liposomes at pH 7.4. Lowering the pH of pure PE liposomes from 9.5 to 5 caused fusion accompanied by a slow leakage of contents. Inclusion of FAs resulted in liposomes that were stable above pH 6.5 and fused at lower pH. Compared with pure PE liposomes, the FA-PE liposomes showed larger leakage rates resulting in a decrease in the extent of content mixing. The increase in leakage rate was a function of FA: AA>OA>EA>SA. Free FA inclusion altered the light-scattering changes that accompanied fusion and altered the phase transition properties of PE. These findings have implications for design of pH-sensitive liposomes for use in drug delivery, and suggest that free FAs could modulate fusion in biological membranes. Supported by ACS grant #PF-2331.

M-Pos124 FREE ENERGY POTENTIAL FOR ADHESION (FOLLOWED BY OCCASIONAL FUSION) OF GIANT PE-PC BILAYER VESICLES. E. Evans, M. Metcalfe, D. Needham, Pathology, Univ. of British Columbia, Vancouver, B.C. V6T 1W5

Adhesion of two giant (2×10^{-3} cm diameter) vesicles was controlled by micromanipulation. The vesicles were made from mixtures of phosphatidylethanolamine (PE) and phosphatidylcholine (PC) with ratios of PE:PC from 1:1 to 9:1. The aggregation was carried out in phosphate buffered saline (100 mM), pH 6.0. The two vesicles were first slightly deflated in hyperosmotic strength buffer while held by suction micropipets. One vesicle was aspirated with sufficiently high suction pressure so that it became a rigid sphere; the other vesicle was held with low suction pressure. The vesicles were then maneuvered into position for contact; the vesicle held with low suction pressure was allowed to adhere (spread-on) to the rigid vesicle with an extent controlled by the suction pressure (i.e. membrane tension). From the observation of membrane tension versus contact area, the free energy potential per unit area of contact was directly determined. The values increased with PE content; the maximum value was three fold greater than that determined previously for pure PC vesicles (1.5×10^{-2} ergs/cm^2; Biophys. J. 46: 423, 1984). With the use of published values for lamellar repeat spacing determined by X-ray diffraction methods, the measured free energy potential for adhesion showed that the Hamaker coefficient for van der Waal's attraction was the same for the PE containing vesicles as for pure PC vesicles. However, the hydration force was greatly reduced. During the course of the adhesion test, fusion of the vesicles was occasionally observed for vesicles with PE content greater than or equal to 4:1 (PE:PC). The event was not predictable but there was some indication that pressurization of the vesicles (to produce high membrane tension) could act to promote fusion.

M-Pos125 ^{2}H NMR STUDIES OF THE ACTION OF BENZYL ALCOHOL ON MODEL LECITHIN AND GRAMICIDIN/LECITHIN BILAYER MEMBRANES. N. Phonphok[+], J.W. Doane*[+] and P.W. Westerman*[+], *Molecular Pathology Program, Northeastern Ohio Universities College of Medicine, Rootstown, Ohio 44272 and [+]Department of Physics and Liquid Crystal Institute, Kent State University, Kent, Ohio 44242.

The effect of the general anesthetic, benzyl alcohol (BzOH) on the structure of dimyristoylphosphatidylcholine (DMPC) bilayer membranes was evaluated by ^{2}H NMR. Time-averaged quadrupole splittings ($\delta\nu$) from DMPC, specifically ^{2}H-labelled in the choline and glycerol backbone moeities, and from BzOH, ^{2}H-labelled in the α-methylene group, were used to determine molecular ordering in the system. Results were analysed by an order matrix approach to estimate how BzOH alters the conformation of the glycerol backbone in DMPC as well as the ordering of its most-ordered molecular axis. Experiments with ^{2}H-labelled BzOH showed the existence of two distinct sites for the anesthetic in the bilayer. It is proposed that the more-ordered population of BzOH molecules is intercalated between lipids in the bilayer while the less-ordered population is adsorbed on the surface. Exchange between the two sites is slow on the NMR time-scale.

The effect of BzOH on protein-lipid interactions in the bilayer was determined with the gramicidin A'-DMPC model system. ^{2}H-labelled sites on both BzOH and DMPC were utilized as probes. Our data show that BzOH probably disrupts H-bond formation between H-bond donor groups on gramicidin and the H-bond acceptor carbonyl group in the sn-1 chain of DMPC. In gramicidin A containing bilayers the presence of two populations of ordered BzOH molecules is still observed. (Supported by NIH GM27127).

M-Pos126 FLUORESCENCE PROPERTIES OF DPHPC: USE AS A BILAYER PROBE. Roberta A.Parente and Barry R. Lentz. (Intr. by J. Hermans) Biochemistry Dept., Univ. of North Carolina, Chapel Hill, NC 27514.

1-palmitoyl-2-(4'-carboxyethyl)-6-diphenyl-*trans*-1,3,5-hexatriene-3-*sn*-phosphatidylcholine (DPHPC) is a fluorescent phospholipid which incorporates the diphenylhexatriene (DPH) moiety in one acyl chain and maintains photophysical properties similar to its parent fluorophore, DPH. We have investigated the behavior of DPHPC in synthetic phosphatidylcholine vesicles. From its behavior in mixed lipid vesicles containing known amounts of coexisting fluid and solid-like phases, DPHPC was found to preferentially partition into fluid lipid ($K_{f/s}$ = 3.3). Consistent with this observation, DPHPC reports a lower phase transition temperature as measured by fluorescence anisotropy than that obtained by differential scanning calorimetry and DPH fluorescence anisotropy. Slight changes in membrane transition temperatures (0.1 to 0.2° C) and no change in transition widths were observed in calorimetric scans performed at different phospholipid to probe ratios. Temperature profiles of steady state fluorescence anisotropy, limiting anisotropy, differential tangent, and rotational rate were similar to those of DPH below the main lipid phase transition, but generally reflected more restricted rotational motion above the phase transition. Finally, the fluorescence lifetime of DPHPC was resolved into two components, both above and below the phase transition, and was roughly 1.5 nsec shorter than that of DPH over the same temperature range (5-60° C). In summary, the lipid-like structure of DPHPC ensures limited perturbation of bilayer components and orients the DPH moiety in the bilayer, making this an ideal probe of membrane structure and dynamics. Supported by USPHS Grant GM 32707 and by an Established Investigator Award to BRL by the American Heart Association.

M-Pos127 INVESTIGATION OF DRUG-MEMBRANE INTERACTIONS USING FLUORESCENCE TECHNIQUES.
C.L. Pryor, C.D. Stubbs and E. Rubin
Department of Pathology and Laboratory Medicine, Hahnemann University, Philadelphia, PA 19102

Drugs, anesthetics and alcohols are known to disorder cell membranes by disturbing lipid organization. The consequences of this on membrane mediated cell functions is less clear and in many cases intereference with protein-lipid interactions and direct effects on the proteins occur. In previous studies fom this laboratory membranes from livers of alcoholic rats were found to be resistant to disordering by in vitro addition of ethanol. In order to clarify which of the four main regions in the membrane are affected, we have made time-resolved and steady state fluorescence measurements on probe molecules which locate specifically at the phospholipid headgroup region, the lipid hydrocarbon core, the protein-lipid interface and directly on membrane proteins. By this means we were able to distinguish between different types of membrane perturbation brought about by various drugs and other agents which interact with membranes.

M-Pos128 THE EFFECTS OF RHODOPSIN AND CHOLESTEROL ON THE PHYSICAL PROPERTIES OF LIPID BILAYERS
Martin Straume and Burton J. Litman, Department of Biochemistry, University of Virginia School of Medicine, Charlottesville, VA 22908

Incorporation of rhodopsin into egg phosphatidylcholine (Egg PC) unilamellar vesicles causes an increase in the static ordering of the bilayer lipids as observed with both diphenylhexatriene (DPH) and trimethylammonium-diphenylhexatriene (TMA-DPH). Rhodopsin therefore increases the average order of bilayer PC molecules both in the membrane interior (as probed by DPH) and at the interfacial, headgroup region of the bilayer (as probed by TMA-DPH). In addition, the rate of fluorophore motion is decreased by rhodopsin in the case of DPH and not much affected when TMA-DPH is observed.

Introduction of cholesterol into Egg PC, POPC (16:0,18:1-PC), and DOPC (18:1,18:1-PC) unilamellar vesicles shows differing effects on lipid structural properties as a function of acyl chain composition. The static order of all three systems was increased by cholesterol as observed by both DPH and TMA-DPH. However, rates of DPH motion in the bilayer interior were increased by cholesterol in Egg PC (a system heterogeneous in acyl chain composition), decreased in DOPC (a homogeneous, di-unsaturated system), and decreased at 37°C but increased at 5°C in POPC (a homogeneous, mixed chain system). TMA-DPH motion at the interfacial, headgroup region of the bilayers was significantly increased by cholesterol in Egg PC, slightly increased in POPC, and unaffected in DOPC. Differential effects of cholesterol on rate of probe motion as a function of acyl chain composition are therefore evidenced in both regions of the bilayers even though Egg PC, POPC, and DOPC show very similar properties when examined as pure PC bilayers.

M-Pos129 THE CONSEQUENCES OF ELEVATING DOCOSAHEXAENOATE IN MEMBRANE PHOSPHOLIPIDS. FLUORESCENCE POLARIZATION MEASUREMENTS ON DIETARY SUPPLEMENTED MEMBRANES AND THEORETICAL STUDIES USING COMPUTER MODELING.

C.D. Stubbs[a], D.M. Conroy[b], S. Islam[c], C.L. Pryor[a] and A.D. Smith[b]
[a]Department of Pathology and Laboratory Medicine, Hahnemann University, Philadelphia, PA 19102
[b]Courtauld Institute, Middlesex Hospital Medical School, University of London, W1P 7PN, UK
[c]Biophysics Department, Kings College, University of London, WC2 B5RL, UK.

Membranes from several different tissues have high levels of docosahexaenoate (22:6) acylated to the phospholipids. We have examined the effect of increasing the level in rat liver membranes by dietary supplementation using fish oil. Large increases in the levels of 22:6 were obtainable causing an increase in the overall fatty acid unsaturation. The 22:6 went mainly into phosphatidylethanolamine and fluorescence polarization measurements using diphenylhexatriene (DPH) and TMA-DPH were therefore made to assess effects on bilayer motional properties. Computer modeling studies on 22:6 showed it to be a bulky and inflexible structure indicating that a decrease in the rate and extent of motion might be expected in membranes with elevated levels. In intact membranes no differences were found with either probe. Differences were found, however, when phosphatidylethanolamine liposomes were examined, with the increased unsaturation leading to lower fluorescence anisotropy values, the differences being greater with TMA-DPH.

M-Pos130 THE STRUCTURE OF IODOLIPID-PHOSPHOLIPID AGGREGATES FOR CT HEPATIC IMAGING. Gordon L. Jendrasiak, Mohsen Eghbal, Department of Physics and the School of Medicine, East Carolina University, Greenville, NC; G. Donald Frey, Medical University of South Carolina, Charleston, SC

We have recently used aggregates, composed of phospholipids and the iodolipid, ethiodol, to obtain enhanced CT liver imaging with diagnostic efficacy in the rabbit model. The structure of these aggregates is of some interest since the use of the aggregates results in rapid hepatic uptake, retention in the liver and low iodine load, in comparison to commonly used imaging agents. Nuclear magnetic (NMR) proton spectroscopy indicates that the great majority of the phospholipids are in the liposomal configuration. Proton relaxation time measurements and phosphorus spectroscopy suggest that the ethiodol sits "down" in the liposome. The presence of micelles seems unlikely. Scanning and transmission electron microscopy show the individual subunits to be in the size range 150Å to 600Å, for most of the subunits; the subunits have a bilayer structure. Filtration of the preparation through a 0.45μ filter and the application of x-ray dispersive and fluorescence techniques show that the phosphorus to iodine ratio before and after filtration is the same. All of these observations taken together suggest that the phospholipids are in the unilamellar and multilamellar liposome configuration with the iodolipid contained in the hydrophobic region of the liposomes.

M-Pos131 THE USE OF DEHYDROERGOSTEROL AND DEHYDROERGOSTERYL LINOLEATE AS PROBES OF STEROL BEHAVIOR IN HUMAN SERUM LOW DENSITY LIPOPROTEINS. Greg Smutzer and Philip L. Yeagle, Dept. of Biochemistry, School of Medicine, State University of New York at Buffalo, Buffalo, New York 14214

The fluorescent probes dehydroergosterol and dehydroergosteryl linoleate were employed to detect phase transitions by fluorescence polarization in human serum low density lipoproteins (LDL). Dehydroergosterol was incorporated into LDL by exchange from dehydroergosterol-containing vesicles, and underwent an increase in anisotropy near 36° C. This temperature region is where the LDL core cholesteryl esters undergo a calorimetric phase transition. This increase in anisotropy occurred over a temperature range of approximately 2° C. Dehydroergosteryl linoleate was synthesized from dehydroergosterol by reaction with linoleic anhydride in the presence of 4-pyrrolidinopyridine as a catalyst. The purified ester was identified by its infra-red and NMR spectra, and possessed spectroscopic characteristics identical to dehydroergosterol. Dehydroergosteryl linoleate was incorporated into LDL by use of lipid exchange factors normally found in plasma (Sklar et al., 1981, J. Biol. Chem. 256: 4286-4292). Dehydroergosteryl linoleate also underwent an increase in anisotropy near 36-37° C, and the amplitude of this increase was approximately half that observed with dehydroergosterol. These results indicate that free cholesterol, in addition to cholesterol esters, is located in the core of human serum LDL. Supported by NIH grant HL 23853.

M-Pos132 ANISOTROPIC ^2H SPIN-LATTICE RELAXATION IN LIPID/CHOLESTEROL BILAYER MEMBRANES D.J. Siminovitch, M.J. Ruocco, E.T. Olejniczak, S.K. Das Gupta and R.G. Griffin F. Bitter Nat'l Magnet Laboratory, Massachusetts Institute of Technology, Cambridge, MA 02139

By adding a sufficiently high concentration (~ 50 mol %) of cholesterol to [7,7-$^2H_2$]N-palmitoylgalactosylsphingosine (NPGS), [4,4-$^2H_2$]-dipalmitoylphosphatidylethanolamine (DPPE) or 1,2-bis (perdeuterio)palmitoyl-sn-glycero-3-phosphocholine (DPPC-d_{62}) bilayers, we have been able to decrease the lipid lateral diffusion rate by almost an order of magnitude, and thus prevent orientational averaging of the ^2H spin-lattice relaxation rate (T_1^{-1}).[1] This reduction is sufficient to render observable the anisotropic relaxation of the ^2H lineshape in a T_1 experiment. The orientation dependence of T_1^{-1} observed in any of the specifically labeled lipid/cholesterol mixtures is not that expected if slow, collective director fluctuations provide the dominant relaxation mechanism, as they appear to do in pure DPPC bilayers.[2,3] Furthermore, measurements of the ^2H-spin-lattice relaxation rates and quadrupolar splittings, $\Delta\nu_Q$, of DPPC-d_{62} in DPPC/CHOL mixtures are not consistent with a square law dependence of T_1^{-1} on the bond segmental order parameter $|S_{CD}|$, as demonstrated earlier for pure DPPC bilayers.[2,3] Simulations of the partially recovered lineshapes, using a model which includes both *gauche-trans* isomerization and axial diffusion, indicate that the observed T_1 anisotropies are consistent with large amplitude molecular reorientation of the C-D bond among a finite number (9) of sites.

1. M.F. Brown and J.H. Davis, Chem. Phys. Lett. 79, 431 (1981).
2. M.F. Brown, J. Chem. Phys. 77, 1576 (1982).
3. M.F. Brown, A.A. Ribeiro and G.D. Williams, Proc. Natl. Acad. Sci. USA 80, 4325 (1983).

M-Pos133 EQUILIBRIA AMONG LOCAL ANESTHETIC SPECIES IN PHOSPHATIDYLCHOLINE LIPOSOMES. H.P. Limbacher, Jr., G.D. Blickenstaff, J.D. Bowen, and H.H. Wang, Biology Department, University of California, Santa Cruz, CA. 95064

The equilibria among spin-labeled amine local anesthetic species in dioleoylphosphatidylcholine liposomes at an anesthetic:lipid mole ratio of 1:100 are investigated. Electron spin resonance (ESR) spectra demonstrate that anesthetic mobility within the bilayer is charge-dependent, with the uncharged species the more mobile. Partition coefficient measurements confirm ESR evidence that changes in anesthetic mobility represent anesthetic-phospholipid interaction and not changes in bilayer fluidity. Spin-exchange attenuation experiments show that anesthetics within the bilayer are accessible to the aqueous medium. Dependence of tertiary-amine anesthetic pK on dielectric constant has been used to estimate the interfacial pK. We propose a model of equilibria among species of the tertiary amine anesthetic in the aqueous medium and those intercalated in the bilayer, including a species electrostatically bound to the lipid phosphate. Using experimentally determined equilibrium constants, the model provides the binding constant between the electrostatically bound and unbound cationic anesthetics within the bilayer. The model simulates the pH dependence of the mobile fraction of total anesthetic population determined by subtraction techniques on experimental ESR spectra.

M-Pos134 PHOSPHOLIPID LATERAL PHASE SEPARATION AS REVEALED BY PYRENE-LIPID PHASE AND MODULATION FLUORESCENCE LIFETIME DATA. R.C. Hresko, Y. Barenholz and T.E. Thompson (Introduced by J.W. Ogilvie) Department of Biochemistry, University of Virginia, Charlottesville, Virginia 22908.

Two pyrene-lipid analogs, 1-palmitoyl-2-(10-(1-pyrenyl) decanoyl phosphatidylcholine (PyrPC), Tm=14°C, and N-(10-(1-pyrenyl) decanoyl sphingomyelin (PyrSPM), Tm=40°C, were used as probes to study the lateral organization of the bilayer in model membrane systems. Previously reported spontaneous phospholipid transfer experiments suggested that small unilamellar vesicles of PyrPC in 1-palmitoyl-2-oleoyl phosphatidylcholine (POPC) at 25°C and PyrSPM in dipalmitoyl phosphatidylcholine (DPPC) at 50°C are randomly mixed in a liquid crystalline state (Frank et al., (1983) Biochemistry 22, 5647). Measurement of the excimer to monomer fluorescence intensity ratio (E/M) as a function of temperature indicates that PyrSPM and DPPC phase separate at 20°C. The two systems were analyzed quantitatively by determining the pyrene rate parameters using phase and modulation lifetime data. Excimer formation, a bimolecular process, is described by a second order rate constant k_{DM}, multiplied by C, the probe concentration in the phospholipid. $k_{DM}C$ for PyrSPM in DPPC at 20°C is 1.5 times larger than that at 50°C. Since k_{DM} varies directly with temperature, the local probe concentration at 20°C must exceed the concentration at 50°C. This result provides direct quantitative evidence that PyrSPM and DPPC phase separate at 20°C. (Supported by USPHS Grants GM-14628 and HL-17576).

M-Pos135 LATERAL DIFFUSION OF GANGLIOSIDES IN DMPC BILAYERS, B. Goins, B.G. Barisas, and E. Freire, Dept. of Biochemistry, University of Tennessee, Knoxville, Tennessee and Dept. of Chemistry, Colorado State University, Fort Collins, Colorado.

The lateral mobility of ganglioside G_{M1}, incorporated into preformed DMPC vesicles was studied using the technique of fluorescence recovery after photobleaching. For these studies, 5-(((2-carbohydrazino)methyl)thio)acetyl) amino eosin (CMTAA-eosin) was covalently attached to the sialic acid moeity of the ganglioside. CMTAA-eosin labeled ganglioside G_{M1} exhibits a behavior similar to that of the unlabeled ganglioside G_{M1} and is able to bind Cholera Toxin. The lateral diffusion coefficient of the ganglioside was dependent upon the gel-liquid crystaline transition of DMPC. Above Tm the lateral diffusion coefficient of the ganglioside was $2x10^{-9}$ cm^2/sec (with >80% fluorescence recovery). This figure is almost one order of magnitude slower than that of the phospholipid. Increasing mole fractions of ganglioside, up to a maximum of 10 mole percent, did not have a measurable effect on the lateral diffusion coefficient or in the percent recovery. At 30°C, the lateral diffusion coefficient remained the same in the absence or in the presence of 5 mM Ca^{2+} suggesting that at least in the fluid phase, Ca^{2+} does not have a crossbridging effect on the ganglioside. Substituting unlabeled ganglioside Gd_{1a} or Gt_{1b} for the unlabeled ganglioside Gm_1 gave similar results at this same temperature. The addition of stoichiometric amounts of Cholera Toxin to samples containing either 1 or 10 mole percent ganglioside G_{M1} produced only a small decrease in the measured diffusion coefficient. Similar results were obtained from additional excimer/monomer ratio experiments using pyrene phospholipid derivatives. (Supported by NIH Grant GM-30819 (E.F.) and NSF PCM-8410763 (B.G.B)).

M-Pos136 ROTATIONAL MOTIONS OF PERYLENE IN LIPID BILAYERS: PRESSURE AND CHOLESTEROL EFFECTS. P.L.-G. Chong[1], B.W. van der Meer[2] and T.E. Thompson[1], [1]Department of Biochemistry, University of Virginia, Charlottesville, VA 22908 and [2] The Netherlands Cancer Institute, Plesmanlaan 121, NL-1066 CX, Amsterdam, The Netherlands.

Using steady state fluorescence polarization measurements, an isothermal pressure-induced phase transition was observed in dimyristoyl-L- -phosphatidylcholine multilamellar vesicles containing perylene. The temperature-to-pressure equivalence, dT/dP, estimated from the phase transition pressure, $P_{1/2}$, is about 22°C $kbar^{-1}$, which is comparable to values determined from DPH polarization (Chong & Weber, 1983, Biochemistry 22, 5544). In addition, we have employed a new method, introduced at this time, to calculate the rate of the in-plane rotation (R_{ip}) and the rate of the out-of-plane rotation (R_{op}) of perylene in lipid bilayers. The effects of pressure and cholesterol on the rotational rates of perylene in two lipid bilayer systems were examined. They are 1-palmitoyl-2-oleoyl-L- -phosphatidylcholine (POPC) multilamellar vesicles (MLV) and 50 mol % cholesterol in POPC (MLV). R_{op} is smaller than R_{ip} due to the fact that the out-of-plane rotation requires a larger volume change than the in-plane rotation. Cholesterol seems not to affect R_{op} significantly, but pressure causes a decrease in R_{op} by about a factor of three. In contrast, the effects of pressure and cholesterol on R_{ip} are less straightforward. At 1 atm, cholesterol increases R_{ip} by a factor of about two. Similarly, in the absence of cholesterol, 1.5 kbar pressure essentially triples R_{ip}. However, if both cholesterol is added and pressure is applied, R_{ip} decreases sharply. The possible interactions between cholesterol and perylene are discussed. (Supported by a NIH grant GM-14628).

M-Pos137 FLOW MICROFLUOROMETRY OF NATIVE LIPOPROTEINS AND SMALL UNILAMELLAR VESICLES.

M. Mims, J.K. Allen, D.K. Dennison and J. Morrisett, Baylor College of Medicine, Houston, Texas.

In the past, flow microfluorometry (FMF) has been used primarily to study large particles such as cells and cellular organelles. Recently, however, our laboratory has used FMF to analyze lipid vesicles 200-300 nm in diameter. We have extended this technique further to detect fluorescently labelled small unilamellar vesicles and lipoproteins ranging in size from 10-300 nm in diameter. Lipoproteins were labelled using a variety of standard techniques with the synthetic lipophile probe sn-1-palmitoyl-sn-2-[12-(N-4-nitrobenzo-2-oxa-1,3-diazole)]-aminocaproyl-phosphatidylcholine (NBD-PC). Small unilamellar vesicles were formed by sonication of egg yolk lecithin containing 2% NBD-PC. Because these particles are $\leq$ the wavelength of the light source (488 nm), the scattered light intensity is much less than for cells, thus very sensitive detection must be employed. Theory for Rayleigh scatterers predicts that scattered light intensity should be greater in the forward scattering lobe than at 90° to the incident beam, this was in fact observed, additionally, the right angle signal is complicated due to internal particle structure. NBD-labelled lipoproteins or vesicles were analyzed using an Ortho Series 50-H Cytofluorograph both for light scattering at low angles (2-5°) to the incident beam and for green fluorescence. Analysis of the histograms and cytofluorograms allowed assessment of the results of the labelling procedures in terms of efficiency, location and distribution of the probe molecules, and effect of the procedures on the structural integrity of the individual lipoprotein particles. The results indicate that the procedures used vary in their capacity to label effectively the lipoproteins, and in some cases to produce artifacts due to aggregated probe.

M-Pos138 ISOLATION AND CHARACTERIZATION OF A HIGH MOLECULAR WEIGHT ACTIN-BINDING PROTEIN FROM DICTYOSTELIUM DISCOIDEUM. Rick S. Hock and John S. Condeelis, Department of Anatomy, Albert Einstein College of Medicine, Bronx, N.Y. 10461.

Dictyostelium amoebae exhibit actin-dependent motile behavior such as phagocytosis, capping, pseudopod formation, and chemotaxis. Several actin-associated proteins (AAP) have been isolated from these amoebae including myosin, and proteins that gel, bundle, and sever actin filaments. The AAP are believed to specify the site of assembly and subsequent function of the actin-containing motile machinery.

We now report the isolation of a new high molecular weight actin-binding protein and its initial characterization. This protein is designated 240K based on its subunit mass on SDS PAGE. The 240K is isolated from a cell extract prepared by homogenizing vegetative amoebae in 5mM EGTA, 5mM PIPES, 1mM DTT, pH 7.0, followed by ultracentrifugation at 100,000g-1hr. The extract is fractionated by ion-exchange chromatography on ATP-saturated DEAE-cellulose. Fractions eluting between 0.17-0.19M KCl are greatly enriched for 240K and myosin. The myosin can be separated from 240K by dialyzing the pooled fractions to low salt and pelleting the myosin as thick filaments. The 240K that remains soluble is further purified by chromatography on hydroxylapatite and BioGel A15M.

The 240K protein binds to and sediments with filamentous actin at low salt (20mM KCl). Covalent crosslinking with dimethylsuberimidate demonstrates that the native protein is at least a dimer and may form larger polymers in 0.2M triethanolamine. Analytical gel filtration demonstrates that native 240K has a Stokes' radius of 11nm and an apparent molecular weight of ~850,000 daltons.

Further characterization of this protein is in progress to determine if it is a spectrin- or filamin-like protein. (Supported by NIH 25813 and a Hirschl Career Scientist Award).

M-Pos139 BINDING OF STREPTOCOCCAL M-6 PROTEIN TO ACTIN. J. M. Chalovich and V. A. Fischetti, East Carolina University, Greenville, NC and the Rockefeller University, New York, NY.

M proteins are antiphagocytic molecules on the surface of group A streptococci having physical characteristics similar to mammalian tropomyosin. Both are alpha-helical coiled-coil fibrous structures with a similar seven residue periodicity of non-polar and charged amino acids. We wish to determine if the observed similarity to tropomyosin could be extended to the ability of M protein to bind actin. Purified M6 protein isolated from an E. coli cloned to contain the streptococcal M6 gene was used for these studies. Binding of M protein to skeletal muscle actin was examined at 25° in a buffer containing 4 mM $MgCl_2$, 10 mM imidazole propionate pH 7.0, 0.5 mM EGTA, 0.5 mM DTT 0.5 mg/ml BSA and either 0 or 100 mM potassium propionate. At low ionic strength, mixtures of M protein and actin were turbid and an actin-M protein complex could be sedimented by brief low speed centrifugation. Using [^{125}I] M protein it was shown that the binding to actin increased in a hyperbolic manner with increasing M protein concentration. The binding constant of this interaction is estimated to be 3×10^4 M^{-1} with what appears to be a 1:1 stoichiometry. Neither tropomyosin nor the troponin-tropomyosin complex affected the binding of M protein to actin. Therefore, while M protein does bind to actin it does so in a way quite distinct from the interaction observed between tropomyosin and actin. Interestingly, myosin subfragment-1 does compete with M protein for binding to actin. In the presence of 100 mM potassium propionate the binding of M protein to actin is weakened considerably. Thus, it is not obvious at this time whether the observed interaction between M protein and actin plays a role in the pathogenicity of the group A streptococcus.

M-Pos140 PURIFICATION AND PROPERTIES OF THE 55,000-DALTON PEPTIDE COMPONENT OF THE ACANTHAMOEBA CYTOSKELETON. Takashi Ueno and Edward D. Korn, Laboratory of Cell Biology, NHLBI, NIH, Bethesda, MD 20205.

The Triton-insoluble cytoskeletal complex isolated from Acanthamoeba castellanii is highly enriched in myosin I, myosin II, actin and a 55,000-dalton polypeptide (Mr by SDS-gel electrophoresis) (T. Ueno and E.D. Korn, J. Cell Biol. 99, 34a). The 55K-protein accounts for 10% of the cytoskeletal protein and occurs in a molar ratio to actin of 1:5-6. The 55K-protein does not react with antibodies raised against tubulins from turkey brain and paramecium. To characterize the 55K-protein, we extracted it from the cytoskeleton with a buffer containing 10 mM imidazole, pH 7.0, 0.3 M NaCl, 5 mM DTT, precipitated it with ammonium sulfate (40-80% saturation), and purified it by DEAE-cellulose and hydroxyapatite chromatography to near homogeneity. By SDS-gel electrophoretic analysis of high speed centrifugal pellets, purified 55K-protein was found to bind to F-actin in 10 mM Tris-Cl, pH 7.5, 50 mM KCl, 2 mM $MgCl_2$, 0.1 mM $CaCl_2$, 0.2 mM ATP. The maximum molar binding ratio of 55K-dalton protein to F-actin subunits was about 1:1 by Coomassie blue staining. The 55K-protein appears to bind to actin more tightly in the absence of Ca^{2+} than in its presence. The 55K-protein increased the low-shear viscosity of F-actin in a concentration dependent manner and accelerated actin polymerization. Sedimentation equilibrium analysis revealed that the 55K-protein exists primarily as a 110K-dimer in 50 mM KCl. In the light of these results, the 55K-protein is assumed to be a new actin-binding protein possibly involved in cross-linking F-actin filaments in the Acanthamoeba cytoskeleton.
T.U. is supported by a fellowship from the Muscular Dystrophy Association.

M-Pos141 COMPARISON OF FLUORESCENCE AND LIGHT SCATTERING ASSAYS OF THE INHIBITION OF THE POLYMERIZATION OF ACANTHAMOEBA ACTIN BY ACANTHAMOEBA PROFILIN. Altaf A. Lal and Edward D. Korn, Laboratory of Cell Biology, NHLBI, NIH, Bethesda, MD 20205.

The critical concentration (Cc) of 5% pyrenyl-actin in 50 mM KCl, 1 mM $MgCl_2$, 0.1 mM $CaCl_2$, 1 mM EGTA, 0.2 mM ATP, 5 mM imidazole, pH 7.5, 25°C was 0.18 μM by light scattering and fluorescence assays. By light scattering, 10 μM profilin caused the same increase in apparent Cc at all actin concentrations consistent with a Kd of 3.9 μM for the 1:1 profilin-actin complex. By fluorescence, a Kd of 3.6 μM was obtained at very low actin concentrations but almost no effect of profilin was seen at higher (3-5 μM) actin. The discrepancy in the fluorescence data results from the very low affinity of pyrenyl-actin for profilin; Kd=39 μM for 100% pyrenyl-actin by fluorescence assay. At high total actin concentrations, therefore, the pyrenyl-actin is enriched in the F-actin. Elongation rates were measured using 1 μM 5% pyrenyl-G-actin and either 25 nm crosslinked dimer or 250 nm unmodified F-actin as seeds. By fluorescence, the inhibition of the elongation rate indicated an apparent Kd of 2.8 μM with 5 μM, 5.4 μM with 20 μM, and 9.9 μM with 50 μM profilin, respectively. On the other hand, by light scattering, a Kd of 2-4 μM was consistently obtained between 2 and 10 μM profilin and, at 20-50 μM profilin, the F-actin seeds depolymerized as expected from a Kd of 2-4 μM; the same results were obtained with unmodified G-actin. Thus, by light scattering assays, the same low Kd was obtained from Cc and elongation rate measurements, and the sequestering of G-actin in the 1:1 complex was sufficient to explain the inhibtion by profilin of actin nucleation, actin elongation and the concentration of F-actin at steady state. Supported in part by Muscular Dystrophy Association.

M-Pos142 ACTIN-ASSEMBLY ACTIVITY OF NEW CYTOCHALASIN ANALOGS. Angel Mozo-Villarias, Bennie R. Ware, Esther Garcia, and Grant A. Krafft, Department of Chemistry, Syracuse University, Syracuse, New York 13210

The cytochalasins are cytotoxic fungal metabolites that elicit a variety of responses in living systems. The cytochalasins are known to interact with actin filaments, and the effects of cytochalasins on actin self-assembly have been studied as a means of elucidating the assembly mechanism. We are particularly concerned with the structure-activity relationships of cytochalasins as they relate to the fundamental parameters of actin self-assembly. We have prepared structurally simplified cytochalasin analogs such as 1. The specific effects of these analogs have been determined using fluorescence photobleaching recovery (FPR). This technique permits the independent measurement of the state of aggregation of unassembled actin, the fraction of actin incorporated into filaments, and the average length of filaments. Sequential FPR measurements also permit determination of the kinetics of assembly. These kinetic data are corroborated using fluorescence enhancement of pyrenyl actin. Our results are significant both for the elucidation of structure-activity relationships in this family of compounds and for the preparation of new chemical probes with more selective molecular activities. (Supported by NIH Grant No. CA 35954 and NSF Grant No. PCM-8306006)

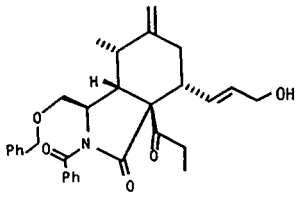

1

M-Pos143 PHOTOAFFINITY LABELING OF RABBIT SKELETAL MUSCLE ACTIN WITH 8-AZIDO-ADP. Charles W. Mahoney*. Biochemistry/Biophysics Program, Washington State University, Pullman, WA.

The photoaffinity analogs 8-azido-ADP and -ATP have been used to label the single ADP/ATP site on skeletal muscle actin. Viscometric analysis indicates that both of these analogs act as substrates for actin polymerization. The final level of polymerization (π_{sp}) in the presence of 5 mM 8-azido-ATP is 30-40% lower and the critical G-actin concentration is elevated 5 fold relative to control (5 mM ATP). The ability of F-actin to bind one non-exchangeable adenosine-5'-diphosphate per G monomer was exploited to stoichiometrically trap 8-azido-ADP in F-actin. This protocol allowed the removal of excess analog from F-actin and site-specific photo-incorporation. To further support site-specific labeling, competition experiments demonstrated that 8-azido-ADP binding and covalent incorporation can be totally inhibited in a linear fashion with increasing levels of ATP. Photolysis (450 W Hg lamp with pyrex filter, 4°C, 60 sec) of [β-^{32}P] 8-azido-ADP·F-actin (1:1, 8-azido-ADP:G monomer) after Dowex 1 removal of excess analog resulted in a maximal photo-incorporation efficiency of 4-5%. Preliminary peptide studies based on reverse-phase HPLC purifications, N-terminal determinations, and amino-acid compositions of tryptic peptides indicate that 60% of the label is located in a C-terminal peptide.

*Present address: Dept. of Physiology & Biophysics, University of Miami School of Medicine, Miami, FL 33101. Supported by N.I.H. grant AM 05195 to R.G. Yount.

M-Pos144 THERMODYNAMICS OF THE POLYMERIZATION OF Mg-ACTIN AND Ca-ACTIN. L.C. Gershman, L.A. Selden, and J.E. Estes: Medical and Research Services, Veterans Administration Medical Center, Albany and Depts. of Medicine and Physiology, Albany Medical College, Albany, NY 12208.

We have shown that exchange of the tightly-bound Ca^{++} in Ca-actin for Mg^{++} (forming Mg-actin) occurs during the lag phase in actin polymerization and that Mg-actin has a lower critical concentration (c_c) and a higher forward rate constant of polymerization (k_+) than Ca-actin (Biochemistry 23:2199, 1984; B.B.R.C. 116:478, 1983). We measured the effect of temperature in the range 5-35°C on the polymerization of pyrene-labelled Mg- and Ca-actin induced by the addition of phalloidin-stabilized actin nuclei and either 1 mM $MgCl_2$, 1 mM $CaCl_2$ or 20 mM KCl. Thermodynamic parameters for both actins were calculated from Arrhenius plots:

Reaction	Parameter	Ca-actin	Mg-actin
G ⇌ F equilibrium	Equilibrium enthalpy change (ΔH)	12	6
Forward polymerization	Activation enthalpy change ($\Delta H^*_{k^+}$)	12	11
Depolymerization	Activation enthalpy change ($\Delta H^*_{k^-}$)	0	5

The c_c values for Mg-actin are less temperature dependent than those for Ca-actin and the difference in these values appears to be a result of differences in the activation enthalpies of depolymerization. The equilibrium ΔH values for Ca-actin agree with published values; however, the activation enthalpy for polymerization is significantly lower than published values and, $\Delta H^*_{k^-}$ for Ca-actin is zero. The larger $\Delta H^*_{k^-}$ for Mg-actin agrees with our earlier conclusion that Mg-actin forms more stable polymers than Ca-actin. Supported by the Veterans Administration.

M-Pos145 HYDROSTATIC PRESSURE STUDIES ON THE POLYMERIZATION OF ACTIN. L.A. Selden, G. Strizich, L.C. Gershman, and J.E. Estes: Medical and Research Services, Veterans Administration Medical Center, Albany, and Depts. of Medicine and Physiology, Albany Medical College, Albany, NY 12208.

Earlier studies of the effect of applied hydrostatic pressure on actin polymerization indicated that the polymer elongation phase is associated with a volume change of activation of 75-100 cc/mole (Estes, J.E., Fed. Proc. 33:1522, 1974). Recent work in our laboratory has demonstrated differences between the polymerization properties of actin containing tightly bound Mg^{++} (Mg-actin) or Ca^{++} (Ca-actin). This was not appreciated at the time of the earlier hydrostatic pressure studies, so it was of interest to compare the effect of applied pressure on Mg- and Ca-actin separately. Pyrene-labelled actin was polymerized by addition of 50 mM KCl and phalloidin-stabilized actin nuclei, and rates of polymerization were determined before and immediately after pressure application (2 min duration) over the range of 0-16,000 psi. From these data estimates were made of the critical concentration (c_c) and forward polymerization rate (k^+m) for Mg- and Ca-actin (m=number concentration of actin nuclei). Values were calculated for the equilibrium volume change (ΔV), and the volume change of activation for the polymerization ($\Delta V^*_{k^+}$) and depolymerization ($\Delta V^*_{k^-}$) reactions. ΔV is approximately 46 cc/mole for Mg-actin and 81 cc/mole for Ca-actin. $\Delta V^*_{k^+}$ was small for Mg-actin and on the order of 40 cc/mole for Ca-actin, suggesting that the monomer conformations of Mg-actin and Ca-actin are different. $\Delta V^*_{k^-}$ was found to be similar for both actins and on the order of -40 cc/mole. The application of hydrostatic pressure thus facilitates depolymerization and increases the c_c. Supported by the Veterans Administration.

M-Pos146 THE EFFECT OF SOLUTION VARIABLES ON THE KINETICS OF MICROTUBULE ASSEMBLY, Janice S. Barton and Daniel Vandivort, Chemistry, Washburn University, Topeka, Ks. 66621.

The kinetic properties of bovine brain tubulin were examined while varying the solutions of conditions of assembly. The type of kinetics observed was dependent on total ionic strength (I). In0.1 M PIPES, pH 6.9 with I = 0.212, one growth step is observed, while at 0.05 M PIPES pH 6.9 with I= 0.106 or 0.1M MES pH 6.5 with I = .069 two steps are observed. Rate constant values were obtained by nonlinear least squares analyses of the data for a range of ionic strengths at constant pH and protein concentration by varying either KCl or PIPES. With increasing I, the fast rate decreased from a plateau value and the slow rate constant increased until the two merged. These rate constants are pseudofirst order and have a term containing the number concentration of microtubules, which equals the number concentration of nuclei. Changes in the rate constants with I could reflect a decrease in the concentration of nuclei for the fast step and a concomitant increase in the concentration of nuclei for the slow step. The extent of assembly evinced a maximum from I = 0.106 to I = 0.212 in PIPES and from I = 0.106 to .146 in KCl. Since PIPES and KCl have similar effects on the forward rate constant, this stabilization at higher I by PIPES could reflect an affect on the dissociation rate constant. These results reconcile the work of Johnson and Borisy (1977) J. Mol. Biol. 117, 1 done at I = 0.212 with that of Barton and Riazi (1980) Biochem. Biophys. Acta. 630,392 where I = 0.082 and Bayley et al., (1983) Biopolymers 22, 87 where I = 0.069 to 0.086. In the range of 6.5 to 6.9, the number of kinetic steps was independent of pH. Acknowledgment is made to the donors of The Petroleum Research Fund, administered by the ACS, for support of this research.

M-Pos147 ACTIVATION AND POTENTIATION OF DYNEIN ATPASE. John A. Evans and I. R. Gibbons, Department of Biochemistry and Biophysics, University of Hawaii, Honolulu, Hawaii.

Dynein ATPase is the mechanochemical transducing enzyme for microtubule-based motility. The principal isoenzymic form, dynein 1, can be solubilized from sperm flagellar axonemes of the sea urchin Tripneustes gratilla with 0.6 M KCl. In such solutions, dynein 1 has a low latent ATPase activity (0.1-0.2 umole Pi mg^{-1} min^{-1}) that can be reversibly activated about 10-fold by moderate concentrations of monovalent inorganic anions, with their relative effectiveness following the Hofmeister lyotropic series. Organic anions, such as acetate, both stabilize the latent state of dynein during storage and antagonize the activation due to chloride. On the other hand, dynein 1 ATPase activity is potentiated (increased irreversibly) 10-fold by exposure to appropriate concentrations of organic solvents or of Triton X-100. ATP largely protects the latent form of dynein 1 against this potentiation by Triton. Determination of the amplitude of the presteady state Pi burst of latent and Triton-potentiated dynein suggests that the dynein 1 molecule of Mr 1,250,000 has two active sites and that the increase in activity upon potentiation does not result from an increase in the number of active sites. These data suggest that the latent and potentiated states of solubilized dynein may be kinetic analogues of the coupled non-motile and the coupled motile states of dynein in the intact axonemal complex. (Supported by NIH Grant GM 30401).

M-Pos148 DIFFERENTIAL CALMODULIN BINDING BY AXONEMAL PROTEINS OF CALCIUM-INHIBITED AND CALCIUM-ACTIVATED CILIA IN MYTILUS GILL. R. E. Stephens and E. W. Stommel, Marine Biological Laboratory, Woods Hole, MA 02543 and Boston University School of Medicine, Boston, MA 02118.

Pure calcium-inhibited lateral cilia and a mixed population of calcium-insensitive and calcium-activated cilia can be isolated selectively from Mytilus gill (Stommel, J. Comp. Physiol. in press, 1984). The respective calcium-mediated inhibition or activation can be reversed by inhibitors of calmodulin. Motility of lateral cilia is activated by serotonin, known to raise cAMP levels. We showed previously (Stommel and Stephens, J. Cell. Biol. abstr., 1984) that cAMP could overcome calcium-induced arrest of ATP-reactivated cilia in cell models of lateral cells and that cAMP caused specific phosphorylation of 3 polypeptides (MW = 23K, 16K, 14K) associated with the dynein fraction of these cilia. Although having virtually identical polypeptide composition, the mixed population axonemes showed little cAMP-dependent phosphorylation. Using gel overlay techniques, with ^{125}I-calmodulin, we now find that the 23K and 16K polypeptides of lateral ciliary axonemes bind calmodulin in a calcium-independent manner, whereas the 14K binds little. Conversely, in axonemes from the mixed population cilia, the 23K and 16K chains bind little calmodulin while the 14K binds calmodulin strongly, in a calcium-dependent manner. Together, these observations suggest that the lateral cilia are activated by serotonin through the cAMP-dependent phosphorylation of 3 regulatory polypeptides but, upon mechanical stimulation (which causes a calcium influx) they are inhibited through calmodulin associated with the 23K and 16K chains. In calcium-activated cilia, where a mechanically-induced calcium flux stimulates movement, calcium may regulate motility by binding to calmodulin associated with the 14K polypeptide. Support: NIH GM 29,503 and GM 20,644.

M-Pos149 MECHANICAL STIMULATION ACTIVATES BEATING IN CALCIUM-ARRESTED LATERAL CILIA OF MYTILUS EDULIS GILL. E. W. Stommel, Marine Biological Laboratory, Woods Hole, MA 02543 and Department of Physiology, Boston University School of Medicine, Boston, MA 02118 (Intro. by E. R. Baylor).

Lateral (L) cilia of Mytilus gill arrest upon mechanical stimulation, the result of calcium influx. A mechanical stimulus which deflects these cilia towards the effective stroke, and is normally sufficient to cause transient arrest in beating L-cilia or transient movement into the recovery stroke in quiescent cilia, initiates beating in Ca^{++}/ionophore arrested cilia at 9-15 Hz, for periods as long as 30 seconds. Movement is restricted to the stimulated cell and the beat pattern appears constrained to the first half of the beat cycle. After application of ionophore in Ca^{++}-free/EGTA seawater, the cilia become quiescent, stopped at the end of the recovery stroke, but beating occasionally at 9-15 Hz. Mechanical stimulation again causes activation of beat, with a similar range of frequencies and duration as in Ca^{++}-arrested L-cilia, but the beat pattern is normal and cilia of adjacent cells may also beat, presumably initiated by mechanical coupling. In the presence of ATP, mechanical stimulation of detergent-permeabilized L-cell models arrested in the presence of 50 μM Ca^{++} will also cause activation comparable in frequency, duration, and beat pattern as seen in Ca^{++} arrested cells, but the initiation is more difficult. Mechanical activation of quiescent lateral cilia by deformation of the basal region with small, slow displacement of the mechanical probe will initiate several beat cycles but will cause Ca^{++} arrested cilia to "snap" into the effective stroke and back. These data indicate that Ca^{++} arrest does not involve any permanent "rigor" dynein bridges and suggest that mechanically-labile attachments, possibly via interdoublet links, are important in holding the axoneme in the arrest position. NIH GM 29,503.

M-Pos150 THE EFFECTS OF NOCODAZOLE, TAXOL AND TUBULAZOLE C ON THE MICROTUBULAR ORGANELLES IN THE CILIATE, STENTOR COERULEUS. V. K-H. Chen, Department of Biophysical Sciences, State Univ. of New York at Buffalo, Buffalo, New York 14214

The ciliate,Stentor coeruleus has several prominent groupings of microtubules: membranellar band, body cilia, Km fibers, ramifying zone,links between marconuclei.These grouping are such that small alterations in the tubules results in marked changes in cell structure and behavior. We found each of these drugs to have very distinctive effects. Nocodazole caused continuous backward swimming to the right. The circular paths continued until the cell began to extend.Forward swimming returned upon maximum extension(2-3x rest length). Cell contraction and relaxation were unhindered even up to 10mg/ml Nocodazole. Feeding,division and conjugation appeared normal except that the cell was a long trumpet rather than a pear shape. Taxol, a microtubule stabilizer Stentor to swim stright backwards continuously. The posterior third of the body quickly became fluted. The cell extended by about 30%. Eversion of the gullet occured. Then shedding of the membranellar band occured with the lifting beginning at the distal end. The cell then spun rapidly in place alternately to the left and then to the right,repeatedly. The effects were not reversible. All effects of Nocodazole were reversible. The extended cell in a mixture of Nocodazole and Taxol had extremely posterior two thirds.Occasionally a sharp spike could be seem to protrude from the side of the cell. When Stentor was exposed to Tubulazole C the membranellar band was immediately shedding from the distal end. Straight backward swimming occured continuously. Contraction and relaxation occured unhindered. The macronuclei fused.The clear strip in the ramifying zone broadened.Self minicing of body pattern occured after pellicel split.

M-Pos151 DIRECT VISUALIZATION OF ORGANELLE MOVEMENT ALONG ACTIN FILAMENTS DISSOCIATED FROM CHARACEAN ALGAE CELLS. B. Kachar, Laboratory of Neurobiology, NIH, Bethesda, MD 20205 (Intr. by R.L. Ornberg).

Binding and continuous unidirectional movement of organelles along isolated transport cables are directly visualized by video light microscopy after the dissociation of the cytoplasm of characean algae cells in a Ca^{++} free buffer containing ATP. Organelles in Brownian motion bind to the cables after random collisions and immediately display smooth movement along its surface. Individual organelles have more than one attachment site and move at mean rates of 11.2 ± 0.1 μm/s or 62.3 ± 1.1 μm/s along multiple parallel pathways on each cable. Organelle movement was undisturbed when rhodamine-phalloidin (0.2 μM), a fluorescent-labelled toxin that binds specifically to actin, was present in the medium. The fluorescent compound specifically labelled the transport cables. Freeze-etching electron microscopy of this preparation shows organelles closely associated with the surface of long cables made of compact bundles of 6-8 nm thick filaments. Individual filaments display substructure similar to that of actin filaments. The estimated number of filaments per cable varies from 10 to more than 80. Since actin filaments are the only detectable linear components of the cables, it is likely that single actin filaments are the structural units of the multiple tracks at the surface of the cables. The requirement of ATP to support movement along the actin filaments suggests that an actin activated ATPase is directly involved in this process. Regulatory proteins associated with the actin filament such as troponin and tropomysin need not be involved in this system since the movement does not require Ca^{++}. It is conceivable that the only elements involved in the mechanism of organelle movement in this system are actin and an actin activated ATPase present at the surface of the organelle. This preparation allows organelle transport to be studied without the influence of an organized cytoplasm. Under these conditions, characteristics of organelle movement should reflect directly the underlying molecular processes of binding and force generation.

M-Pos152 STEADY CURRENTS GO THROUGH ACETABULARIA CRENULATA: A VIBRATING PROBE ANALYSIS. N.S. Allen and E.A. Bowles, Dept. of Biology, Wake Forest University, Winston-Salem, N.C. 27109. (Intr. by G. Holzwarth).

Large, steady light responsive currents have been found to go through the giant marine unicellular alga, A. crenulata as measured with a vibrating probe (Jaffe and Nucitelli 1974, J. Cell Biol. 63:614-628). Currents of Acetabularia grown at 27°C in a 8/16 hour light/dark regime were measured at the midpoints of each light and dark period. Large currents, with current densities (δ) ranging from 10-500 μA cm^{-2} enter the rhizoid of A. crenulata (light regime) cells illuminated with actinic light at an intensity of 300-500 μA cm^{-2}. Smaller currents (δ = 1-20 μA cm^{-2}) leave the stalk along its entire length, diminishing towards the apical end. The same cells were measured during the middle of the dark regime under 546 nm green light and all the currents were dramatically diminished (δ = 1-5 μA cm^{-2}). Rough calculations indicate that inward and outward currents were approximately equal. These currents are light responsive. When lights were extinguished during the light regime, currents decayed within 2 minutes to values near or at zero. Exposure of cells to white light during the dark period, caused currents to rise dramatically. Increasing the intensities of light resulted in increased currents with maximal currents measured at intensities between 300 and 700 μW cm^{-2}. Future studies of these currents will attempt to characterize the ionic components, map cells in all stages of growth, examine currents in regenerating nucleate and anucleate cell fragments and investigate the relationships of these ionic currents to cytoplasmic streaming. (This work was performed at the National Vibrating Probe Facility, MBL, Woods Hole, MA. 02543 with the invaluable help of L. Jaffe, C. Scheffey, A. Shipley and K. Robinson. Supported by Carswell and Archie Funds, Wake Forest University.)

M-Pos153 LOWERING PH_i INHIBITS PLATELET SHAPE CHANGE. Vivianne T. Nachmias, Department of Anatomy, School of Medicine, University of Pennsylvania, Philadelphia, PA 19104

To test further the hypothesis that platelet pH is a significant variable for platelet activation, we diluted platelet-rich plasma (PRP) with 135 mM NaCl, 5 mM KCL, 100 mM EGTA and 30 or 100 mM imidazole to yield final pH_e 6.0-7.2 and used salts of weak acids to replace NaCl. We measured shape change, platelet volume, and internal pH at differing pH_e. Shape change was measured by rate of rise in A and change in oscillation signal of 10^8/ml stirred platelets at 37°C after 10 µM ADP at 609nm in a Gilford spectrophotometer; chart speed 10 sec/inch. Platelet volumes were estimated by double label counting (^3H-H_2O and ^{14}C-sucrose). Platelet pHs were measured by ^{14}C-DMO distribution. Data were analyzed with a visicalc program. Platelet shape change (PSC) was relatively independent of pH_e in NaCl. Sustained inhibition of PSC was seen with all weak acids studied as a negative function of pH_e to 90% inhibition at pH_e 6.0; pH_i in propionate was 0.3-0.4 pH units below that in NaCl. Level of imidazole affected pH_i and PSC. Platelet volumes increased 6% in NaCl and 10-50% in propionate; the increases were inhibited 100% with 1 mM amiloride, but inhibition of PSC was unaffected or slightly increased. Rapid reversal of the inhibition of PSC was caused by alkalinization of pH_e without additional ADP; an overshoot in rate was observed. A-23187 induced PSC was also inhibited by weak acids, suggesting that perhaps cytoskeletal response is affected by low pH_i.

Supported by HL-15835 to the Pennsylvania Muscle Institute. I thank M.C. Glennon for outstanding technical assistance.

M-Pos154 THRUST GENERATION BY MAMMALIAN SPERMATOZOA AGAINST THE ZONA PELLUCIDA D.F. Katz[1] and N.J. deMestre[2], [1]Department of Obstetrics and Gynecology, University of California School of Medicine, Davis, Ca. 95616 and [2]Department of Mathematics, Royal Military College, Duntroon, Australia.

Mammalian spermatozoa must penetrate an accellular, proteinaceous vestment, the zona pellucida, immediately before fertilizing the ovum. In most mammals, only one sperm penetrates the zona, and thus monospermic fertilization is assured. The physicochemical mechanisms of zona penetration are not well understood. Thrust generated by the beating sperm flagellum must be the driving force, but sperm lytic enzymes might also act to lessen the zona resistance. We have begun to analyze the biomechanics of this process, and present here the results of our initial hydrodynamic computations of sperm thrust against the zona. Our technique consists of determining flagellar thrust in an infinite fluid and, in a separate computation, determining the extent to which this is augmented by the fluid-constraining presence of the zona. The methods of slender body theory at low Reynolds number are employed. Experimental data from our high-speed videomicrographic studies of sperm penetration of the zona serve as input to the computations. We have found that if a spermatozoan is oriented at right angles to the zona surface, it thrusts approximately 20% harder than in free fluid. If, however, the sperm is oriented obliquely, which is typical of most mammals, thrust amplification can be as much as 85%. Typical forces generated by human, rabbit, and hamster spermatozoa against the zona material are, respectively, 0.38×10^{-5}, 0.80×10^{-5}, and 3.57×10^{-5} dynes. (Supported by NIH grant HD12971).

M-Pos155 COMPLEX BACTERIAL FLAGELLA OF *RHIZOBIUM LUPINI* ARE PERTURBED FORMS OF PLAIN FLAGELLA. S. Trachtenberg, S.I. Aizawa+, D.J. DeRosier and R.M. Macnab+, Rosenstiel Center, Brandeis Univ., Waltham, MA 02254 and +Dept. of Molecular Biophysics & Biochemistry, Yale Univ., New Haven, CT 06577 .

The bacterial flagellum consists of a basal body (motor), a hook (universal joint), and a filament (propellor). There are two morphologically distinct kinds of bacterial flagella: Plain — present in most bacterial species, and complex — found only in *R. lupini*, *R. meliloti*, and *Pseudomonas rhodos*, and having an apparent three-stranded outer helical sheath. However, both kinds of filament are made from only one species of protein-flagellin. Based on diffraction studies of negatively stained low dose images of plain (*Salmonella typhimurium*, *Escherichia coli*) and complex (*R. lupini*, *P. rhodos*) filaments, we demonstrate that the symmetry is easily derived from that of plain filament: the unit cell of complex filaments is twice as wide as that of plain filaments. Based on STEM mass measurement, monomer molecular weight and rise per subunit, we find that the unit cell of the complex filaments is occupied by two flagellin molecules. A three-dimensional reconstruction of *R. lupini* H13-3 filaments was carried out to 26Å resolution. The main features of the reconstruction are: an outer three-start helix with deep grooves between windings, a solid eleven-start cylinder, three inner helical tubes and a central channel. The filament is thus constructed from four concentric cylinders which contribute to its rigidity without addition of mass. The rigidity is believed to be an adaptation to motility in viscous media. We suggest the evidence points to the complex filament as a variant of the plain filament structure in which there is a pairwise perturbation of neighboring subunits.

M-Pos156 EVALUATION OF THE INHIBITORY ACTION OF cAMP ON CELL DIVISION IN TERMS OF TRANSITION PROBABILITY THEORY. Mary N. Stamatiadou, Department of Biology, Nuclear Research Center "Demokritos", Aghia Paraskevi Athens, Greece.

Non-dividing quiescent Balb/c-3T3 cells, maintained in culture, can be stimulated by serum to reenter the process of cell division. In such stimulated cells the mean length of the prereplicative (G_0-G_1) phase is about 14 h and is independent of serum concentration or of cell density. At some point during the prereplicative phase the stimulated cells become irreversibly committed to proceed to DNA synthesis and mitosis. Despite their previous synchronization in G_0, serum-stimulated cells exhibit a spread of about 3-4 h in S phase initiation times. Exogenously administered cAMP at 0.5 mM elicits a 100% inhibition of DNA synthesis and mitosis, if administered to the cells throughout the prereplicative phase. The early part (up to 8 h) of the prereplicative phase is 59% less susceptible to the action of exogenous cAMP than the later part during which the cells become irreversibly committed to proceed to completion of the cell cycle. cAMP has no effect if administered during S phase. When added to continuously dividing cells for a period equal to one generation time, under the above conditions, cAMP elicits only a partial inhibition, the extent of which correlates with the percentage of cells in G_0-G_1 within the random population. Probabilistic models of the cell cycle can satisfactorily account for the observed kinetics of entry into S phase. The described traits of cAMP inhinition of cell division are compatible with a two-transition model in which the first transition occurs during the early part of the prereplicative phase and may be out of phase with the conventional cell cycle in continuously dividing cells, while the second transition occurs at or near the G_1/S boundary.

M-Pos157 STUDY OF CELL-SUBSTRATE CONTACT BY TOTAL INTERNAL REFLECTION FLUORESCENCE MICROPHOTOMETRY. F. Lanni and D. L. Taylor, Center for Fluorescence Research in Biomedical Sciences, and Dept. of Biological Sciences, Carnegie-Mellon Univ., 4400 Fifth Ave., Pittsburgh, PA 15213.

Total internal reflection fluorescence (TIRF) microscopy was introduced by Axelrod (J. Cell Biol. 89, 141-145, 1981) as a means to form images of only the contact regions of cells attached to a planar substrate. The brightness of any zone of a TIRF image is a function of the multi-layer structure of the specimen, the refractive index of each layer and of the substrate, and the distribution of fluorescent dye in the specimen within roughly 200nm of the substrate. By measuring TIRF emission as a function of excitation angle-of-incidence, the distance between the substrate and the fluorescent structures in or on adherent cells can be estimated. 3T3 cells growing on microscope slides were stained by loading fluorescein-dextran or carboxyfluorescein into the cytoplasmic compartment. Close-contact and focal-contact zones, as defined by Izzard and Lochner (J. Cell Sci. 21, 129-159, 1976), were located in the reflection interference image, and measurements of TIRF emission were made at those locations. Our data indicate that the boundary of the cytoplasmic compartment is about 20nm from the substrate in close contact zones, if the cytoplasmic refractive index in the cortex is about 1.37. Essentially the same result was obtained for focal contacts. By labeling different components or compartments of a cell, such as the plasma membrane, actin, vinculin, etc., a structural model of the cell-substrate contact zone can be developed by study of only intact cells.

This work was supported by a grant from the Council for Tobacco Research-U.S.A. (#1412).

M-Pos158 MONITORING CELL BEHAVIOR IN TISSUE CULTURE BY MEASUREMENTS OF ELECTRICAL IMPEDANCE, **I. Giaever and C.R. Keese, General Electric Research and Development Center, P.O. Box 8, Schenectady, NY 12301.**

Mammalian fibroblasts have been cultured on evaporated gold electrodes subjected to an alternating electric field at 4000 Hz (1). When cells attach and spread on the electrodes, the measured impedance of the system increases and following cell spreading begins to fluctuate with time. The amplitude of these fluctuations is greatly reduced by cytochalasin B suggesting they are a consequence of cell motion. We have determined the power spectrum of these fluctuations in the range of 10^{-3} to 1 Hz for both the normal human diploid WI-38 line and its transformed counterpart (WI-38/VA-13). The power spectra for these cell lines have similar shapes but are approximately an order of magnitude lower for the normal WI-38 cells than for the transformed line.

The system has also been employed to study the dynamics of cell attachment and early spreading, where the electrodes have been precoated with specific proteins. The slope of the initial increase in impedance is highly dependent upon both the adsorbed protein coat and the type of cell line studied. This application of the system provides a new method to study the time course of early events in cell-substrate interactions.

(These studies were conducted in part pursuant to a contract with the National Foundation for Cancer Research.)

(1) Giaever, I. and C.R. Keese, Proc. Natl. Acad. Sci. USA 81, 3761 (1984).

M-Pos159 STRENGTH OF ACTIVATION IN CONTRACTING MUSCLE FIBERS AS REVEALED BY LIGHT DIFFRACTION. A. F. Leung and M. K. Cheung, Department of Physics, The Chinese University of Hong Kong, Hong Kong.

Single semitendinosus muscle fibers of frog were illuminated with a He-Ne laser. The intensity and substructure pattern of the first-order diffraction were measured during isometric contractions. The intensity decreased to a minimum at the peak of shortening and then returned to its original value at the end of relaxation of the fiber. During the initial phase of contraction the substructure pattern remained the same. However, a new pattern developed at the peak of shortening. The basic unit of light diffraction is the sarcomere. The intensity is mainly determined by the internal properties of individual sarcomeres (structural factor) and the relative optical positions of the sarcomeres (interference). If the interference factors of the resting and activated sarcomere arrays of the same sarcomere length are equal, the diffraction substructure patterns of these two arrays would be the same and the intensity difference between the two patterns would indicate the degree of sarcomere activation. The intensity difference could be caused by a decrease in the refractive index of the activated sarcomeres resulting from the interaction between the thick and thin filaments. The intensity difference decreases linearly with sarcomere length. This relationship is consistent with the crossbridge model. The intensity difference can be a measure of the strength of activation between the contractile proteins or the crossbridge population.

M-Pos160 OPTICAL ELLIPSOMETRY OF SINGLE FIBER DIFFRACTION ORDERS. Y. Yeh, R. J. Baskin, K. Burton. Depts. of Applied Science and Zoology, University of California, Davis, CA 95616.

The optical depolarization signal on the diffraction pattern obtained when light is scattered from single fibers of skeletal muscle contains information on molecular orientation and dynamics. In previous reports, the measured phase angles, δ, of the resulting elliptically polarized light have been interpreted as arising from optical anisotropy within the sarcomeric unit. This anisotropy, however, has as its sources, both intrinsically anisotropic elements and form anisotropy from the orderly arrangement of isotropic elements. Thus, this measurement is very similar to transmission birefringence experiments except that the birefringent elements now exhibit the added feature of sarcomeric periodicity. We have now studied the anisotropy of the signal amplitudes or intensities along and perpendicular to the fiber axis. These signals are uniquely attributable to the intrinsically anisotropic elements of the sarcomere whose polarizabilities are α_1 and α_2, parallel and perpendicular respectively to the fiber axis. The orientation of intrinsically anisotropic elements can also be estimated using a model where all these elements are assumed to have the same angle of declination. The isometric relaxed-to-rigor transition has been re-examined using this new technique. Measurements were conducted at several ATP concentrations and different sarcomere lengths. The measured difference between the diffraction order birefringence and the polarizability changes provides us with a new handle on crossbridge dynamics.

Work supported by NIH AM 26817 (YY) and NSF PCM 83-00046 (RJB)

M-Pos161 THEORETICAL FRAUNHOFER LIGHT DIFFRACTION PATTERN OMEGA SCANS CALCULATED FROM REAL AND MODIFIED STRIATED MUSCLE 3-D SARCOMERE ARRAYS. K.P. Roos and A.F. Leung. Dept. of Physiology, UCLA, Los Angeles, Ca. 90024 and Dept. of Physics, The Chinese Univ. of Hong Kong, Hong Kong.

We recently demonstrated that Fraunhofer diffraction patterns could be calculated by numerical methods from real 3-D sarcomere position data of resting heart muscle cells (Roos and Leung, Proc. 8th Intl. Biophys. Cong., 1984). These theoretical diffraction patterns have the same characteristic features observed in real resting striated muscle patterns including omega (Ω) scans (layer line intensity vs. data array rotation angle Ω). Over the range of a calculated $\pm 30°$ Ω scan, the intensity of each layer line varies smoothly and reaches a maximum at a specific Ω angle for a given cell. The shapes of corresponding right and left Ω scans are qualitatively the same, but the major peaks are shifted from each other by an angle equal to the diffraction angle of that order. Furthermore, these paired peaks are not necessarily symmetrical about $\Omega=0°$ which may indicate striation skewing between focal planes. In order to determine the spatial dependence of diffraction pattern layer lines upon discrete sarcomere structures, 3-D data arrays were modified and Ω scans recalculated. A complete $180°$ Ω rotation of the data yields identical diffraction patterns and Ω scans to control. A focal plane reverse stacking (only changes along the optical axis) yields mirror image theoretical diffraction patterns including the fine structure and Ω scans. Random ordering of the focal planes yields the same diffraction angular separations but different fine structures and Ω scans. These data suggest that the 3-D structural ordering within striated muscle plays a significant role in diffraction pattern layer line intensities and fine structure, but not in average layer line angular separations. (Supported by USPHS HL29671).

M-Pos162 ANALYSIS OF 3D CELL IMAGES FOR GRAPHIC MODELLING AND ANALYSIS. Fredric S. Fay, Kevin E. Fogarty & James M. Coggins. Univ. Mass. Med. Ctr., Dept. of Physiol., Worc., MA 01605 and Comp. Sci. Dept., Worc. Poly. Inst.

Computer analysis of cell images often requires location of structures of interest and measurement of salient features of those structures for use either in developing models or in automatic decision making. Ongoing studies of the mechanism of force generation in smooth muscle require a model for the location and orientation (in 3D) of elongated bodies rich in α-actinin. These bodies are believed to be integral to the contractile apparatus whose organization we wish to understand. In relaxed cells these bodies are on average 1.25 μm long, 0.25 μm wide, and oriented within 15° of the cells' long axis. To assess the pattern of organization of these bodies we obtain a set of optical sections of fluorescence due to fluorescently labelled anti-α-actinin in a single cell. An iterative deconvolution procedure is applied to the 3D data to reduce distortion caused by the image acquisition system. Subsequent analysis to determine the position and orientation of all α-actinin rich bodies is performed by an artificial visual system consisting of three 3D spatialfilter sets. In the first stage of analysis, local maxima in the output of one filter are thresholded to locate body centers. Next, the pattern of responses of each body to a set of 4 filters is used to determine the angle between the long axis of the body and the long axis of the cell. A set of 6 filters is used to determine the orientation of the projection of the long axis of the body on a plane normal to the long axis of the cell. The resulting information about 3-D position and orientation of all α-actinin rich bodies is used to analyze the organization of the contractile apparatus in smooth muscle. The use of this artificial 3D visual system in analyzing other aspects of cell organization is presently being explored. Supported by grants from NIH (HL14523) and the MDA.

M-Pos163 CROSS-BRIDGE INTERCONNECTIONS BETWEEN THICK FILAMENTS IN STRETCHED SKELETAL MUSCLE FIBERS. A. R. Crooker and G. H. Pollack, Center for Bioengineering, WD-12, University of Washington, Seattle, WA 98195.

Cross-bridge interconnections between thick filaments have recently been observed in stretched skeletal muscle fibers by the freeze-fracture/etch method (Suzuki and Pollack, Biophys. J. 45:104a, 1984). Observations are reported here that confirm the presence of these thick-thick interconnections in serial ultrathin sections of chemically fixed, plastic embedded fibers.

Single fibers were isolated from the semitendinosus muscle of the frog, Rana temporaria, in Ringer's solution, mechanically skinned in a relaxing solution, then stretched to 40% greater than resting length to reduce the overlap of thick and thin filaments. Primary fixation was in 2.5% glutaraldehyde in 0.1 M sodium cacodylate buffer and 1% tannic acid following gradual replacement of the relaxing solution by the fixative. Post-fixation was in 2% osmium tetroxide in distilled water followed by dehydration in a graded ethanol series and subsequent embedding in Medcast. Serial ultrathin sections were stained with uranyl acetate followed by Reynold's lead citrate, then examined in the electron microscope.

Micrographs of ultrathin serial cross sections through entire sarcomeres revealed the presence of interconnections between thick filaments not only in the M region at the center of the sarcomere, but also in the remaining regions throughout the H zone. The latter interconnections were not as robust or as intensely staining as those in the M region, and were more readily observed in fibers prepared in low ionic strength solutions. The nature of these interconnections is not known, but the structures may be formed by the joining of two opposed myosin S-1 heads projecting from adjacent thick filaments.

M-Pos164 RESTING TENSION IN FROG SKELETAL MUSCLE IS BORNE MAINLY BY MYOFIBRILS. Douglas J. Law and Alan Magid. Department of Anatomy, Duke University Medical Center, Durham, NC 27710.

The relation between sarcomere length (s.l.) and passive tension has been determined for the semitendinosus muscle (dorsal head) of R. pipiens, from slack length ($s.l._o$) to beyond filament overlap. S.l. was measured by light diffraction using a He-Ne laser. Stepwise stretches caused stepwise increases in force which partially decayed. S.l. remained unchanged during stress relaxation. The time-course of decay was analysed (in one experiment) into two exponential components. The faster component was too small to measure accurately. The time constant of the slower component increased from 50 sec at s.l. 2.7 μm to 1180 sec at s.l. 4.2 μm. Tension (σ) at long times was reasonably well described by the expression $\sigma = E_o/\alpha(e^{\alpha\epsilon_s}-1)$, where ϵ_s is sarcomere strain, $\frac{s.l. - s.l._o}{s.l._o}$. For 12 muscles, $s.l._o$ = 2.14±0.06SD μm, α = 4.28±0.64SD, and the initial modulus, E_o, = 2.6±0.8 × 10^3 N/m^2. Muscle cross-sectional area was estimated from width and thickness measurements, assuming an elliptical profile. These mechanical parameters were the same for muscles studied in either normal or calcium-free Ringer's. These values for $s.l._o$, α, and E_o do not differ significantly from those found for mechanically-skinned fibers from semitendinosus muscle (Magid, ms submitted). During stress relaxation, skinned fibers also maintain constant s.l. and show similar rates of tension decay. We conclude that, up to s.l. 4.0 μm, resting tension arises entirely from the intrinsic elasticity of the myofibrils with no detectable contribution from connective tissue. Supported by NIH grant AM27763 and the N.C. United Way.

M-Pos165 INHOMOGENEITY AND OSCILLATION IN THE ACTIVATION PATTERN OF SKELETAL MUSCLE FIBERS DURING THE PLATEAU OF FUSED TETANIC CONTRACTION. Mark Sharnoff and Lawrence P. Brehm, Department of Physics, University of Delaware, Newark, DE 19716

We have used a coherent, microdifferential imaging method to study changes in the appearance of isolated frog tibialis or semitendinosus fibers after the creep phase of tetanus is complete. The changes we observe are far more inhomogeneous and striking than suggested by ordinary, white light microscopic observations of the tension plateau, which indicate only gradual, slow sliding of myofibrils or myofibrillar bundles past one another. Our differential images frequently show very bright, longitudinal filamentary structures which appear to be thin bundles of myofibrillar segments of length ca. 40 striation periods. These bundles are often transversely clumped and well-separated longitudinally. A weak, finely grained speckle pattern normally occupies the space between the clumps. The bright filaments are regions of pronounced or rapid configurational change apparently organized along myofibrillar lines. The changes which occur within the speckled regions are much slower, and they are apparently confined to individual sarcomeres distributed at random. In a sequence of images made with the first exposure flash occurring at a common point on the plateau and the second flash progressively delayed from 3 to 50 msec (20°C), the filamentary structures may fade and disappear, or they may appear and enlarge, with the passage of time. Occasionally, having disappeared, they reappear at locations they previously occupied.

These results suggest that even under maximal activation of a fiber as a whole, and during tension which appears to be steady, the local strain or level of activation may fluctuate, and even oscillate, widely in time.

M-Pos166 COHERENT IMAGING OF REACTIVATION PATTERNS IN PARTIALLY ACTIVATED SKELETAL MUSCLE FIBERS Lawrence P. Brehm and Mark Sharnoff, Department of Physics, University of Delaware, Newark, DE 19716

The maximal isometric tension developed during a single twitch of a well-rested muscle fiber is invariably smaller than that which appears during fused tetanic contraction, a situation normally attributed to the failure of a single stimulus to produce total activation of the fiber. It may be asked whether the incremental activation produced by subsequent stimuli is qualitatively similar to the initial activation manifest just at the end of latency relaxation, before active shortening occurs, as an abrupt increase in fiber stiffness. We have used a holographic technique to study the spatial distribution of activation in frog tibialis fibers given one or a pair of brief stimuli. When applied, the second stimulus was interposed between two holographic exposure flashes and delivered at the peak of the twitch evoked by the first. Holographic images made in the presence of the second stimulus showed a normal filamentary structure of activated myofibrillar segments (Science 223, 822 (1984)). Images made under identical conditions, but without the second stimulus, were highly speckled and showed superficial connective tissue prominently, thus demonstrating both more gross motion of the fiber and more random, local motion in individual sarcomeres than in the doubly stimulated counterparts. In any fiber, the spatial distribution of activation evoked by the second stimulus appears not to have elements in common with that evoked by the first stimulus.

M-Pos167 STRUCTURAL CHANGES IN THE THICK FILAMENTS OF FROG SKELETAL MUSCLE AS EXTERNAL PRESSURE ON THE FILAMENT LATTICE IS VARIED. T. C. Irving and B. M. Millman, Biophysics Interdepartmental Group, Physics Department, University of Guelph, Guelph, Ontario, Canada, N1G 2W1.

Thick filament lattice spacings as a function of external osmotic pressure have previously been determined for the A-band of chemically-skinned frog skeletal muscle under relaxed and rigor conditions (Millman et al., 1983, Biophys. J. 41:259; Irving & Millman, 1984, Biophys. J. 45:101a). The intensity ratio of the 1,1 and 1,0 equatorial X-ray reflections (I_{11}/I_{10})increases significantly as the external pressure increases and the lattice spacing decreases. From Fourier reconstructions, the diameter of the electron density distribution at the thick filament positions in the lattice of relaxed muscle decreases by about 20% over an applied pressure range from 0 to 20 torr. It then remains nearly constant as pressure is increased from 20 to 200 torr. Over the same pressure range in rigor muscle, the change in electron density distribution is much less. At low pressure, the thick filament electron density diameter in rigor muscle is smaller than in relaxed muscle. These changes parallel those observed for the effective thick filament charge diameters determined from comparison of lattice spacing/pressure curves with calculated electrostatic pressure curves. Comparison of electron density maps with effective charge diameters has allowed identification of the radial position of charge on the thick filaments. This appears to coincide with the S1-S2 junction on heavy meromyosin. Furthermore, small external pressures (~20 torr) appear to compress the thick filament projections against the filament backbone in relaxed muscle, but in rigor muscle, much greater pressures are required for similar compression.

M-Pos168 MORPHOMETRIC ANALYSIS OF VENTRICULAR TRABECULAE AND PAPILLARY MUSCLES FROM GUINEA PIG.
B.R. Eisenberg, D.S. Bruner and R.T. Mathias, Department of Physiology, Rush Medical College, Chicago, IL 60612.

Impedance studies of guinea pig ventricle are interpretable in a unique way only if one has an estimate of the structurally based equivalent circuit (see the abstract by Mathias et al., 1985). Furthermore, electrical parameter values are scaled by the sizes of structural components, hence a morphometric analysis of the preparation is an essential step in obtaining an understanding of electrophysiological properties. Relative volumes are estimated from light and electron micrographs by point count ratios and relative surface areas by intersection count ratios. Both preparations have a thin interrupted epithelial layer but papillary muscles also have a thicker outer connective tissue sheath; in other anatomical respects they are similar. Both contain myocytes, blood vessels, and loose connective tissue. The myocytes occupy two thirds of the tissue volume, the blood vessels occupy about 10% tissue volume, and the extracellular space makes up the remainder. T-system and other small spaces (under 1 μm wide) occupy only 2-4% of the myocyte volume. The myocyte interior contains about 50% by volume as myofibrils, and about 25% as mitochondria. Of the plasma membranes of the myocyte that face the extracellular spaces only about 10-15% face the narrow spaces (under 0.1 μm) of the intercalated disc; about a third of the membrane faces the T-system whose lumen has a minor diameter under a half micron; and the remaining half face wide extracellular space of over a micron. The ratio of total surface area (including T-system and discs) to myocyte volume is about 9,500 cm^{-1}. The outer sarcolemmal membrane (excluding T-system and discs) per unit volume of tissue is about 2,800 cm^{-1}. The morphometric and electrical estimates are in good agreement. Supported by grants from AHA and NIH HL-29205.

M-Pos169 CULTURED MICROSPHERES OF CARDIAC MUSCLE: GROWTH, CRYOPRESERVATION AND MORPHOLOGY.
A. LeFurgey, S.C. Henry, N. Wallace, M. Lieberman, J. Sommer, Departments of Physiology and Pathology, Duke University and VA Medical Centers, Durham, NC

Our objective was to obtain a preparation of cardiac muscle suitable for studying the ionic mechanisms associated with EC coupling. Correlative morphological and microchemical analysis of intracellular compartments involves the use of scanning transmission electron microscopy and energy dispersive x-ray spectroscopy. Such analyses require that cells function until they are snap frozen at a rate which minimizes ice crystal formation and translocation of ionic constituents. Embryonic chick heart cells were grown on spherical microcarriers (≈170μm diameter dextran or gelatin beads) to take advantage of their simple geometry for cryopreservation. After a 24-hour cell attachment period, the beads were triturated and maintained in a medium containing conditioned M-199, fetal bovine serum and chick embryo extract. After 3 or 4 days in culture, quick freezing and freeze substitution of individual microspheres were performed (Sommer et al., Proc. Electron Microsc. Soc. Amer. p. 464-465, 1983). No detectable ice crystals were found within at least 2 layers of cells. The majority of cells were muscle in origin, containing mitochondria, sarcoplasmic reticulum, developing myofibrils, and specialized intercellular junctions. These results suggest that cultured microspheres can be used to characterize the relationship between structural and elemental (ionic) compartmentation in small myocardial cell aggregates. Supported by grants HL 28280, HL 17670, HL 12486, and VA Research Service.

M-Pos170 THE LOCATION OF CYSTEINE-374 IN F-ACTIN DETERMINED BY GOLD CLUSTER LABELING AND SCANNING TRANSMISSION ELECTRON MICROSCOPY.
Daniel Safer, James Hainfeld and Joseph S. Wall. Department of Biochemistry and Biophysics G-4, University of Pennsylvania, Philadelphia, PA 19104 and Department of Biology, Brookhaven National Laboratory, Upton, NY 11973.

We have prepared a new water-soluble, monomaleimidopropyl undecagold cluster, $Au_{11}P_7(PhCONHCH_3)_{20}PhCONHC_3H_6NC_4H_2O_2(HCO_3)_3$, and have used it to label actin and actin-tropomyosin filaments. Reaction at neutral pH with a 4-fold excess of reagent results in the incorporation of 0.75-0.8 gold cluster per actin monomer as determined by spectroscopic measurement. Prereaction of actin with N-ethylmaleimide reduces the incorporation of gold cluster to 0.1 or less per actin monomer, indicating that the reaction is predominantly at cysteine-374 (J.H. Collins and M. Elzinga, J. Biol. Chem. 250, 5915-5920, 1975). Preliminary examination of labeled specimens by high-resolution STEM shows a pattern of bound gold clusters consistent with a two-stranded actin helix, an axial subunit repeat of 5.5 nm, and 13-15 subunits per turn. Gold clusters are bound at or near the outer radius of the actin filament, which is about 3.5 nm in unstained, freeze-dried specimens.

Supported by NIH Grants AM 31,984 to John S. Leigh and Daniel Safer and RR 01777 to Joseph S. Wall.

M-Pos171 **ULTRASTRUCTURE OF THE FROG THICK FILAMENT.** **Robert W. Kensler and Murray Stewart. Department of Anatomy, The Medical College of Pennsylvania, Philadelphia, PA 19129 and the MRC Laboratory of Molecular Biology, Cambridge, England.**

In a preliminary report (Kensler and Stewart. 1983. J. Cell Biol. 96: 1791-1802), we reported that frog skeletal muscle thick filaments can be isolated with the periodic ordering of the myosin crossbridges substantially preserved. Computer image analysis of electron micrograph images of the filaments provided strong evidence that the crossbridges lie along three approximately helical strands, but because of a perturbation of the crossbridge arrangement from perfect helical symmetry we were not able to compute a three-dimensional reconstruction of the crossbridge arrangement on the filaments. From analysis of micrographs of individual filaments tilted about their long axes from -60^{o} to $+60^{o}$, we have now computed a preliminary three-dimensional reconstruction of the frog thick filament. The reconstruction clearly confirms the three-stranded arrangement of the myosin heads and suggests that the position of the heads may deviate in a periodic way from the expected helical path. A density which may correspond to C-protein has also been identified, but further work will be necessary to confirm this identity. Platinum-shadowed images of the filaments (both unidirectional and rotary shadowing) appear consistent with a three-stranded arrangement of the crossbridges.

This work was supported in part by UPHS grant AM30442 to R.W.K.

M-Pos172 A RAPID-FREEZING/STOPPED FLOW METHOD TO PREPARE THE INTERMEDIATES IN THE ACTIN-MYOSIN ATPase CYCLE FOR ELECTRON MICROSCOPY.

T.D. Pollard, A.G. Weeds & H.E. Huxley. MRC Laboratory of Molecular Biology, Cambridge, U.K.

We have combined the rapid mixing techniques used in enzyme kinetic analysis with rapid freezing by a -190^{o}C propane jet to prepare intermediates in rapid reactions for electron microscopy. The freezing machine is designed to stop reactions at known times after mixing on a millisecond time scale. The sample is frozen in a 1.5 mm diameter copper tube with walls 20 μm thick, then freeze fractured, deep etched and rotary shadowed. This method produces replicas of actin filaments (diameter 9-11 nm, helical repeat 5.5 nm) and actin filaments fully decorated with myosin subfragment-1 (S-1) (diameter 22 nm, helical repeat 36 nm) identical to those prepared by impact freezing at 4^{o}K (J. Heuser and R. Cooke, J. Mol. Biol., 1983). Actin filaments mixed with substoichiometric concentrations of S-1 have random teardrop-shaped particles protruding 5-6 nm from their surfaces. Actin filaments saturated with heavy meromyosin (HMM) are 27 nm in diameter and have much more irregular surfaces than the filaments saturated with S-1. The filaments decorated with HMM show occasional slender strands 50-70 nm long cross-linking adjacent filaments, but individual subfragment-2 rods do not project regularly from the surface. Substoichiometric HMM decorates actin filaments non-randomly. In 0.5 mM ATP, 1 mM $MgCl_2$, 5 mM imidazole (pH 7.0) at 20°C, 30 μM S-1 and 40 μM actin hydrolyze ATP at 7.0 s^{-1} in the steady-state phase of 2.4 s, with 40% of the S-1 bound to the actin filaments, as judged from light scattering. Samples frozen during the steady state reaction have actin filaments decorated with random particles that look superficially similar to S-1 bound in the absence of ATP. This established the feasibility of using electron microscopy to examine directly intermediates in rapid enzymatic reactions.

M-Pos173 ENVIRONMENTAL EFFECTS ON LIMULUS CROSSBRIDGES IN VITRO. Rhea J.C. Levine, John S. Wray* & John L. Woodhead. Dept. Anatomy, The Medical College of PA, Phila. PA 19129 & Dept. Biophysics, Max-Planck Institut für Medizinische Forschung, Heidelberg, Fed. Rep. Germany.

Within the filament lattice of skinned fibers, unattached crossbridges are affected by environmental conditions (Wray et al. J. Mol Biol 88:343 '74; unpublished results). Here we report the effects of changes in the composition of the surrounding medium on the crossbridge orientation of native thick filaments isolated from Limulus telson muscles. These filaments were chosen as a model system since we have shown that the helical parameters of the crossbridge array are preserved during isolation and negative staining and these have been analysed (Stewart et al. J. Mol Biol 153:781'81; Kensler & Levine, J. Cell Biol 91:443 '82).

Filament preparations that appeared highly periodic by electron microscopy and exhibited well-ordered relaxed diffraction patterns were exposed to one or more environmental modifications prior to or during negative staining. ATP depletion, pyrophosphate substitution for ATP in the presence of EDTA, increased pH, increased ionic strength and exposure to 50% glycol at any preparative step but during UAc staining, all caused crossbridges to move away from the filaments' shafts. This was apparent on electron micrographs and by the loss of the 1st and 4th layer lines from the optical transforms. Reincubation with relaxing solution tended to restore both the periodic appearance of the crossbridge array and portions of the diffraction pattern relating to the helical arrangement of crossbridges. These results suggest that isolated filaments may be used as model systems to examine crossbridge positions relating to the contractile cycle, in the absence of a thick-thin filament array. Work supported in part by grants: AM33302 and HL15835 to The Pennsylvania Muscle Institute.

M-Pos174 MORPHOLOGICAL CHANGES IN THE CARDIAC SARCOMERE DURING EXTREME ACTIVE & PASSIVE SHORTENING
John W. Krueger & Barry London, The Albert Einstein College of Medicine, Bronx, N.Y. 10461

The ultrastructural appearance of the cardiac sarcomere commonly changes from a barrel shape at rest to one where the smallest diameter occurs at the center of the A-band in the actively shortened sarcomere. The light microscopic appearance of sarcomeres in single, isolated myocytes was recorded during rapid fixation (2% glutaraldehyde & 0.1% tannic acid in a physiological salt sol'n), an event which arrests the unattached cell at the apex of its contractile shortening cycle. Longitudinal dimensions in electron microscopy were then corrected by sarcomere length in the pre-embedded cell, and the lateral separation of the thick filaments was evaluated where one-of-two uniform patterns occurred across the longitudinally sectioned myofibril. The ratio of the respective separations was $\sqrt{3}$, as expected by the ratio of the (1,0/1,1) X-ray diffraction planes, and the uncorrected separation of the thick filaments in resting cells was >90% of the value predicted by cardiac X-ray diffraction data (Matsubara & Millman, 1974). The separation of the thick filaments at the A-I jct increased with sarcomere shortening as predicted by a constant volume behavior, but the separation of the thick filaments in the middle of the A-band did not change. The differences in protein concentration resulting from alterations in thick filament spacing explains the optical properties of the shortened sarcomere. Not seen in actively shortening sarcomeres, discrete shearing occurred between bundles of thick filaments at the level of the M-line in the passively shortened, buckled sarcomere. The bundles separate at these points after treatment of the cells with mild detergent (0.5% w/v Brij). Lateral organization of the cardiac A-band may prevent constant volume behavior and promote relengthening of the shortened sarcomere. (NIH HL21325 & T32-GM7288 and the NYHA)